DOKUZ EYLÜL UNIVERSITY
GRADUATE SCHOOL OF NATURAL AND APPLIED SCIENCES

COMPUTER AIDED DESIGN AND OPTIMIZATION OF HEAT EXCHANGERS

by
Bayram IRMAKLIOĞLU

June, 2006
İZMİR

COMPUTER AIDED DESIGN AND OPTIMIZATION OF HEAT EXCHANGERS

A Thesis Submitted to the
Graduate School of Natural and Applied Sciences of Dokuz Eylül University
In Partial Fulfillment of the Requirements for the Degree of Master of Science
in Mechanical Engineering, Energy Program

by
Bayram IRMAKLIOĞLU

June, 2006
İZMİR

M.Sc THESIS EXAMINATION RESULT FORM

We have read the thesis entitled **"COMPUTER AIDED DESIGN AND OPTIMIZATION OF HEAT EXCHANGERS"** completed by **BAYRAM IRMAKLIOĞLU** under supervision of **ASST. PROF. DR. DİLEK KUMLUTAŞ** and we certify that in our opinion it is fully adequate, in scope and in quality, as a thesis for the degree of Master of Science.

Asst. Prof. Dr. Dilek KUMLUTAŞ

Supervisor

(Jury Member)

(Jury Member)

Prof. Dr. Cahit HELVACI
Director
Graduate School of Natural and Applied Sciences

ACKNOWLEDGEMENTS

I would like to thank to my supervisor Asst. Prof. Dr. Dilek KUMLUTAŞ for her unlimited support and guidance during the study. I also thank to Ege University for FLUENT support. Special thanks to my family.

Bayram IRMAKLIOĞLU

COMPUTER AIDED DESIGN AND OPTIMIZATION OF HEAT EXCHANGERS

ABSTRACT

Heat exchangers are the devices to exchange heat between hot and cold fluid. Many types of heat exchangers are used in various applications. Evaporators are used in refrigeration and air-conditioning systems.

In this study, a two-row aluminum plate fin and copper tube blast freezer evaporator is analyzed for different geometrical parameters, numerically. The evaporator is used in fish blast freezing process at -25°C. The effects of fin pitch, fin thickness, fin material, tube diameter, longitudinal and transverse tube pitches on heat transfer and pressure drop are investigated in 14 different geometrical models for actual boundary conditions and turbulent flow by using a CFD software (Fluent). R404A is used as refrigerant. The air inlet velocity ranges between 2 m/s to 4 m/s. Theoretical study is also completed in order to compare with the numerical study, very close results are obtained.

As a result of this study, the fin pitch has a considerable effect on heat transfer and pressure drop. As the fin pitch decreases, heat transfer rate and pressure drop increases. The fin thickness has an insignificant effect on heat transfer and pressure drop. Another important result of the study is the heat transfer rate and pressure drop increases as the tube diameter increases. Basically, staggered tube arrangement increases heat transfer and pressure drop. The transverse tube pitch effect on heat transfer rate is negligible whereas pressure drop has a considerable increase when the transverse tube pitch decreases. Greater heat transfer rates are obtained as the longitudinal tube pitch increases, due to the increased heat transfer area. The pressure drop increases with a reduction of longitudinal tube pitches. Greater heat transfer rates are obtained as the copper fin is selected. The pressure drop has no change for different fin material.

Keywords: Heat exchanger, evaporator, numerical, Fluent

ISI DEĞİŞTİRGEÇLERİNİN BİLGİSAYAR DESTEKLİ TASARIMI VE OPTİMİZASYONU

ÖZ

Isı değiştirgeçleri, sıcak ve soğuk iki akışkan arasındaki ısı transferini sağlayan araçlardır. Birçok uygulamada birçok tipte ısı değiştirgeci kullanılmaktadır. Evaporatörler, soğutma ve iklimlendirme sistemlerinde kullanılmaktadır.

Bu çalışmada, iki sıralı alüminyum kanatlı ve bakır borulu bir şoklama evaporatörü, değişik geometrik parametreler için nümerik olarak incelenmiştir. Evaporatör, -25°C de balık şoklama işleminde kullanılmaktadır. Kanat aralığı, kanat kalınlığı, kanat malzemesi, boru çapı, yatay ve dikey boru aralıkların ısı transferi ve basınç düşümüne etkisi 14 değişik geometrideki modelde gerçek sınır şartları ve türbülanslı akış için Fluent yardımıyla incelenmiştir. Akışkan olarak R404A kullanılmıştır. Evaporatör girişi hava hızları 2 ila 4 m/s arasında seçilmiştir. Yapılan teorik çalışma, nümerik çalışmayla karşılaştırılmış ve çok yakın sonuçlar elde edilmiştir.

Bu çalışmanın sonucunda, kanat aralığının ısı transferi ve basınç düşümüne önemli ölçüde etkisi olduğu görülmüştür. Kanat aralığı azaldıkça ısı transferi ve basınç düşümü artmaktadır. Kanat kalınlığının ısı transferi ve basınç düşümüne önemli bir etkisi yoktur. Diğer bir önemli sonuç ise, boru çapı arttıkça ısı transferi ve basınç düşümünün artmasıdır. Temel olarak, şaşıtılmış boru yerleşimi ısı transferini ve basınç düşümünü arttırmaktadır. Dikey boru aralığın ısı transferine etkisi ihmal edilebilecek kadar küçüktür, ancak aralık azaldıkça basınç düşümü önemli ölçüde artmaktadır. Yatay boru aralığı arttıkça, ısı transferi alanı da arttığı için daha büyük ısıl kapasite değerleri elde edilmektedir. Ayrıca bu aralık azaldıkça basınç düşümü artmaktadır. Kanat malzemesi olarak bakır kullanıldığında ısı transferi çok fazla artmaktadır. Kanat malzemesinin basınç düşümüne herhangi bir etkisi yoktur.

Anahtar sözcükler: Isı değiştirgeci, evaporator, nümerik, Fluent

CONTENTS

Page

CHAPTER ONE
INTRODUCTION

The process of heat exchange between two fluids that are at different temperatures and separated by a solid wall occurs in many engineering applications. The device used to implement this exchange is termed a heat exchanger, and specific applications may be found in space heating and air-conditioning, refrigeration systems, power production, waste heat recovery, and chemical processing (Incropera, 2002). Boilers, evaporators, super heaters, condensers, and coolers are all considered heat exchangers.

Fin and tube heat exchangers are used extensively in various industrial applications. A number of experimental and numerical studies on heat transfer and pressure drop for fin and tube heat exchangers are presented in the literature. Shepherd (1956) studied the heat transfer characteristics of a single row aluminum fin and tube heat exchanger, experimentally. Rich (1973, 1975) investigated the effects of both fin pitch and the number of tube rows on the air side heat transfer and pressure drop for plate fin and tube heat exchangers. Saboya & Sparrow (1974, 1976a, 1976b) studied heat transfer characteristics of one, two, and three-row fin and tube heat exchanger configurations. Elmahdy & Biggs (1979) developed an empirical technique to predict air side Colburn factor based on the Reynolds number. Eight-row coils with circular or continuous plate fins and circular tubes were used in the experiment. Gray & Webb (1986) developed correlations for air side heat transfer coefficient and friction factor as a function of the Reynolds number and the geometrical parameters. The results were applicable to any number of tube rows. Wang et al. (1996 – 2001) studied the effects of number of tube rows, tube diameter, fin pitch, and fin thickness on heat transfer and pressure drop characteristics for different fin surfaces.

Turaga et al. (1988) studied plate fin and tube direct expansion heat exchanger refrigerant air cooling and dehumidifying heat exchangers, to determine the effects of the geometric and the fluid flow parameter on coil performance. Horuz et al.

(1998) analyzed the theoretical and experimental performance of air-cooled evaporators. Abu Madi et al. (1998) tested 28 heat exchanger samples in an open circuit thermal wind tunnel for different geometries. Kim & Kim (2005) developed a heat transfer correlation to be used in the optimal design of evaporators for refrigerators and freezers.

Rosman et al. (1984) performed a numerical two-dimensional heat transfer analysis for plate fin and tube heat exchangers in order to obtain fin efficiency. Jang et al. (1996) investigated the effects of different geometrical parameters on the average heat transfer coefficient and pressure drop for plate fin and tube heat exchangers, numerically and experimentally. Rocha et al. (1997) studied fin efficiency for elliptical tubes. Jang & Chen (1997) investigated wavy fin and tube heat exchangers. Jang et al. (1998) studied fluid flow and heat transfer characteristics over circular fin and tube heat exchangers with staggered arrangement. Romero-Mendez et al. (2000) investigated the effects of fin pitches on a single-row fin and tube heat exchanger. Shih (2003) performed a numerical simulation on predicting the pressure drop and heat transfer coefficient for the evaporator of domestic refrigerator. Mon & Gross (2004) investigated annular fin and tube heat exchangers.

In this study, a two-row plate fin and tube blast freezer evaporator model is analyzed for different geometrical parameters, numerically. The evaporator is used in fish freezing process at -25°C. The geometrical parameters are taken from commercially available products. The effects of fin pitch, fin thickness, fin material, tube diameter, longitudinal and transverse tube pitch on the air side heat transfer and pressure drop of aluminum plate fin and staggered tube heat exchangers are investigated for actual boundary conditions and turbulent flow. R404A is used as refrigerant. The air inlet velocity ranges from 2 m/s to 4 m/s.

CHAPTER TWO
CLASSIFICATION OF HEAT EXCHANGERS

Heat exchangers are devices that provide the flow of thermal energy between two or more fluid at different temperatures. Heat exchangers are used in various applications. In power production, industrial processes, air-conditioning and refrigeration, heat exchangers are used extensively. In Figure 2.1, classification of heat exchangers according to 5 main criteria is shown (Kakaç, 1998) :

1. Recuperators and regenerators
2. Transfer processes: direct contact and indirect contact
3. Geometry of construction: tubes, plates, and extended surfaces
4. Heat transfer mechanisms
5. Flow arrangements: parallel, counter, and cross flows

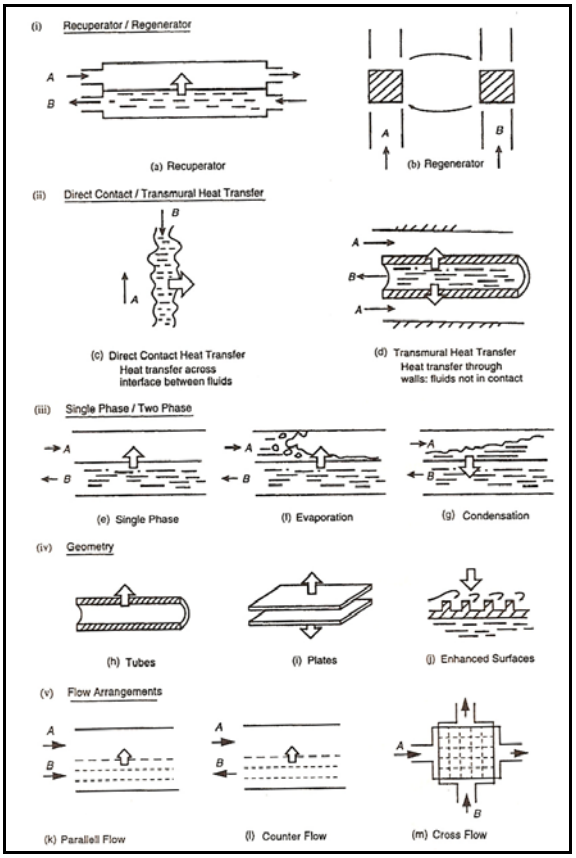

Figure 2.1 Classification of heat exchangers

2.1 Recuperation and Regeneration

In Figure 2.1a, a recuperator is shown, with heat transfer between two fluids. The hot stream A recuperates some of the heat from stream B. As shown in Figure 2.1c, in direct contact type heat exchangers, the heat transfer is through a separating wall or through the interface between the streams. Some of the recuperative-type exchangers are shown in Figure 2.2 (Kakaç, 1998).

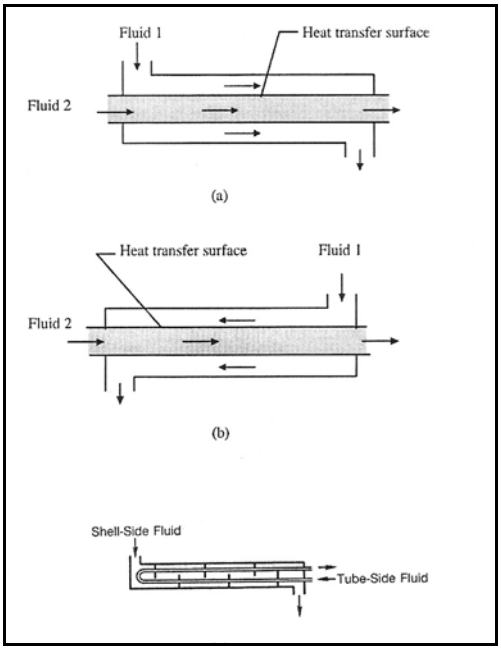

Figure 2.2 Indirect contact types of heat exchangers. (a), (b) Double-pipe type, (c) shell and tube type

The same flow passage is alternately occupied by one of the two fluids in regenerators (storage-type heat exchangers). As shown in Figure 2.1b, thermal energy is not transferred through the wall as in a direct transfer type of heat exchanger. Regenerators can be classified as:

1. Rotary regenerator
    (a) Disk-type
    (b) Drum-type
2. Fixed-matrix regenerator

Rotary regenerators are used in preheating air in large coal-fired steam power plants, gas turbines, fixed-matrix air preheating for blast furnace stoves, steel furnaces, open-hearth steel melting furnaces, and glass furnaces. Rotary regenerators can be classified as:

The disk-type and drum-type regenerators are shown in Figure 2.3, schematically. The heat transfer surface is in a disk form and fluids flow axially in disk-type regenerators. In drum-type regenerators, the matrix is in a hollow drum form and fluids flow radially.

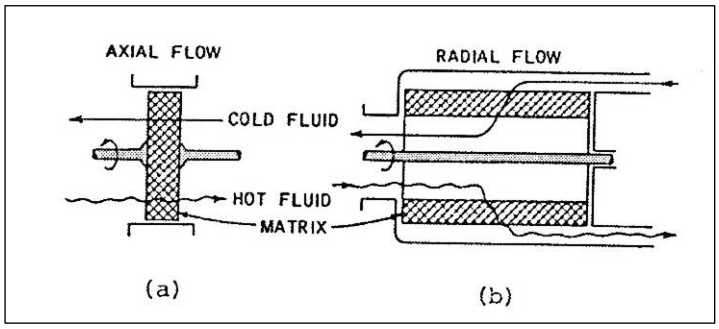

Figure 2.3 Rotary regenerators. (a) Disk type. (b) Drum type

2.2 Transfer Processes

Heat exchangers are classified as direct contact type and indirect contact type (transmural heat transfer) according to transfer processes (Kakaç, 1998).

In direct contact type heat exchangers, heat is transferred through a direct contact between the cold and hot fluids. As shown in Figure 2.1c, since there is no wall between hot and cold streams, the heat transfer occurs through the interface of two streams. The streams are two immiscible liquids, a gas-liquid pair, or a solid particle-fluid combination in direct contact type heat exchangers. Cooling towers, spray and tray condensers are good examples of such heat exchangers.

In indirect contact type heat exchangers, heat is transferred through a heat transfer surface between the cold and hot fluids, as shown in Figure 2.1d. The fluids are not mixed. This type of heat exchanger examples are shown in Figure 2.2.

Indirect contact and direct contact type heat exchangers are also called recuperators. Tubular (double-pipe, shell and tube), plate, and extended surface heat exchangers; cooling towers; and tray condensers are examples of recuperators.

2.3 Geometry of Construction

Indirect contact type heat exchangers are often described in terms of their construction features. Tubular, plate and extended surface heat exchangers are the major construction types (Kakaç, 1998).

2.3.1 Tubular Heat Exchangers

Circular tubes are used in these heat exchangers. One fluid flows inside the tubes and the other fluid flows outside of the tubes. Tube diameter, number of tubes, tube length, tube pitch, and tube arrangement are the construction parameters; there is a considerable flexibility in tubular heat exchanger design. Tubular heat exchangers can be classified as:

1. Double-pipe
2. Shell and tube
3. Spiral-tube

2.3.1.1 Double-Pipe Heat Exchangers

A typical double-pipe heat exchanger consists of one pipe placed concentrically inside another of larger diameter with appropriate fittings to direct the flow from one section to the next, as shown in Figure 2.4. Double-pipe heat exchangers can be arranged in various series and parallel arrangements to meet pressure drop and mean

temperature difference requirements. In sensible heating or cooling of process fluids where the small heat transfer areas (to 50 m^2) are required, double-pipe heat exchangers are used extensively. Double-pipe heat exchangers can be built in modular concept (i.e., in the form of hairpins).

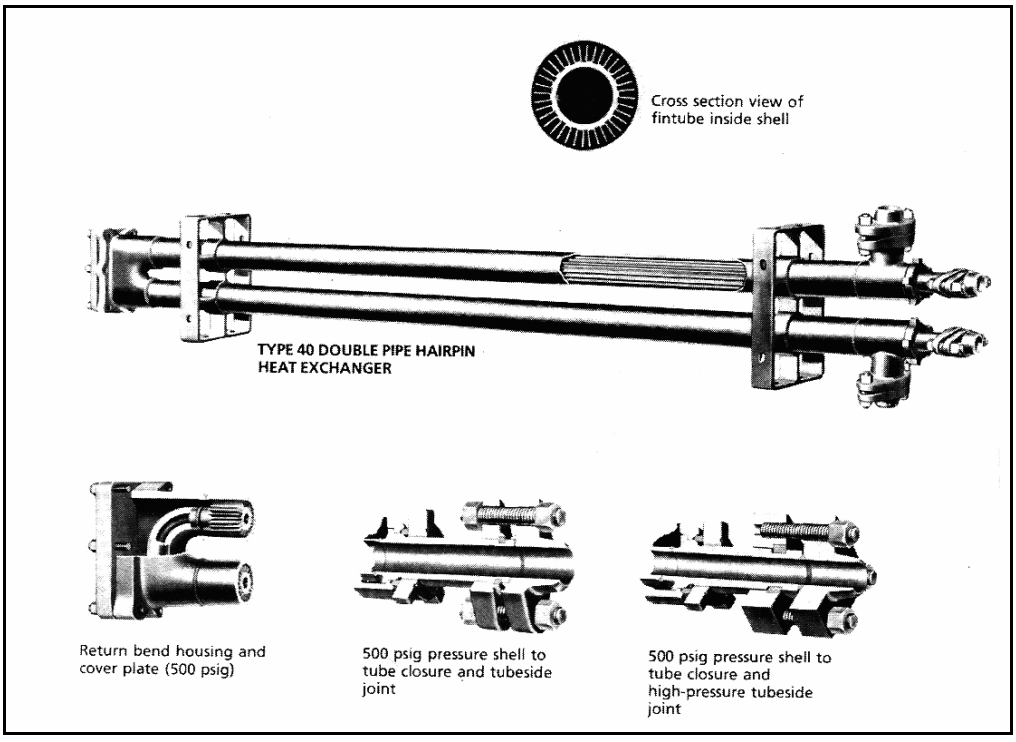

Figure 2.4 Double-pipe hairpin heat exchanger

2.3.1.2 Shell and Tube Heat Exchangers

Shell and tube heat exchangers are built of round tubes mounted in large cylindrical shells with the tube axis parallel to that of the shell. They are used as oil coolers, power condensers, preheaters in power plants, steam generators in nuclear power plants, and in process and chemical industry applications, extensively. A horizontal shell and tube condenser is shown in Figure 2.5. One fluid flows through the tubes while the other flows on the shell side, across or along the tubes. The baffles are used to promote a better heat transfer coefficient on the shell side and to support the tubes. In a baffled shell and tube heat exchanger, the shell side fluid flows across between pairs or baffles and then flows parallel to the tubes as it flows from one baffle compartment to the next. There are many different shell and tube

heat exchangers depending on the application. The most representative tube bundle types are used in shell and tube heat exchangers are shown in Figure 2.6 and 2.7. Since only one tube sheet is used, the U-tube is the least expensive construction. But the tube side cannot be mechanically cleaned because of the sharp U-bend.

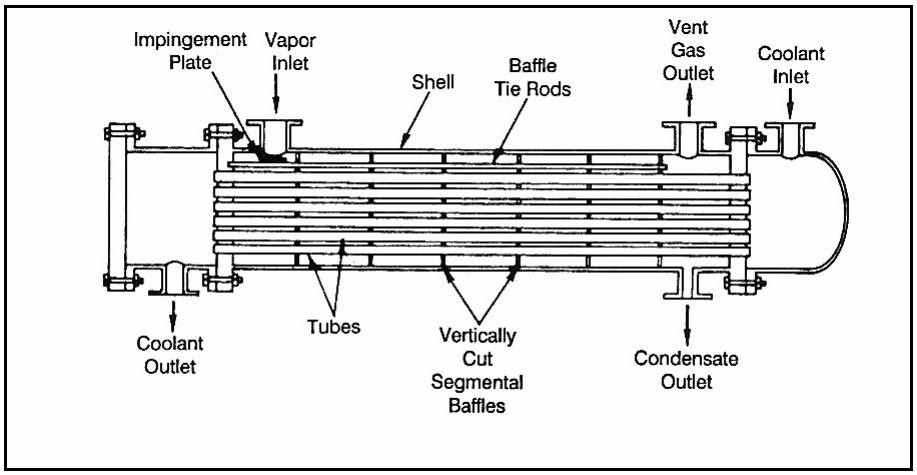

Figure 2.5 Shell and tube heat exchanger as a shell side condenser

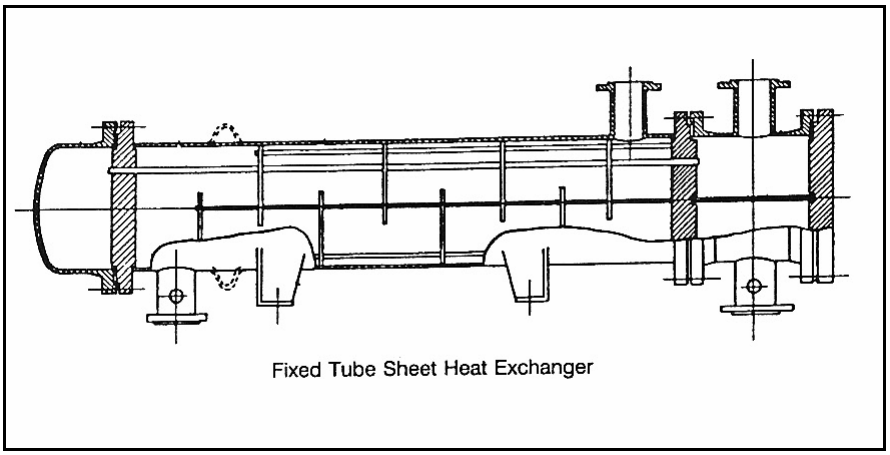

Figure 2.6 Two-pass tube, baffled single-pass shell, shell and tube heat exchanger

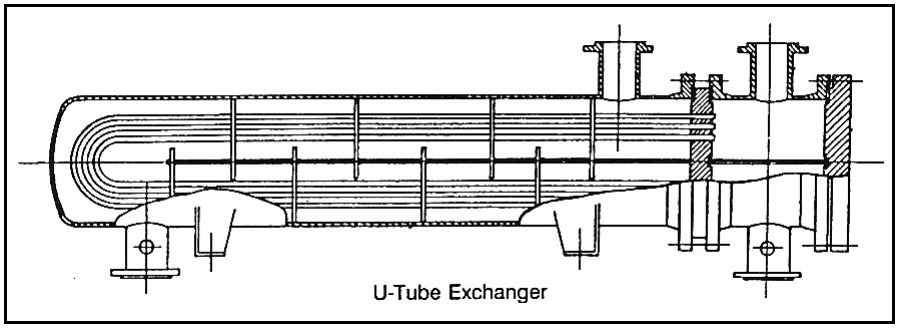

Figure 2.7 U-tube, baffled single-pass shell, shell and tube heat exchanger

2.3.1.3 Spiral-Tube Heat Exchangers

Spiral-tube heat exchangers are spirally wound coils placed in a shell, or coaxial condensers and coaxial evaporators used in refrigeration systems. The heat transfer coefficient is higher than straight tubes. They are suitable for thermal expansion and clean fluids, because it is almost impossible to clean a spiral-tube heat exchanger.

2.3.2 Plate Heat Exchangers

Plate heat exchangers are made of thin plates forming flow channels. The fluid streams are separated by flat plates that are either smooth or between which are sandwiched corrugated fins. They are used for heat transfer between any gas, liquid, and two-phase stream combinations. Plate heat exchangers are classified as:

1. Gasketed-plate
2. Spiral plate
3. Lamella

2.3.2.1 Gasketed-Plate Heat Exchangers

A typical gasketed-plate heat exchanger and the flow paths are shown in Figure 2.8 and 2.9. A gasketed plate consists of a series of corrugated or wavy thin plates that separates the fluids. Gaskets are used to prevent the leakage to the outside and direct the fluids in the plates. The countercurrent flow pattern is generally selected for the fluids. Because of the small flow passages, strong eddying gives high heat transfer coefficients, high-pressure drops, and high local shear that minimizes fouling. Gasketed-plate heat exchangers provide relatively compact and lightweight heat transfer surface. They are typically used for heat exchange between two liquid streams. Because of easy cleaning and sterilization, they are extensively used in the food processing industry.

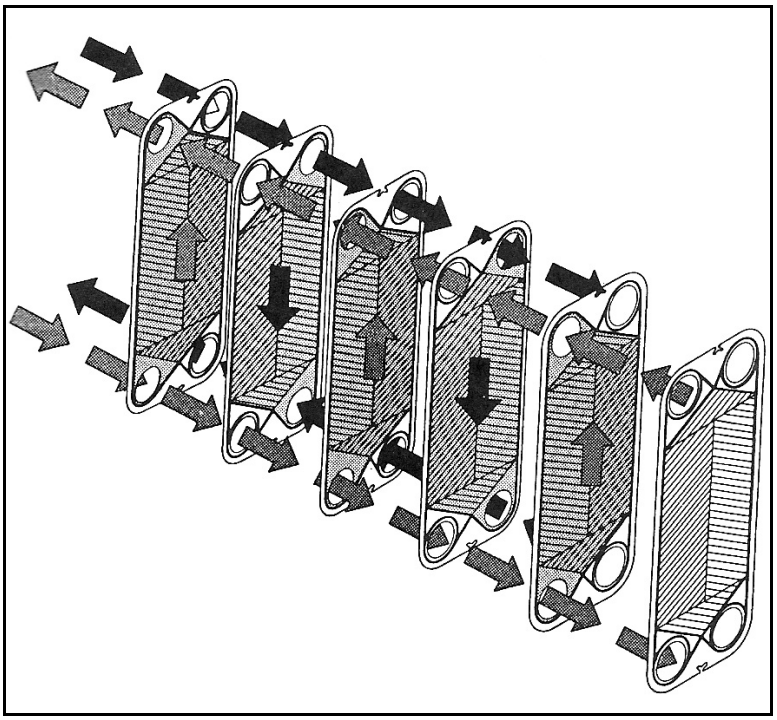

Figure 2.8 Gasketed-plate heat exchanger and flow paths

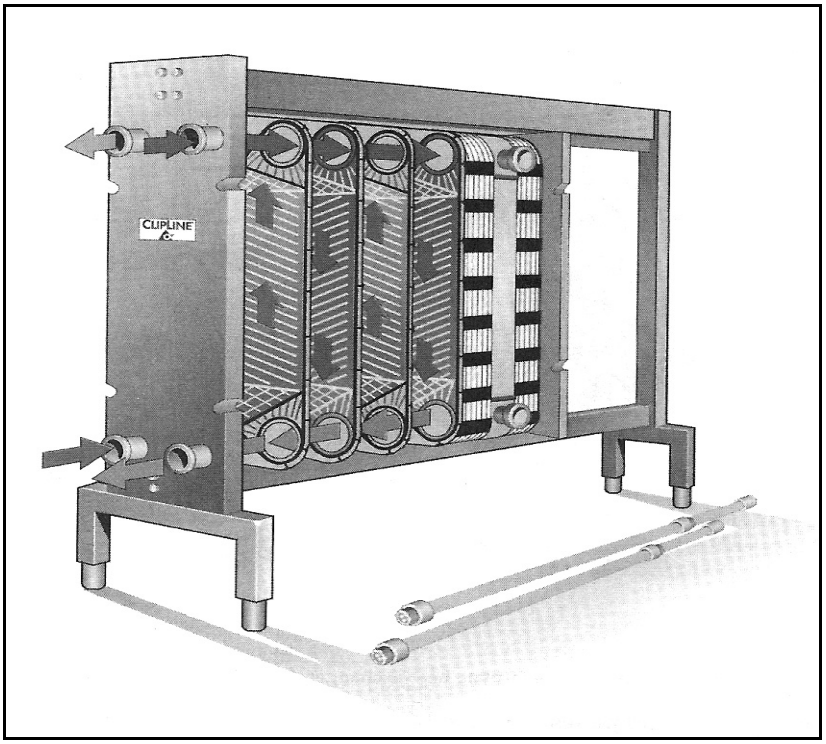

Figure 2.9 Gasketed-plate heat exchanger

2.3.2.2 Spiral Plate Heat Exchangers

As shown in Figure 2.10, spiral heat exchangers are formed by rolling two long, parallel plates into a spiral using a mandrel and welding the edges of adjacent plates to form channels. The distance between the metal surfaces in both spiral channels is maintained by means of distance pins welded to the metal sheet. The length of the distance pins may vary between 5 and 20 mm. It is possible to choose between different channels spacing according to the flow rate and ideal flow conditions and smallest possible heating surfaces can be obtained.

Two spiral paths introduce a secondary flow, increasing the heat transfer and reducting fouling deposits. These heat exchangers are quite compact, but are relatively expensive due to their specialized fabrication. Sizes range from 0.5 to 500m² heat transfer surface in one single spiral body.

The spiral heat exchanger is particularly effective in handling sludges, viscous liquids, and liquids with solids in suspension including slurries. A cross flow type spiral heat exchanger is shown in Figure 2.11.

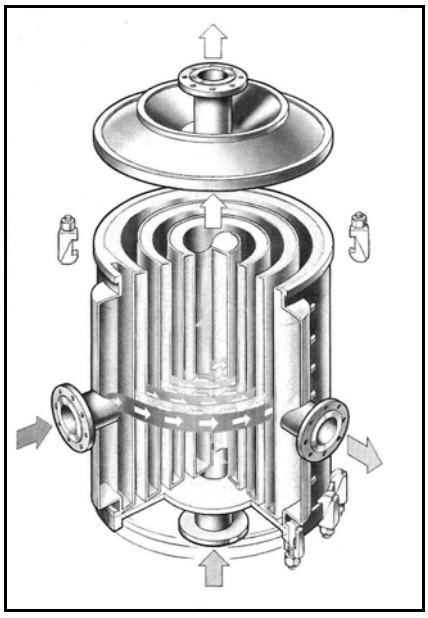

Figure 2.10 Counter-flow spiral heat exchanger

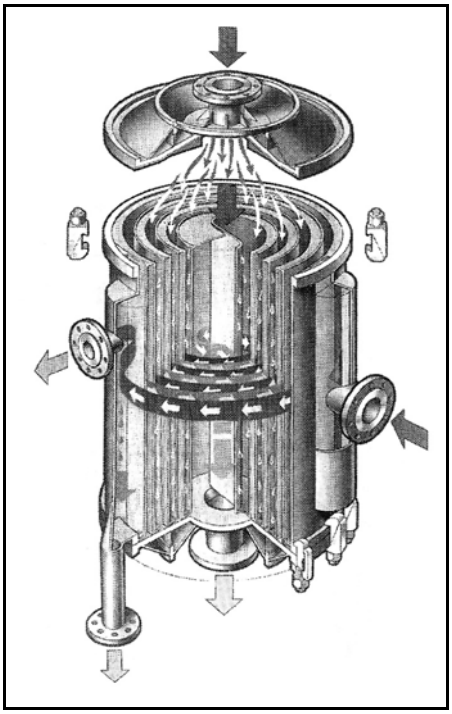

Figure 2.11 Cross-flow spiral heat exchanger

2.3.2.3 Lamella Heat Exchanger

As shown in Figure 2.12, the lamella (Ramen) type heat exchangers consists of a set of parallel, welded, thin plate channels or lamellae (flat tubes or rectangular channels) placed longitudinally in a shell. It is a modification of the floating-head type of shell and tube heat exchanger. These flattened tubes (lamellas) are made up of two strips of plates, profiled and spot or seam welded together in a continuous operation. The lamellas are welded together at both ends by joining the ends with steel bars in between, depending on the space required between lamellas. Both ends of the lamella bundle are joined by peripheral welds to the channel cover, which at the outer ends is welded to the inlet and outlet nozzle. The lamella side is thus completely sealed in by welds.

Lamella heat exchangers can be arranged for true countercurrent flow, since there are no shell side baffles. Because of high turbulence, uniform flow distribution, and smooth surfaces, the lamellas do not foul easily. They can be used up to 35 bar, 200°C for Teflon gaskets, and 500°C for asbestos gaskets.

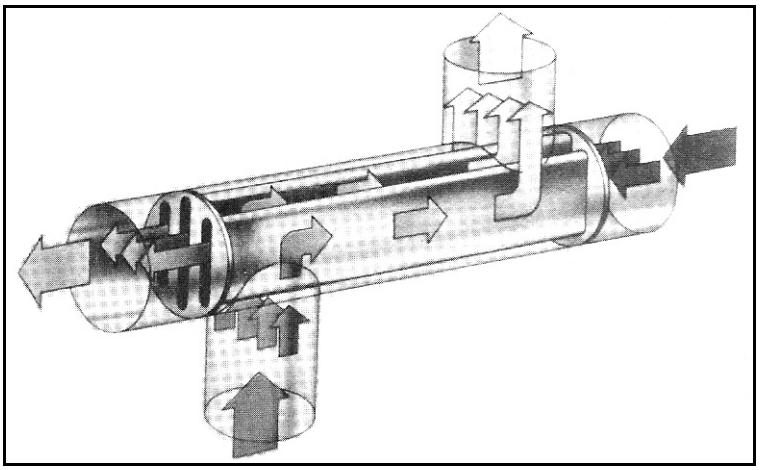

Figure 2.12 Lamella heat exchanger

2.3.3 Extended Surface Heat Exchangers

Extended surface heat exchangers have fins or appendages on the primary heat transfer surface (tubular or plate) to increase heat transfer area. Since gas side heat transfer coefficient is much lower than liquid side, finned surfaces are used to increase the heat transfer area. Fins are extensively used in gas-to-gas and gas-liquid heat exchangers. The most common types of the extended surface heat exchangers are

1. Plate-fin
2. Tube-fin

2.3.3.1 Plate-Fin Heat Exchangers

Plate-fin type heat exchangers are primarily used in gas-to-gas applications and tube-fin type heat exchangers are used in liquid-air applications. Since mass and volume reduction is important in most of the applications, compact heat exchangers are widely used in air-conditioning, refrigeration and process industries. Basic construction of a plate-fin heat exchanger is shown in Figure 2.13. The fluids are separated by flat plates between which are sandwiched corrugated fins. Figure 2.13 shows the arrangement for parallel flow or counter flow and cross flow between the streams.

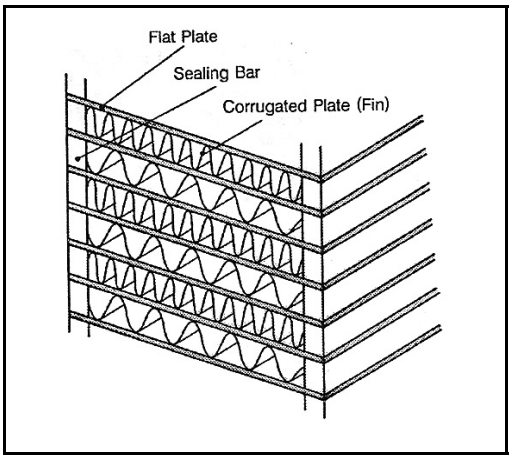

Figure 2.13 Basic construction of a plate-fin heat exchanger

The corrugated sheets that are sandwiched between the plates serve both to give extra heat transfer area and to give structural support to the flat plates. The most common types of corrugated sheets are shown in Figure 2.14.

1. Plain fin
2. Plain-perforated fin
3. Serrated (interrupted, louver) fin
4. Herringbone or wavy fin

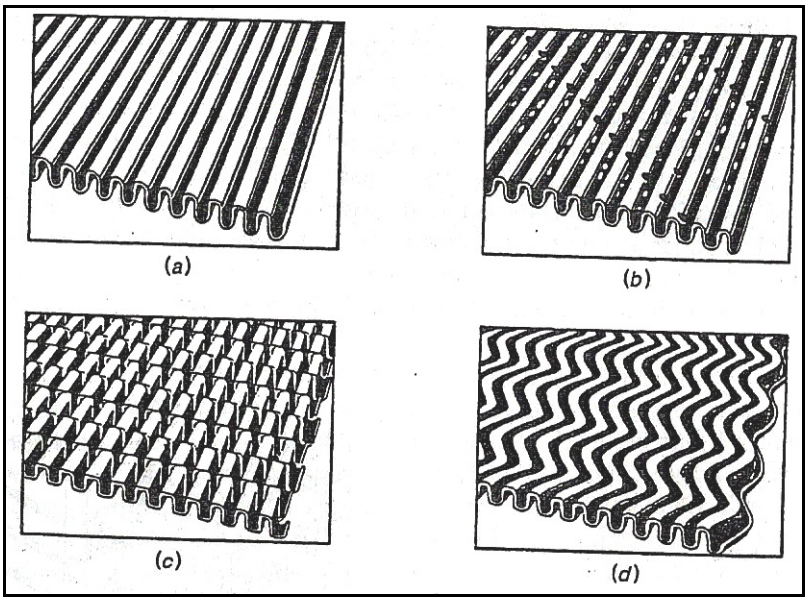

Figure 2.14 Fin types in plate-fin heat exchangers. (a) Plain, (b) perforated, (c) serrated, (d) herringbone

2.3.3.2 Tubular-Fin Heat Exchangers

Tubular-fin heat exchangers are used as gas-to-liquid heat exchangers. Since the gas side heat transfer coefficients are generally much lower than the liquid side, fins are required. As shown in Figures 2.15 and 2.16, a tubular-fin heat exchanger consists of an array of tubes with fins fixed on the outside. The fins may be normal on individual tubes, transverse or helical, or longitudinal (Figure 2.16). Longitudinal fins are commonly used in double-pipe or shell and tube heat exchangers with no baffles. As can be seen from Figure 2.15, continuous plate-fin sheets may be fixed on the array of round, rectangular, or elliptical tubes. Plate fin and tube heat exchangers are commonly used in air-conditioning and refrigerating systems.

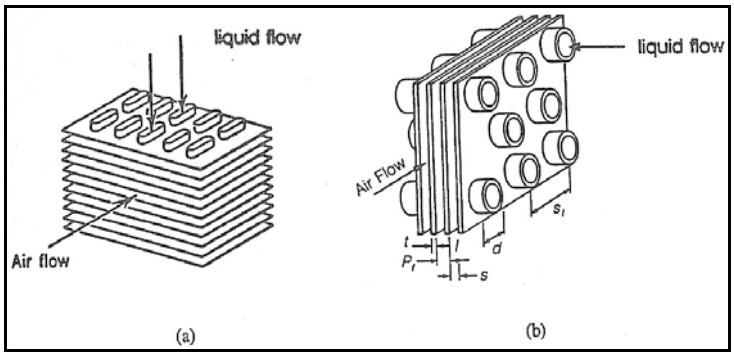

Figure 2.15 Tube-fin heat exchangers. (a) Flattened tube-fin, (b) round tube-fin.

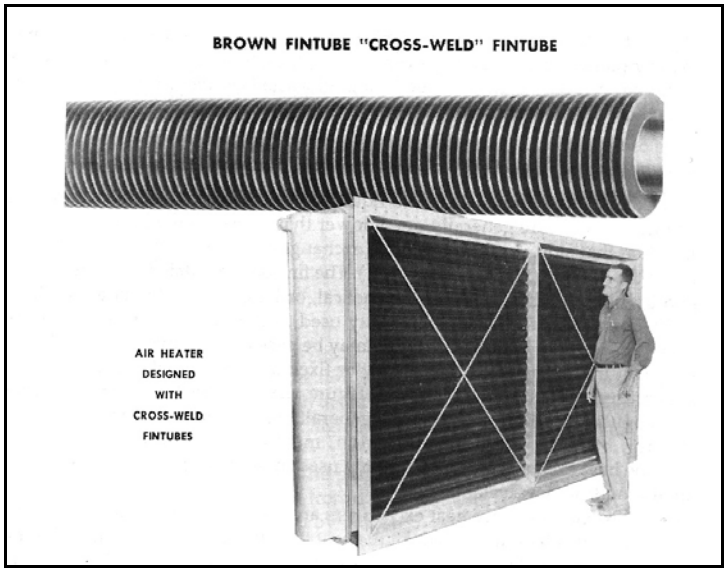

Figure 2.16 Fin-tube air heater

2.4 Flow Arrangement

Heat exchangers may be classified according to the fluid-flow path through the heat exchanger (Kakaç, 1998). Three basic flow arrangements are

1. Parallel flow
2. Counter flow
3. Cross flow

As shown in Figure 2.17a, in parallel flow heat exchangers, the two fluid streams enter together at one end, flow through the same direction, and leave together at the other end. In counter flow heat exchangers, two fluid streams flow in opposite direction (Figure 2.17b). In single-cross flow heat exchangers, one fluid flows through the heat exchanger surface at right angles to the flow path of the other fluid. Cross flow arrangements with both fluids unmixed, and one fluid mixed and the other fluid unmixed are shown in Figures 2.17c and 2.17d, respectively.

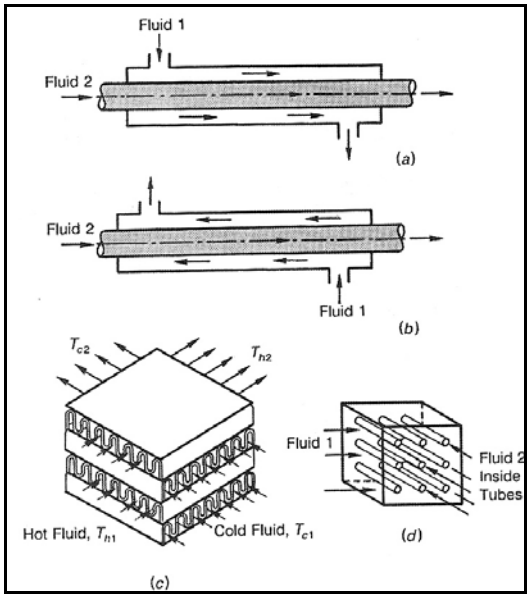

Figure 2.17 Heat exchanger classification according to flow arrangement. (a) Parallel-flow, (b) counter flow, (c) cross flow-both fluids unmixed, (d) cross flow-fluid 1 mixed, fluid2 unmixed.

CHAPTER THREE
EVAPORATORS

Two-phase flow heat exchangers in the refrigeration and air-conditioning industry can be classified as coils when the refrigerant boils inside the tubes and air flows over fin and tubes (Figure 3.1). Shell and tube evaporators are used when the second fluid is a liquid that flows either through the tubes (shell-and-tube flooded evaporators) or over the tubes (shell-and-tube direct expansion evaporators). Flooded evaporators and direct expansion (DX) evaporators perform similar functions. The five types of heat exchangers shown in Figure 3.1 represent the majority of heat exchanger types used in the refrigeration and air-conditioning industry. However, other types such as plate-fin and double-pipe heat exchangers are also used for automotive air-conditioning systems and low-tonnage liquid cooling systems, respectively (Kakaç, 1998).

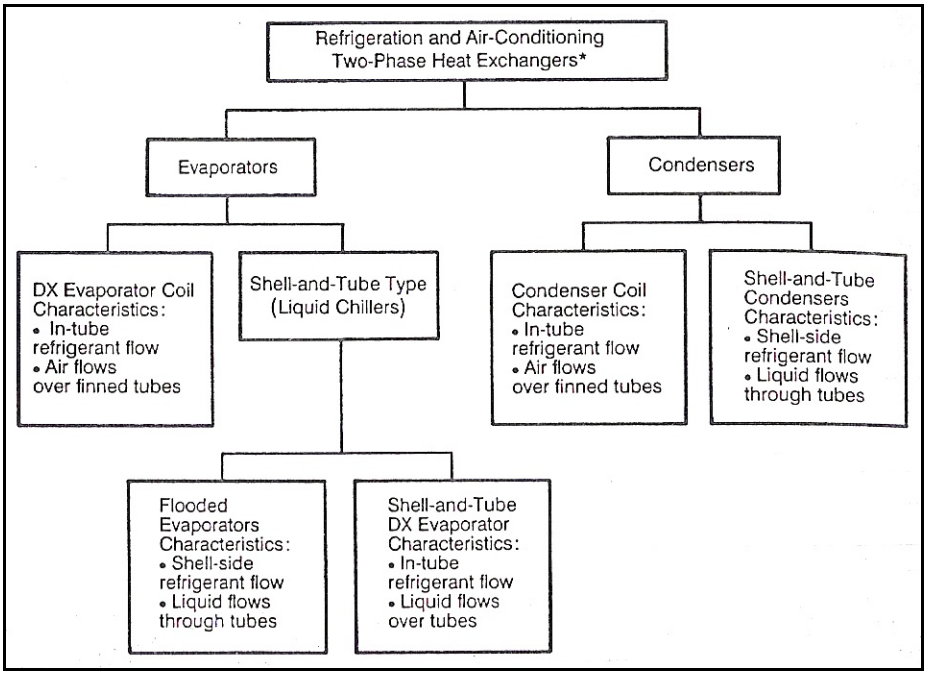

Figure 3.1 Common heat exchanger types used in the refrigeration and air-conditioning industry

3.1 Water-Cooling Evaporators (Chillers)

Evaporators, while the refrigerant boils inside the tubes, are the most common commercial evaporators; boiling in the shell, outside the tubes is an important class of liquid-chilling evaporators' standard in centrifugal compressor applications. Examples of liquid-cooling-flooded evaporators are shown in Figures 3.2 and 3.3 (Kakaç, 1998).

Direct expansion evaporators are usually of the shell-and-tube type with the refrigerant inside the tubes, cooling the shell-side fluid (Figures 3.2 and 3.3). Two crucial items in the direct expansion shell and tube evaporators are the number of tubes (refrigerant passes) and the type of tubes.

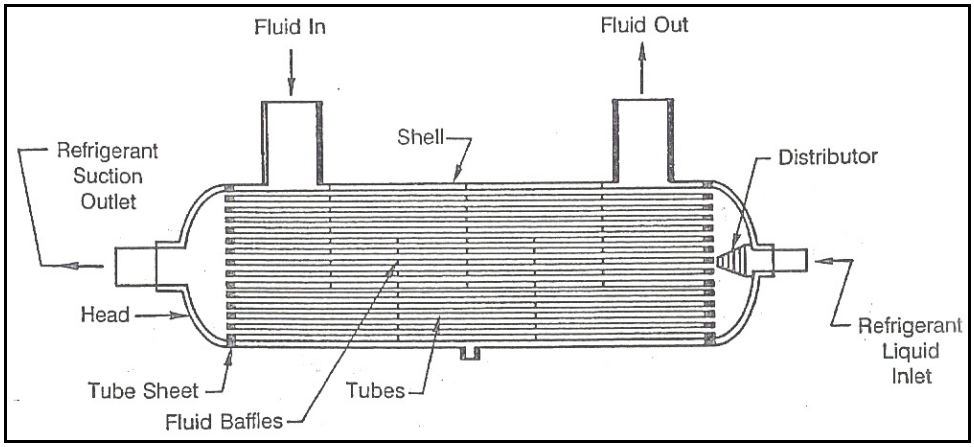

Figure 3.2 Direct (straight-tube type) expansion evaporator

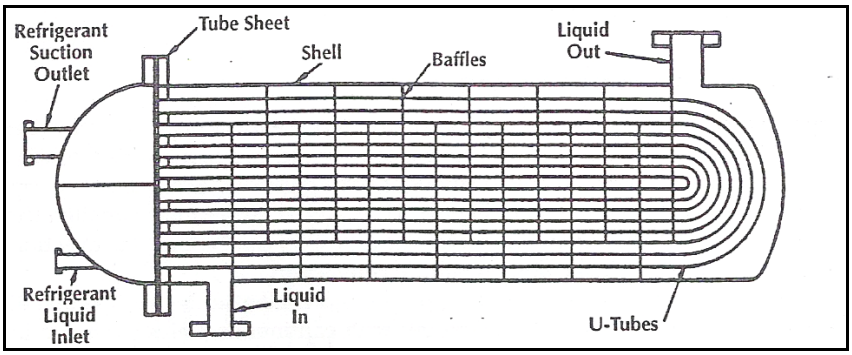

Figure 3.3 Direct (U-type) expansion evaporator

Another type is the flooded shell-and-tube evaporator that cools liquid flowing through tubes by transferring heat to the evaporating refrigerant on the shell side; the tubes are covered (flooded) with a saturated mixture of liquid and vapor (Figure 3.4).

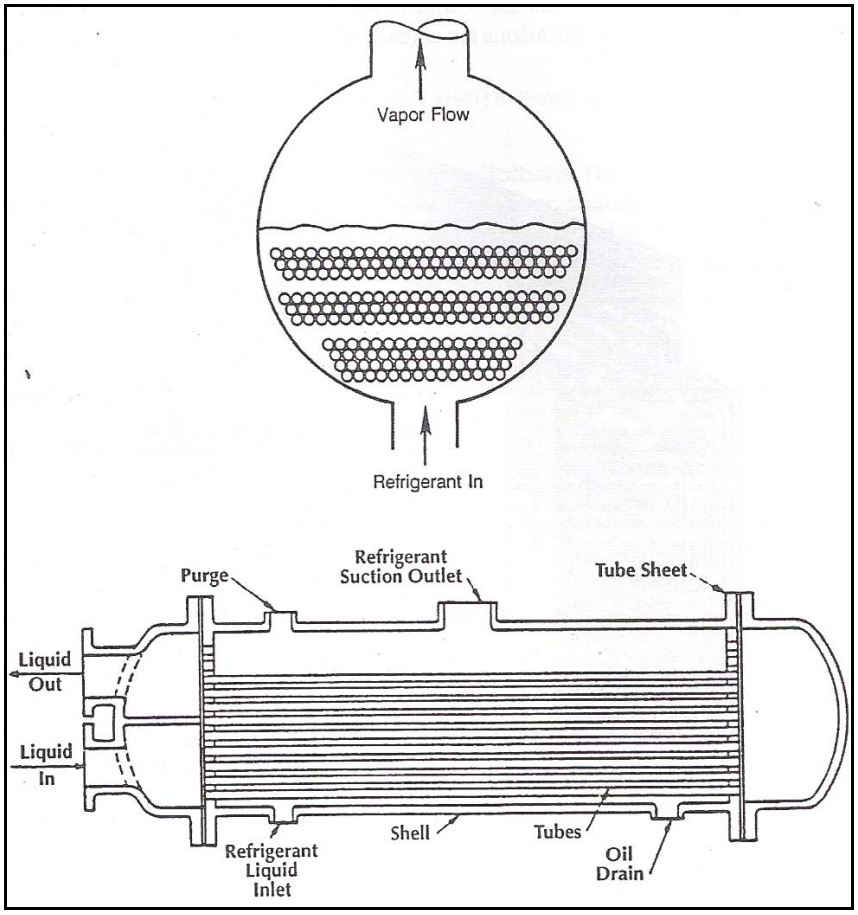

Figure 3.4 Flooded shell and tube evaporator (liquid cooler)

Baudelot evaporators, also used in industrial applications, are used for cooling a liquid to near its freezing point. The liquid is circulated over the outside of a number of horizontal tubes one above the other. The liquid is distributed uniformly along the length of the tube and flows by gravity to the tubes below. The cooled liquid is collected by a pan from which it is pumped back up to the source of heat and then to the cooler again (Figure 3.5).

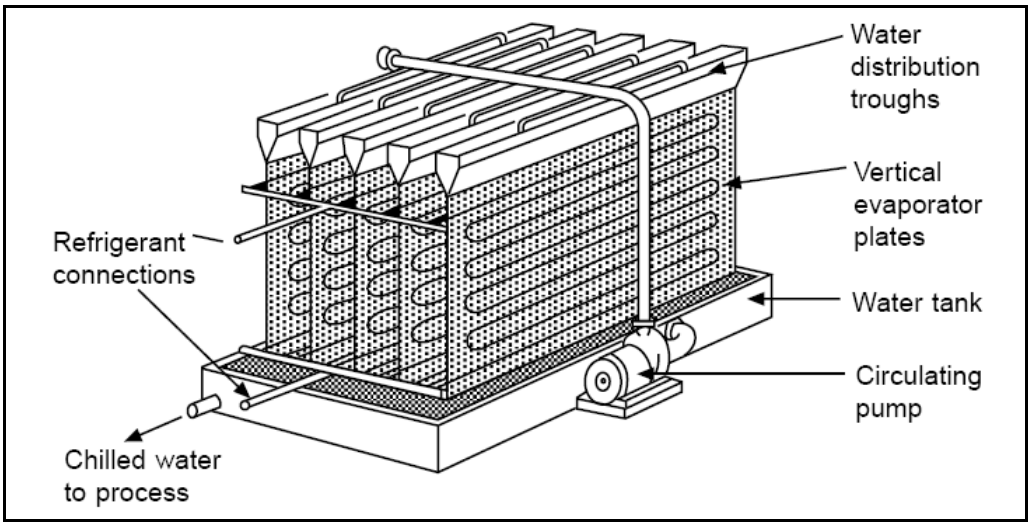

Figure 3.5 Baudelot evaporator

3.2 Air-Cooling Evaporators (Air Coolers)

The dry expansion coil is a type of air evaporator. It is the most popular and widely used air cooler. The refrigerant entering the coil is mostly liquid and as it passes through the coil picking up heat from the air outside the tubes, it evaporates and exists as mostly vapor. The typical dry expansion coils shown in Figures 3.6 and 3.7 are multicircuited (from 2 to 22 circuits) and fed by one expansion valve. The air cooler can be forced convection implementing the use of a fan, or can rely on natural convection (Kakaç, 1998).

The most common air-conditioning evaporator and condenser is the type that air flows over a circular tube bank that has been finned with continuous plates as shown in Figure 3.7; hence it is a plate fin and tube heat exchanger. The evaporating or condensing refrigerant flows through tubes that are mounted perpendicular to the air flow and arranged in staggered rows. The end views in Figure 3.7 show that the tubes can be connected and coiled to form any number of passes, rows, and parallel paths, hence the name evaporator and condenser coil. Evaporator coils use round tubes for the most part. Typical tube sizes representing a wide range of applications are outside diameter of 5/16, 3/8, 1/2, 5/8, 3/4, and 1 in. Oval tubes are also used for special applications. The fins and tubes are generally made of aluminum and copper respectively; however, sometimes both components are manufactured from the same

material. The fins are connected to the tubes by inserting the tubes into holes stamped in the fins and then expanding the tubes by either mechanical or hydraulic means.

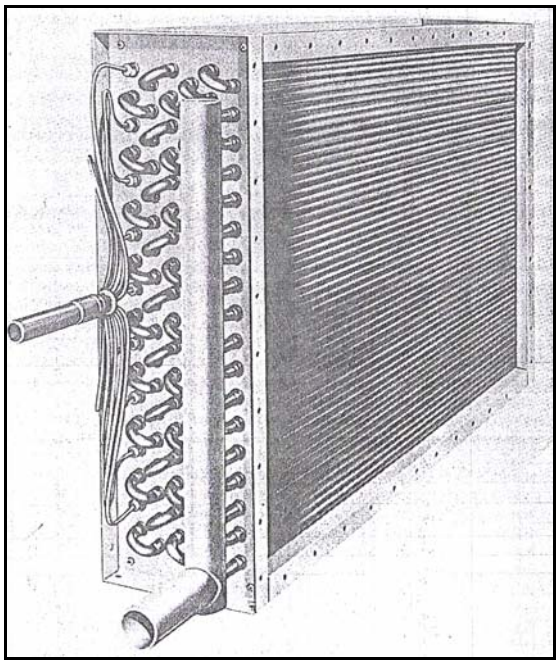

Figure 3.6 Dry expansion coil fin and tube bank for an air-conditioning system

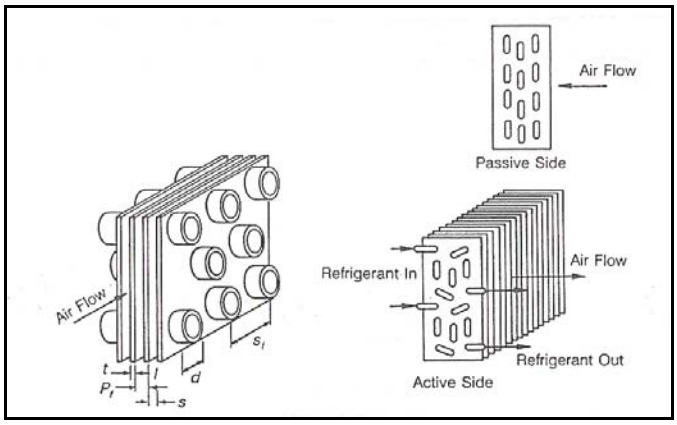

Figure 3.7 Dry expansion coil (air evaporator)

Most refrigeration and air-conditioning air coils, whether evaporators or condensers, use circular-finned tubes rather than plate fin and tubes (the exception is evaporators in automotive air-conditioning). The fin plates used on the air side can be flat or plain surfaces, standard or sine-wave corrugated surfaces, or louvered

surfaces. Examples of some of these fin surfaces are shown in Figure 3.8. The order presented represents increasing heat transfer performance; however, additional manufacturing effort is required to either deform or shape the surface or, in the case of louvering, to cut slits in the surface. It should also be noted that even though the heat transfer performance increases, the pressure drop on the air side, and, hence, required fan power, also increases. Several flat or plain surfaces used in refrigeration and air-conditioning applications are shown in Figure 3.9. Several wavy (corrugated and ripple) fin surfaces used in refrigeration and air-conditioning applications are shown in Figure 3.10. Several types of louvered and strip fins are shown in Figure 3.11 (Kakaç, 1991).

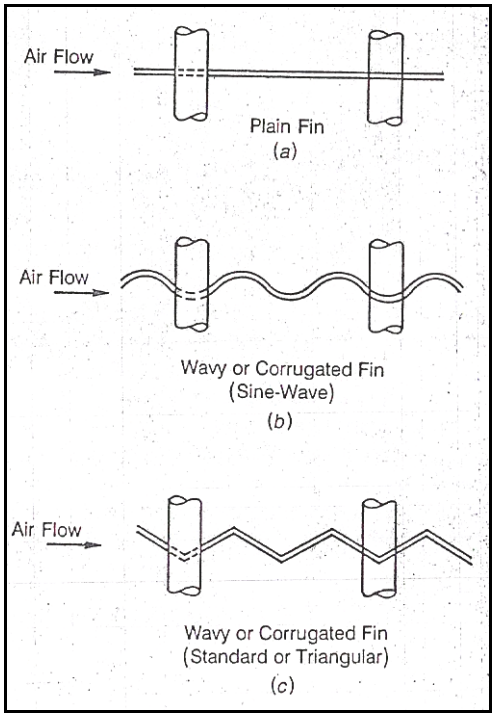

Figure 3.8 Comparison of several fin plates used on the air side

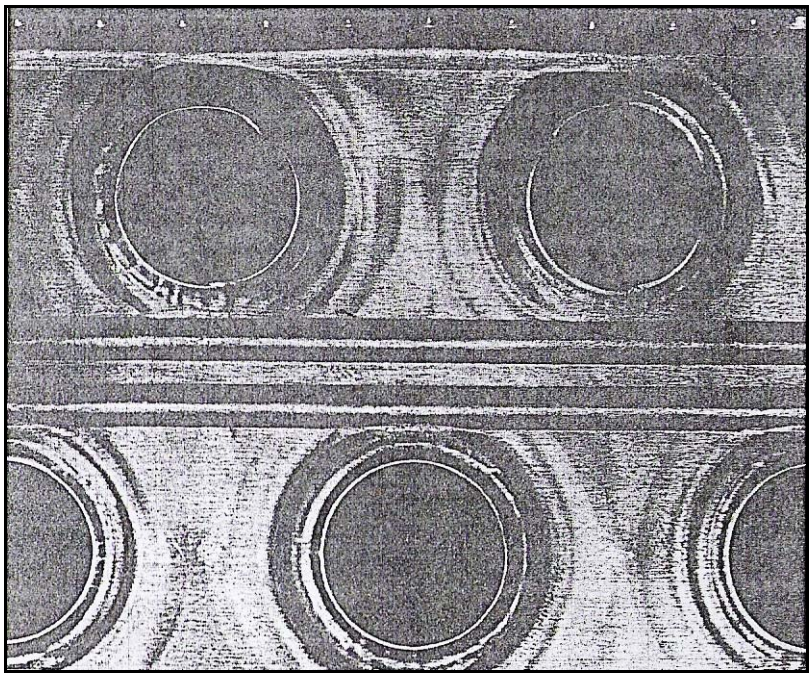

Figure 3.9 Plain (flat) fin surfaces used in refrigeration and air conditioning applications

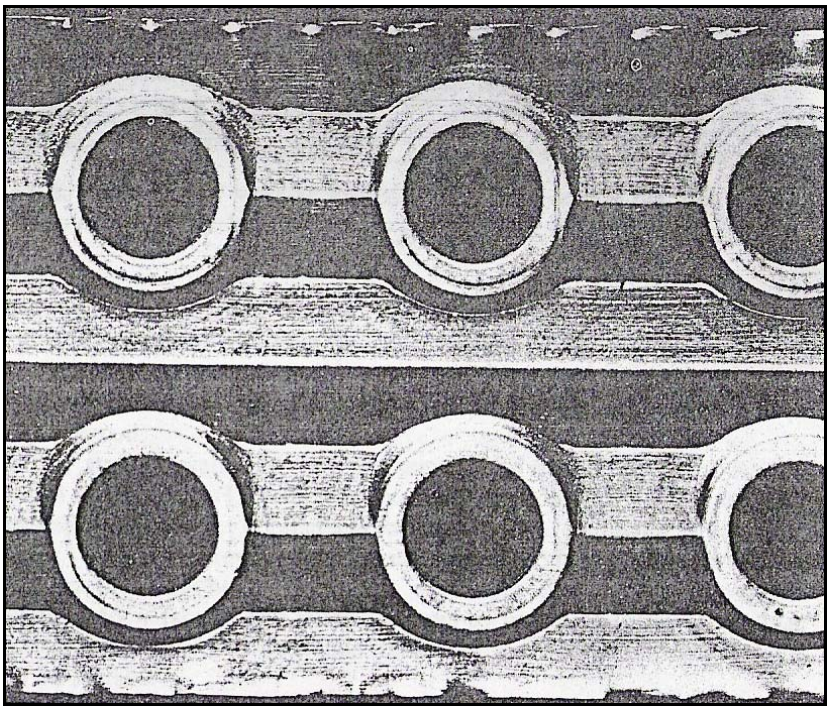

Figure 3.10 Wavy (corrugated and ripple) fin surfaces used in refrigeration and air-conditioning applications

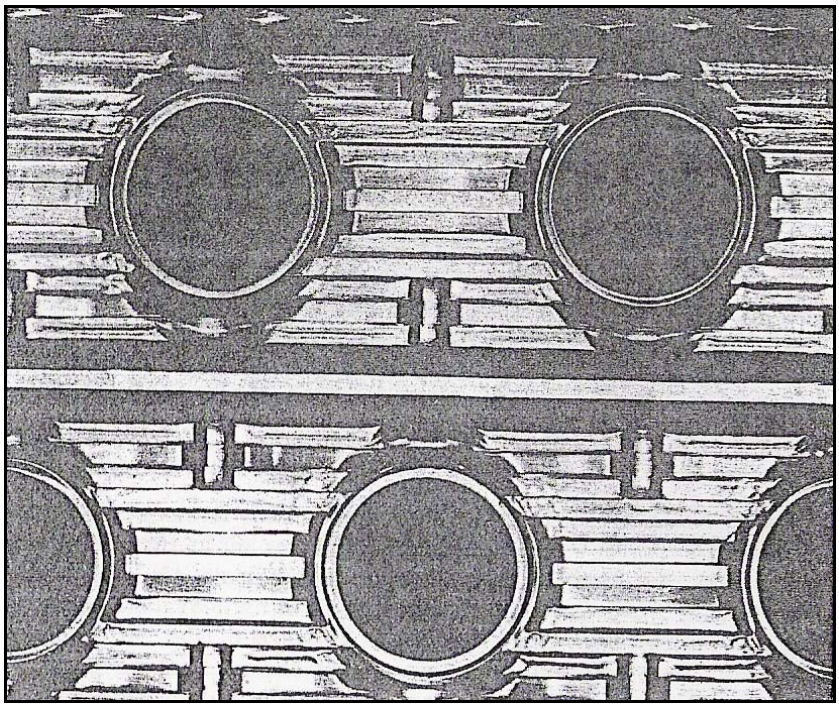

Figure 3.11 Louvered fins (also referred as strip fins, slot fins, and offset strip fins) used in refrigeration and air-conditioning applications

3.3 Plate Evaporators

Plate evaporators (Figure 3.12) are formed by cladding a tubular coil with sheet metal, welding together two embossed plates, or from aluminum extrusions. The extended flat face may be used for air cooling, for liquid cooling if immersed in a tank, or as a Baudelot cooler. The major use for flat plate evaporators is to cool a solid product by conduction, the product being formed in rectangular packages and held close between a pair of adjacent plates (Trott & Welch, 2000).

In the horizontal plate freezer (Figure 3.13a), the plates are arranged in a stack on slides, so that the intermediate spaces can be opened and closed. Trays, boxes or cartons of the product are loaded between the plates and the stack is closed to give good contact on both sides. When the necessary cooling is complete, the plates are opened and the product removed.

The vertical plate freezer (Figure 3.13b) is used to form solid blocks of a wet product, typically fish. When frozen solid, the surfaces are thawed and the blocks

pushed up and out of the bank. To ensure good heat transfer on the inner surface of the plates and achieve a high rate of usage, liquid refrigerant is circulated by a pump at a rate 5–12 times the rate of evaporation. If a plate evaporator is partially filled with brine (see Figure 3.12d) this can be frozen down while the plate is on light load, and the reserve of cooling capacity used at other times. The freezing point of the brine can be formulated according to the particular application and the plate can be made as thick as may be required for the thermal storage needed. The major application of this device is the cooling of vehicles. The plates are frozen down at night, or other times when the vehicle is not in use, and the frozen brine keeps the surface of the plate cold while the vehicle is on the road. The refrigeration machinery may be on the vehicle or static.

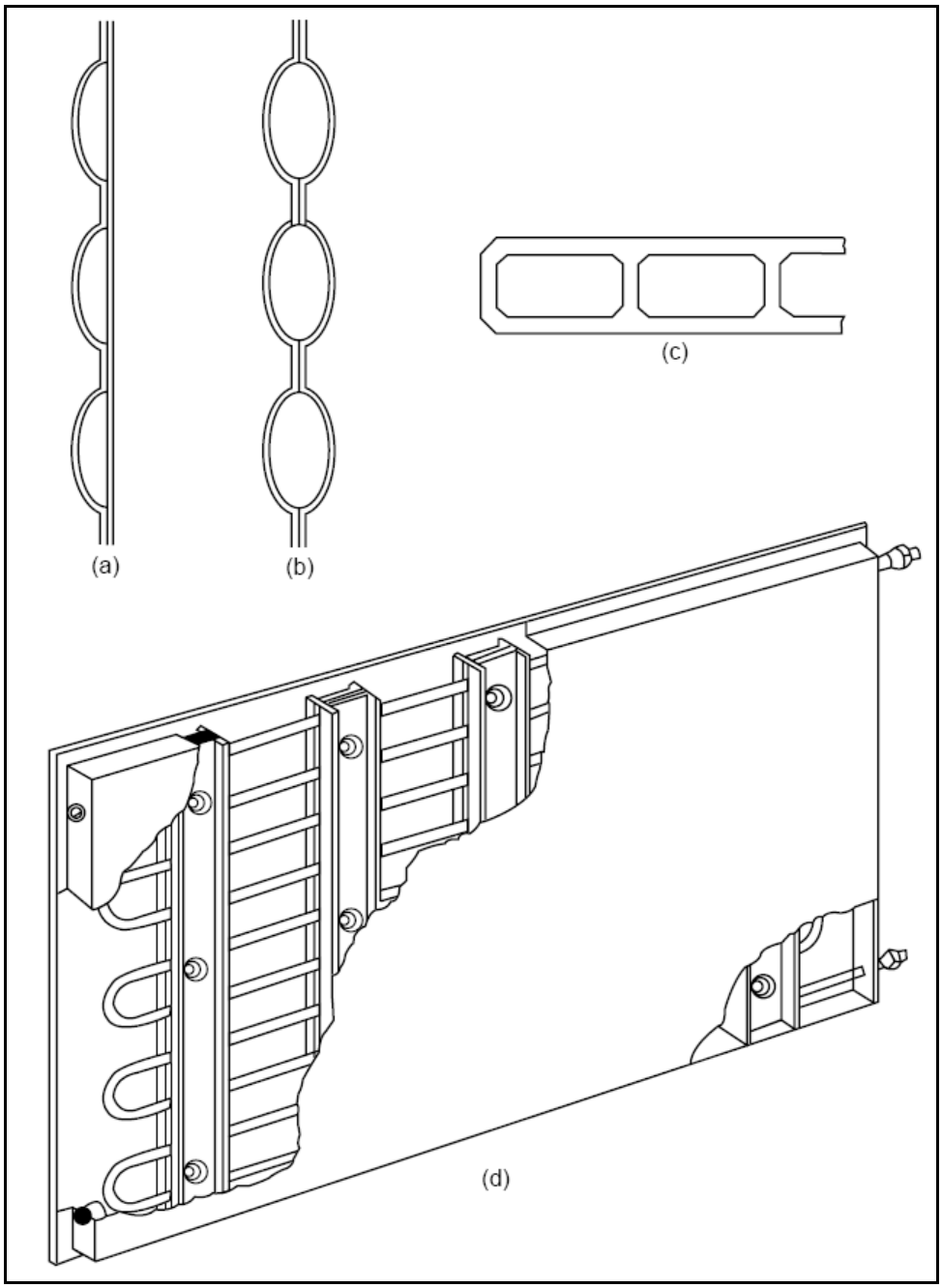

Figure 3.12 Plate evaporators. (a) Single embossed, (b) double embossed, (c) extruded, (d) holdover (brine filled).

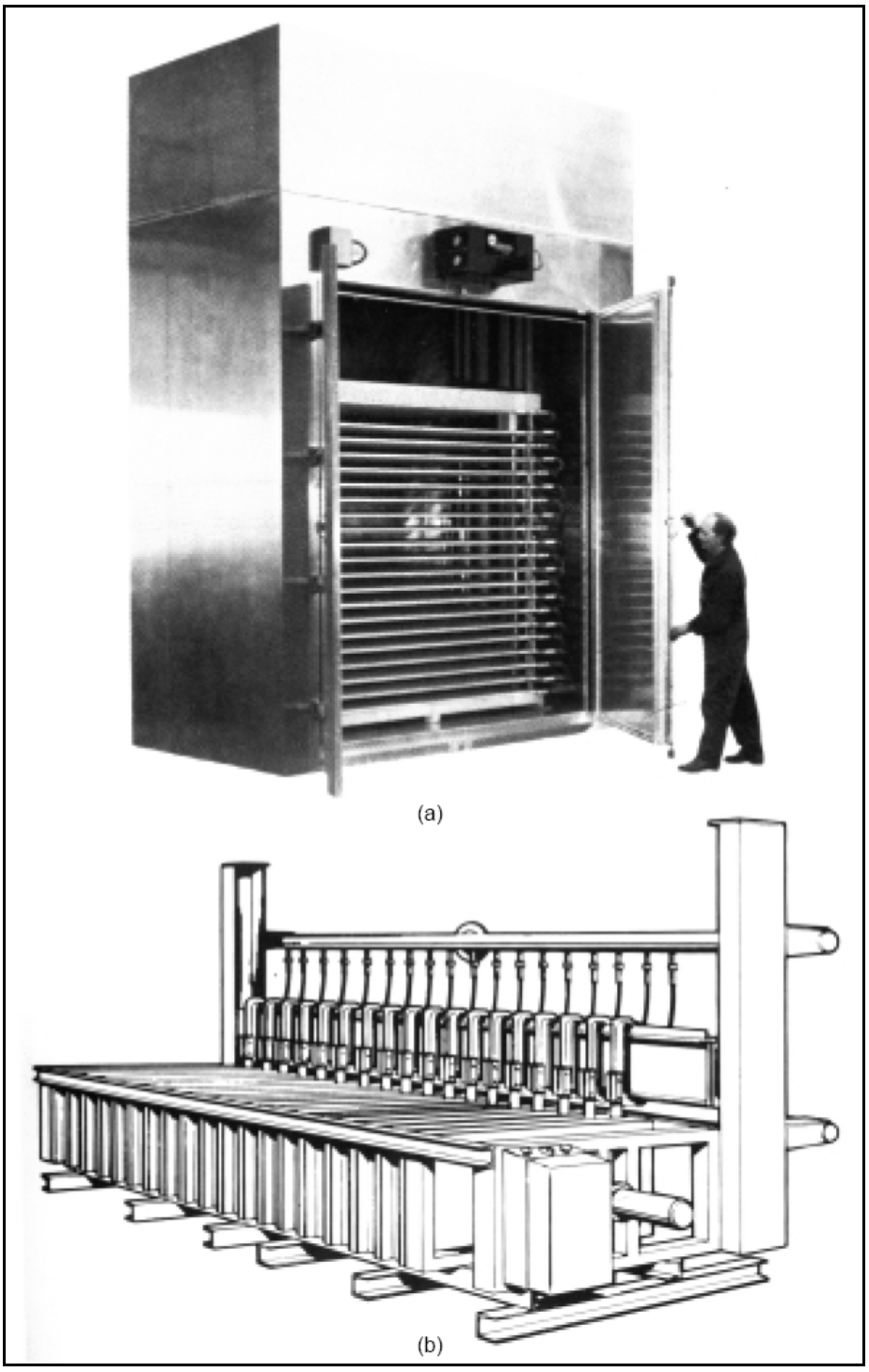

Figure 3.13 Plate freezers. (a) Horizontal, (b) vertical.

CHAPTER FOUR
INDUSTRIAL FOOD FREEZING SYSTEMS

Freezing is a food preservation method which slows the physical changes, chemical and microbiological activity that causes deterioration in foods. Reducing temperature extends useful storage life by slowing molecular and microbial activity in food. Most frozen food products are stored at -18 to -35°C, in fact every product has an individual storage temperature (ASHRAE, 2002).

Freezing reduces the temperature of a product from ambient to storage temperature and changes most of the water in the product to ice. Figure 4.1 shows the three phases of freezing: (1) cooling, which removes sensible heat, reducing the temperature of the product to the freezing point, (2) removal of the products latent heat or fusion changing the water to ice crystals, and (3) continued cooling below the freezing point, which removes more sensible heat, reducing the temperature of the product to the desired or optimum frozen storage temperature.

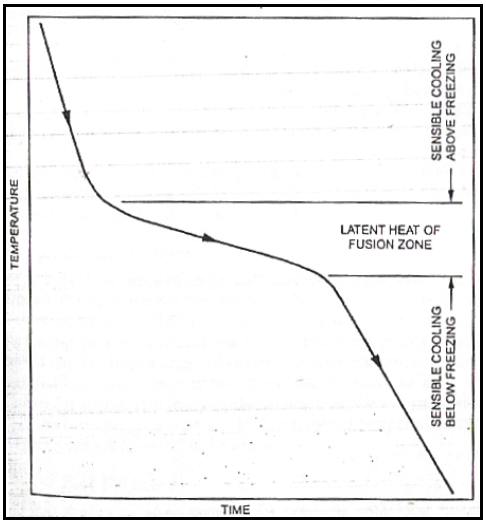

Figure 4.1 Typical freezing curve

The longest part of the freezing process is the removal of the latent heat of fusion as water turns to ice. Many food products are sensitive to freezing rate, which affects yield (dehydration), quality, nutritional value, and sensory properties. The freezing method and system selected can thus have substantial economic impact.

The following factors should be considered in the selection of freezing methods and systems for specific products: special handling requirements, capacity, freezing times, quality consideration, yield, appearance, first cost, operating costs, automation, space availability, and upstream/downstream processes.

4.1 Freezing Methods

Freezing systems can be grouped by their basic method of extracting heat from food products:

Blast freezing (convection): Cold air is circulated over the product at high velocity. The air removes heat from the product and releases it to an air/refrigerant heat exchanger before being recirculated.

Contact freezing (conduction): Food, packaged or unpackaged, is placed on or between cold metal surfaces. Heat is extracted by direct conduction through the surfaces, which are cooled by a circulating refrigerated medium.

Cryogenic freezing (convection and/or conduction): Food is exposed to an environment below -60°C, which is achieved by spraying nitrogen or liquid carbon dioxide into the freezing chamber.

Cryomechanical freezing (convection and/or conduction): Food is first exposed to cryogenic freezing and then finish-frozen through mechanical refrigeration.

4.2 Blast Freezers

Blast freezers use air as the heat transfer medium and depend on contact between the product and the air. Sophistication in airflow control and conveying techniques varies from crude blast freezing chambers to carefully controlled impingement freezers.

The earliest blast freezers consisted of cold storage rooms with extra fans and a surplus of refrigeration. Improved airflow control and mechanization of conveying techniques have made heat transfer more efficient and product flow less labor-intensive.

Although batch freezing is still widely used, more sophisticated freezers integrate the freezing process into the production line. This process-line freezing has become essential for large-volume, high-quality, cost-effective operations. A wide range of blast freezer systems are available, including

Batch	Continuous/Process-line
• Cold storage rooms	Straight belts (two-stage, multi pass)
• Stationary blast cells	Fluidized beds
• Push-through trolleys	Fluidized belts
	Spiral belts
	Carton (carrier)

4.3 Cold Storage Rooms

Although a cold storage room is not considered a freezing system, it is sometimes used for this purpose. Because a storage room is not designed to be a freezer, it should only be used for freezing in exceptional cases. Freezing is so slow that quality of most products suffers. The quality of the already frozen products stored in the room is jeopardized because the temperature of the frozen products may rise considerably due to the frozen products may rise considerably due to the excess refrigeration load. Also, flavors from the warm products may be transferred.

4.4 Stationary Blast Cell Freezing Tunnels

The stationary blast cell (Figure 4.2) is the simplest freezer that can be expected to produce satisfactory results for most products. It is an insulated enclosure equipped with refrigeration coils and axial or centrifugal fans that circulate air over

the products in a controlled way. Products are usually placed on trays, which are then placed into racks so that an air space is left between adjacent layers of trays. The racks are moved in and out of the tunnel manually using a pallet mover. It is important that the racks be placed so that air bypass is minimized. The stationary blast cell is universal freezer – almost all products can be frozen in a blast cell. Vegetables and all other products (e.g., bakery items, meat patties, fish fillets, and prepared foods) may be frozen either in cartons or unpacked and spread in a layer on trays. In some instances, this type of freezer is also used to reduce to -18°C or below the temperature of palletized, cased products that have previously been frozen through the latent heat of fusion zone by other means The flexibility of a blast cell makes it suitable for all small quantities of varied products; however, labor requirements is relatively high and product flow is slow.

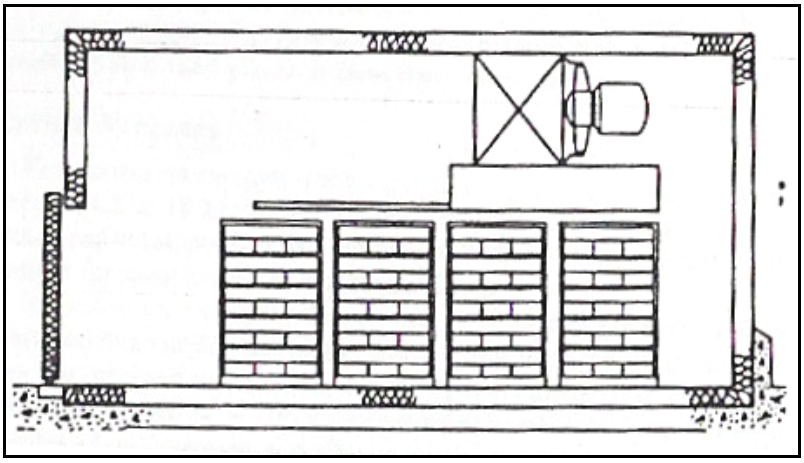

Figure 4.2 Stationary blast cell

4.5 Push-Through Trolley Freezers

The push-through trolley freezer (Figure 4.3), in which the racks are fitted with wheels, incorporates a moderate degree of mechanization. The racks are usually moved on rails by a pushing mechanism, which can be hydraulically or electrically powered. This type of freezer is similar to the stationary blast cell, except that labor costs and product handling time are decreased. This system is widely used to crust-freeze (quick-chill) wrapped packages or raw poultry and for irregularly shaped products.

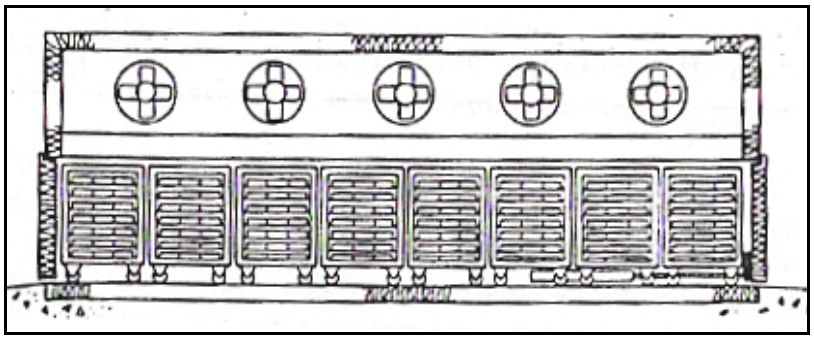

Figure 4.3 Push-through trolley freezer

4.6 Straight Belt Freezers

The first mechanized blast freezers consisted of a wire mesh belt conveyor in a blast room, which satisfied the need for continuous product flow. A disadvantage to these early systems was the poorly controlled airflow and resulting inefficient heat transfer. Current versions use controlled vertical airflow, which forces cold air up to through the product layer, thereby creating good contact with the product particles. Straight belt freezers are generally used with fruits, vegetables, French fried potatoes, cooked meat toppings (e.g., diced chicken), and cooked shrimp.

The principal design is the two-stage belt freezer (Figure 4.4), which consists of two mesh conveyor belts in series. The first belt initially pre-cools or crust-freezes an outer layer or crust to condition the product before transferring it to the second belt for freezing and sensible cooling to -18°C or below. To ensure uniform cold air contact and effective freezing, products should be distributed uniformly over the entire belt. Two-stage freezers are generally operated at -10° to -4°C refrigerant temperature in the pre-cool section and at -32 to -40°C in the freezing section. Capacities range from 0.9 to 18 tones of product per hour, with freezing times from 3 to 50 min.

When products to be frozen are hot (e.g., French fries from the fryer at 80 and 95°C), another cooling section is added ahead of the normal pre-cooling section. This section supplies either refrigerated air at approximately 10°C or filtered ambient air

to cool the product and congeal the fat. Refrigerated air is preferred because filtered ambient air has greater temperature variations and may contaminate the product.

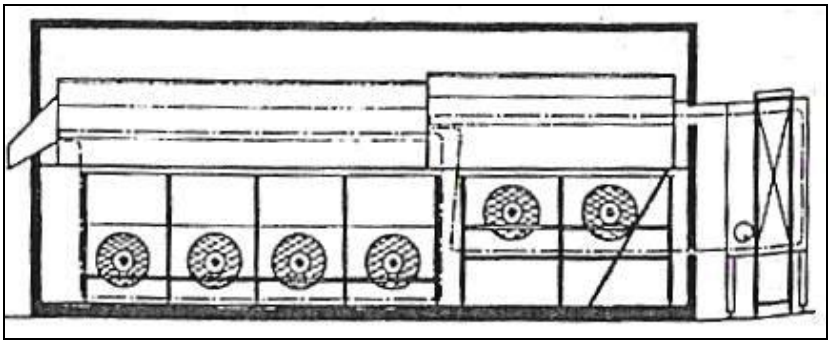

Figure 4.4 Two-stage belt freezer

4.7 Multipass Straight Belt Freezers

For larger products with longer freezing times (up to 60 min) and higher capacity requirements (0.5 to 5.4 tones), a single straight belt freezer would require a very large floor space. Required floor space can be reduced by stacking belts above each other to form either (1) a single-feed / single-discharge multipass system (usually three passes) or (2) multiple single-pass systems (multiple infeeds and discharges) stacked one on top of the other. The multipass (triple-pass) arrangement (Figure 4.5) provides another benefit in that the product, after being surface frozen on the first (top) belt, may be stacked more deeply on the lower belts. Thus, the total belt area required is reduced as is the overall size of the freezer. However, this system has a potential for product damage and product jams at the belt transfers.

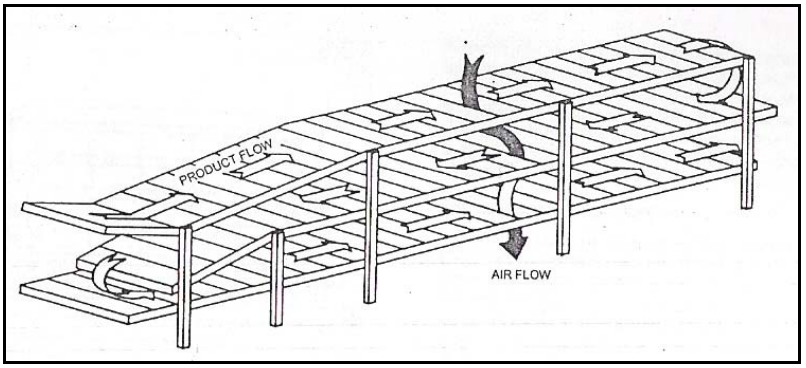

Figure 4.5 Multipass, straight belt freezer

4.8 Fluidized Bed Freezers

This freezer uses air both as the medium of heat transfer and for transport; the product flows through the freezer on a cushion of cold air (Figure 4.6). This design is well suited for small, uniform-sized particulate products such as peas and diced carrots.

The high degree of fluidization improves the heat transfer rate and allows good use of floor space. The technique is limited to well-dewatered products of uniform size that can be readily fluidized and transported through the freezing zone. Because the principle depends on rapid crust-freezing of the product, the operating refrigerant temperature must be -40 °C or lower. Fluidized bed freezers are normally manufactured as packaged, factory-assembled units with capacity ranges of 0.9 to 4.5 tones/h. The particulate products generally have freezing time of 3 to 11 min.

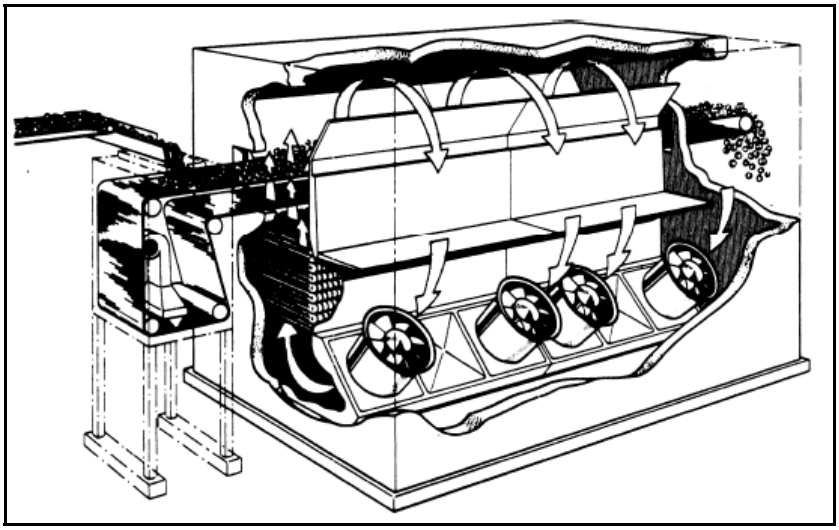

Figure 4.6 Fluidized bed freezer

4.9 Fluidized Belt Freezers

A hybrid of the two-stage belt freezer and the fluidized bed freezer, the fluidized belt freezer has a fluidizing section in the first belt stage. An increased air resistance is designed under the first belt to provide fluidizing conditions for wet incoming product, but the belt is there to help transport heavier, less uniform products that do

not fluidize fully. Once crust-frozen, the product can be loaded deeper for greater efficiency on the second belt. Two-stage fluidized belt freezers operate at -34 to -37 °C refrigerant temperature and in capacity ranges from 0.9 to 14 tones/h.

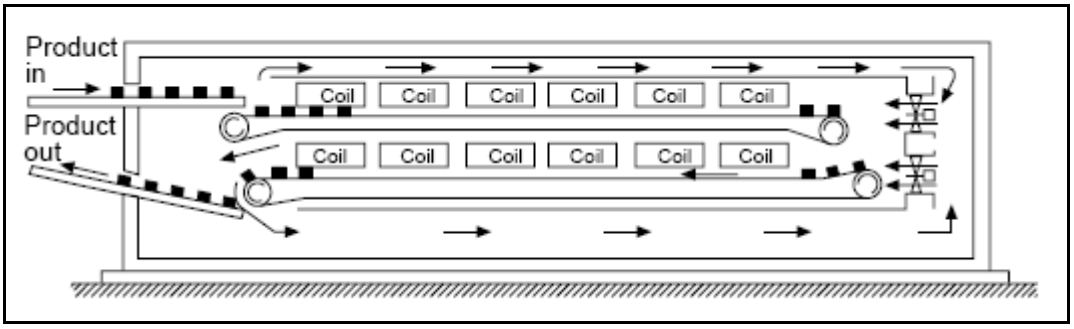

Figure 4.7 Fluidized belt freezer

4.10 Spiral Belt Freezers

This freezer is advantageous for products with long freezing times (generally 10 min to 3 h), and for products that require gentle handling during freezing. An endless conveyor belt that can be bent laterally is wrapped cylindrically, one tier below the last; this is a configuration that requires minimal floor space for a relatively long belt. The original spiral belt principle uses a spiraling rail system to carry the belt, while more recent designs use a property self-stacking belt requiring less overhead clearance. The number of tires in the spiral can be varied to accommodate different capacities. In addition, two or more spiral towers can be used in series for products with long freezing times. Spiral freezers are available in arrange of belt widths and are manufactured as packaged, modular and field-erected models to accommodate various upstream processes and capacity requirements.

Airflow varies from open, unbaffled spiral conveyors to flow through extensive baffling and high-pressure fans horizontal air-flow is applied to spiral freezers (Figure 4.8) by axial fans mounted along one side. The fans blow air horizontally across the spiral conveyor with minimal baffling limited to two portions of the spiral circumference rotation of the cage and belt produces a rotisserie effect, with product moving past the high-velocity cold air near the discharge, aiding in uniform freezing.

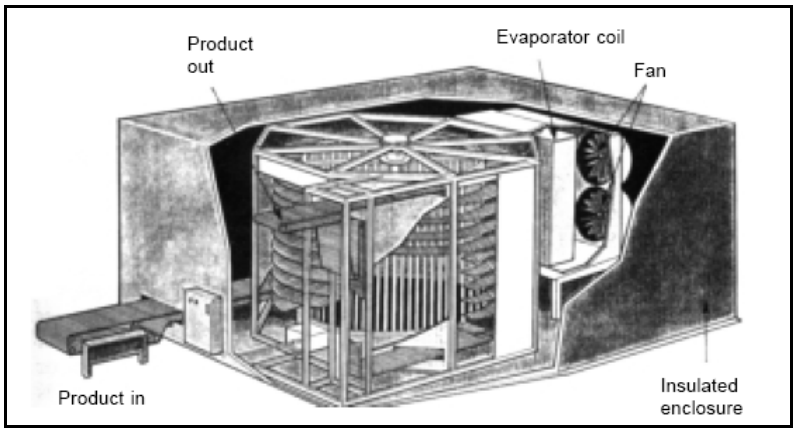

Figure 4.8 Horizontal airflow spiral freezer

Several property designs are available to control air flow. One design (Figure 4.9) has a mezzanine floor that separates the freezer into two pressure zones. Baffles around the outside and inside of the belt form and air duct so that air flows up or down around product as the conveyor moves the product. The controlled air flow reduces freezing time for some products.

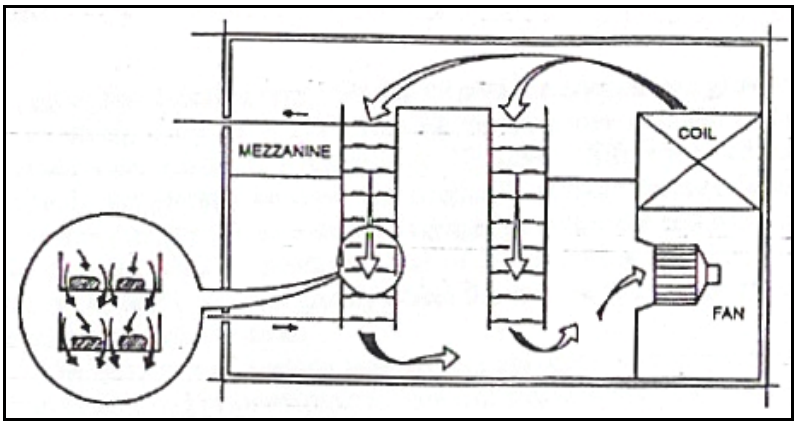

Figure 4.9 Vertical airflow spiral freezer

Another design (Figure 4.10) splits the air flow so that the coldest air contacts the product both as it enters and as it leaves the freezer. The surface heat transfer and freeze the surface more rapidly, which may reduce product dehydration.

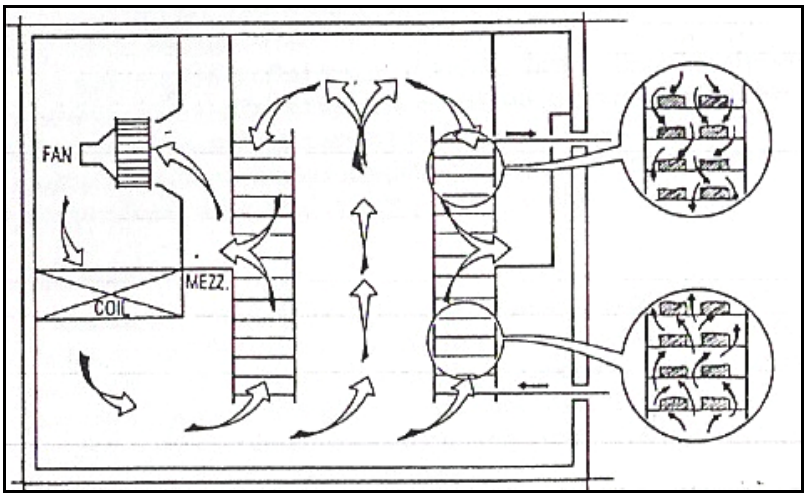

Figure 4.10 Split airflow spiral freezer

Typical products frozen in spiral belt freezers include raw and cooked meat patties, fish fillets, chicken portions, pizza, and a variety of packaged products. Spiral freezers are available in a wide range of capacities, from 0.5 to 5.4 tones/h. They dominate today's frozen food industry and account for the majority of unpackaged non particulate frozen food production.

4.11 Impingement Freezers

In this design (Figure 4.11), cold air flows perpendicular to product's largest surfaces at a relatively high velocity. Thousands of air nozzles with corresponding return ducts are mounted above and below the conveyors. The air flow constantly interrupts the boundary layer that surrounds the product, enhancing the surface heat transfer rate. The technique may therefore reduce the freezing time of products with large surface-two-mass ratios (thin hamburger patties, for example). Impingement freezers are designed with single-pass or multi-pass straight belts. Freezing times are 1 to 4 min. Applications is limited to thin products (less than 25 mm thick).

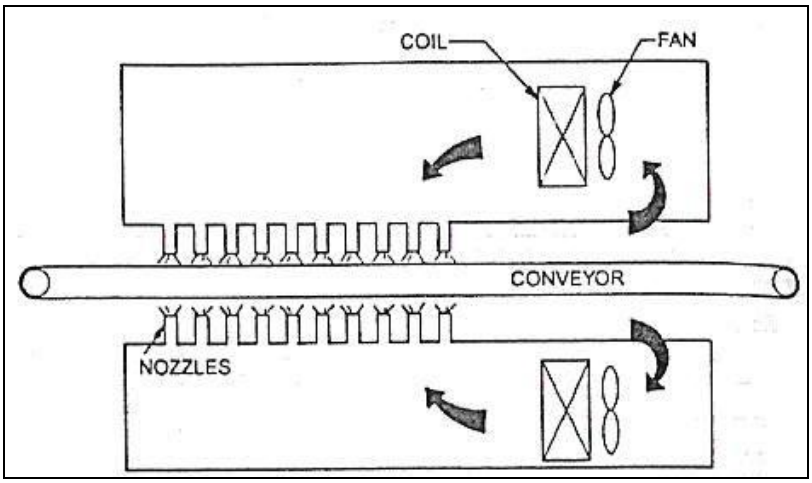

Figure 4.11 Impingement freezer

4.12 Carton Freezers

The carton (or carrier) freezer (Figure 4.12) is a very high capacity freezer (4.5 to 18 tones/h) for medium to large cartons of such products as red meat, poultry, and ice-cream. This units are also used as chillers for meat products and block cheese.

In the top section of the freezer a row of loaded product carriers is pushed toward the rear of the freezer, while on the lower section they are returned to the front. Elevating mechanisms are located at both ends. A carrier is similar to a book case with shelves. When it is indexed in the loading / discharge end of the freezer, the already frozen product is pushed of each shelf one row at a time on to a discharge conveyor. When the carrier is indexed up this shelf aligns with the loading station, when new products are continuously pushed onto the carrier before it is moved once again to the rear of the freezer. Refrigerated air is circulated over the cartons by forced convection.

Computerized systems are now available to control shelf loading, unloading, and movement to freeze and/or cool products with different retention times in the same unit simultaneously. This increased flexibility is particularly useful and cost-effective where different sizes and cuts are prevalent (e.g., red meat and poultry products).

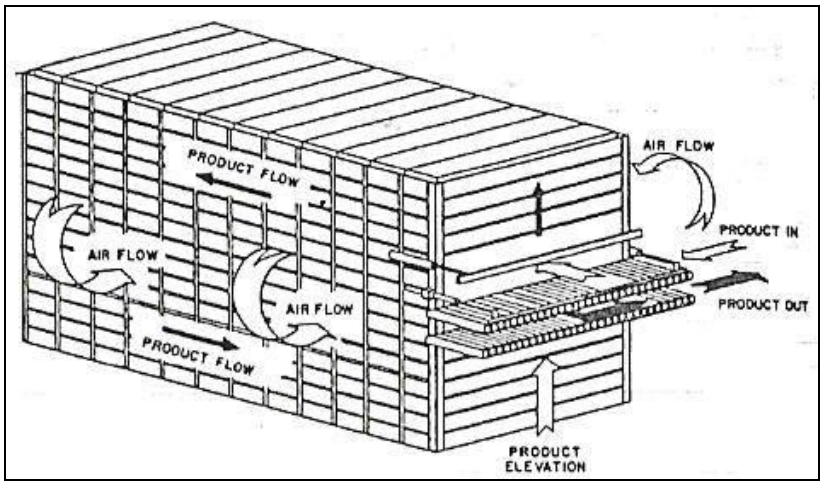

Figure 4.12 Carton (carrier) freezer

CHAPTER FIVE
AIR BLAST FREEZERS

5.1 Air Blast Freezer

Air blast freezers are not readily available off the shelf as packaged units. They usually have to be tailor-made to suit individual requirements (Graham, 2001).

The two most common types of freezer in use in the fish industry are the plate freezer and the air blast freezer. The plate freezer usually takes up less space and requires less power than a blast freezer with the same output, but its use is normally confined to freezing packs of uniform thickness with smooth flat surfaces.

The big advantage of the blast freezer is its versatility; it can cope with a variety of irregularly shaped products. Wherever there is a wide range of shapes and sizes to be frozen, the blast freezer is the better choice. However, because of the versatility of the blast freezer, it is often difficult for the potential user to specify precisely what work he expects it to do and, once it is installed, it is all to easy to use it inefficiently.

5.2 Types of Air Blast Freezer

There are considerable numbers of designs and arrangements of air blast freezer, but there are two main types. In one, the product moves through the freezer during the process; this is a continuous freezer. In the other the product remains stationary; this is a batch freezer.

In the continuous freezer the product is carried through on trucks or on a conveyor; this method is most suited to mass production of standard packs with similar freezing times. When trucks are used they are normally operated on a semi-batch principle; the trucks remain stationary except when a fresh truck is pushed into one end of the tunnel, thus moving the others along to release a finished one at the other end.

Continuous freezers can be further divided into series-flow and cross-flow types. In a series-flow freezer the air flow is in line with the trucks or conveyor; in a cross-flow freezer the air flow is across the line of movement of the product.

In a series-flow freezer, normally only one fan and one cooler are used, and the product is moved in the opposite direction to the air flow; thus the coldest air meets the coldest, or nearly frozen, product at the exit end. In this type of freezer it is essential to switch off the fan during the short period of loading and unloading so that warm air is not drawn into the freezer. A switch should be located near the input door, or contact switches should be fitted to both doors so that the fan is off when either door is open.

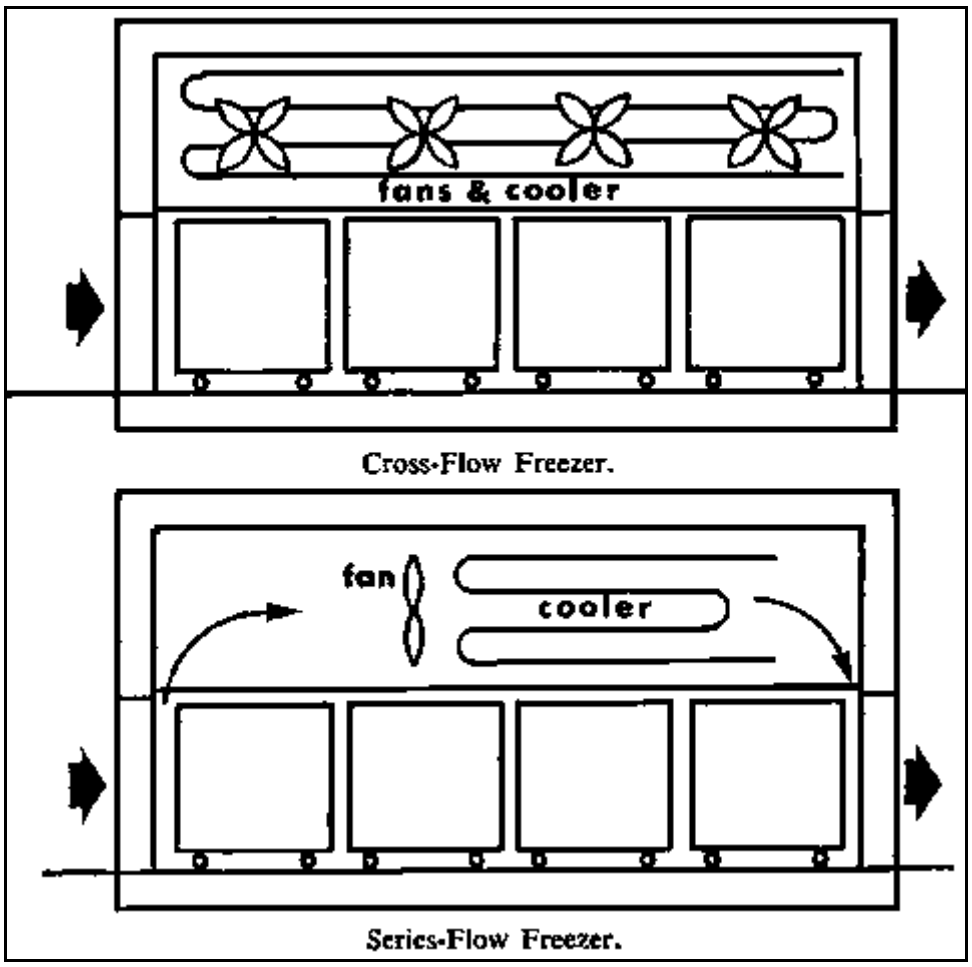

Figure 5.1 Typical freezer arrangements

In the cross-flow freezer there are usually several fans and often more than one cooler unit; trucks entering or leaving the freezer interfere very little with the air flow. Where a conveyor is used with permanent flap openings at loading and discharge ends, the cross-flow arrangement is essential. A slight disadvantage of a cross-flow tunnel is that the cooler nearest the entrance has the most work to do and therefore accumulates more frost than the other coolers. To avoid having to defrost it more often than the others, the entrance cooler can be made with more widely spaced fins.

The batch freezer is more flexible and is used when a variety of products is to be frozen, often at the same time, on individual trolleys or pallets.

When the batch freezer is used for mixed loads in this way it requires close supervision to maintain maximum output without overloading.

The choice of type of freezer depends very much on the kinds and quantities of product to be frozen, and on whether single-shift or round-the-clock operation is contemplated. The precise style and layout of the freezer will often depend on the space available and on its location in relation to other steps in the process, such as filleting, packing and cold storage.

The final choice of freezer is therefore an individual one which can be made only when the product, process and location have been examined in detail.

5.3 Air Circulation

In a well designed and correctly operated air blast freezer, the air speed over the fish should be about the same everywhere in the freezer, thus ensuring uniform freezing of the product. It is very important that the tunnel be designed so that the resistance to the air flow created by the products to be frozen is spread evenly over the whole cross section of the tunnel. The spaces between the trays should all be the same and the gap above, below and at the sides of the truck should be as small as possible; otherwise the air flow will take the path of least resistance and freezing will be inefficient.

Air has a low heat capacity, and still air is a poor conductor of heat so that a fairly high air speed is necessary. However, high air speeds mean powerful fans and these generate heat which has to be removed by the refrigeration machinery. Consequently, there is little to be gained by using a very high air speed, and a speed range of 3 to 6 m/s has been found to be most suitable for economic freezing. An average design air speed of about 5 m/s over the product, with good air distribution across the working section, should ensure air speeds within the recommended range over all the fish in the freezer.

Occasionally, however, higher air speeds may be justified if space is limited and a shorter freezing time is necessary in order to comply with a code of practice or to make freezing time fit the working period.

The air as it moves across the fish will rise in temperature, because it is taking heat away from the product. The extent to which the air is allowed to warm will directly influence the size and power of the fans. When the rise in temperature is too great, the fish at the downstream end of the freezer will encounter much warmer air than the fish at the upstream end, and therefore will freeze more slowly. On the other hand, when the design temperature rise is very small, and when the freezer layout and the spacing of the trays is not perfect, unnecessarily powerful fans may be needed to maintain the required air speed.

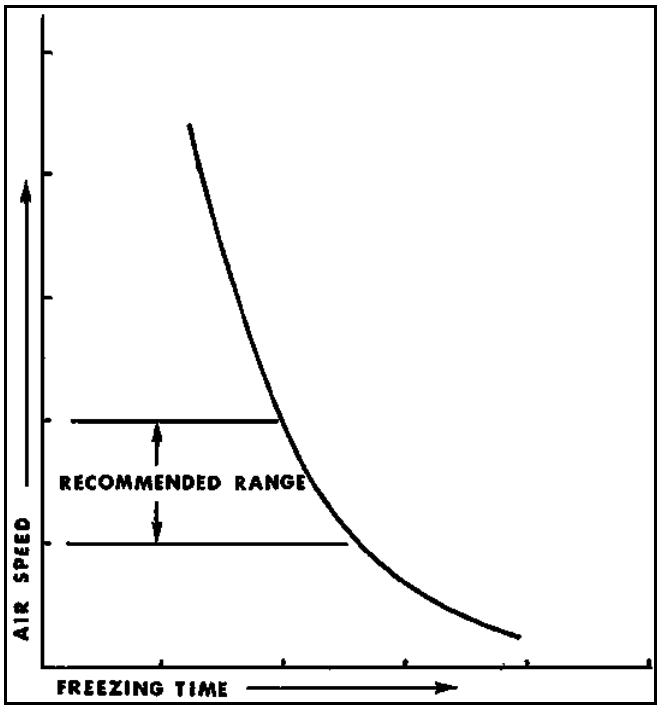

Figure 5.2 Variation of freezing time with air speed

Even in a properly designed layout the fan heat load on the refrigeration system will be about 25 to 30% of the load imposed by the product. The fan load therefore can be considerable and, in extreme cases with a poor layout of freezer, it can be as high as the product load itself.

The rise in air temperature that can be tolerated depends very much on the total freezing time. When the freezing time is 20 min, a difference of 2 min, which is 10% of the total time, between the coldest and the warmest fish may not be important. On the other hand, when the freezing time is 10 h, a 10% difference means 1 h; such a big difference in freezing time between fish in the same batch may not be acceptable.

No hard and fast rule can be made about permissible rise in temperature of the air during its passage over the fish. As a general guide, however, an average rise of 1,2 - 3°C during the freezing period is usually reasonable. With air entering the freezing space at -35°C, such a rise will give a difference in freezing time between the best and the worst packs in the batch of 3-8% of the total time. In practice, the rise in temperature will be higher at the start of freezing than at the end; the suggested permissible rise given is an average over the whole freezing time.

5.3.1 Evaporator and Product Locations in a Cold Room

Four standard evaporator constructions and product locations in a cold room are shown in Figure 5.3 to 5.6 (Şahin, 2005).

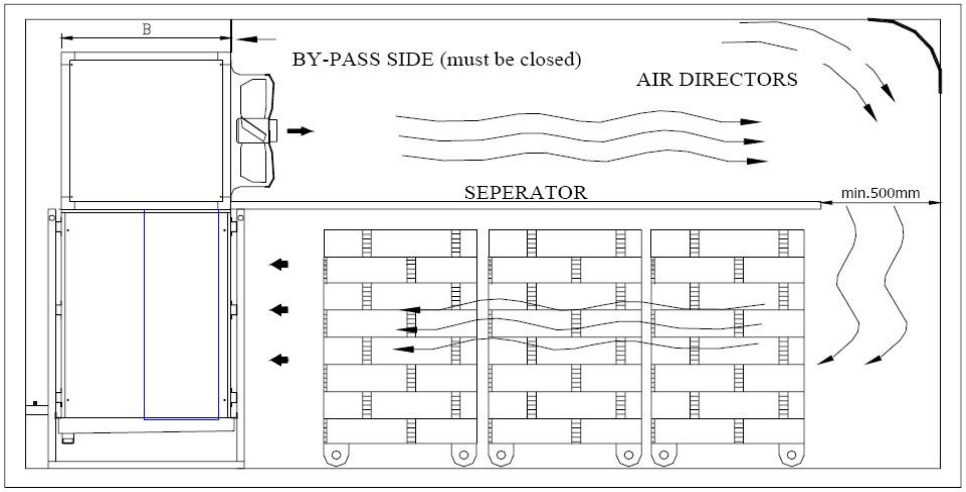

Figure 5.3 Floor unit mounting

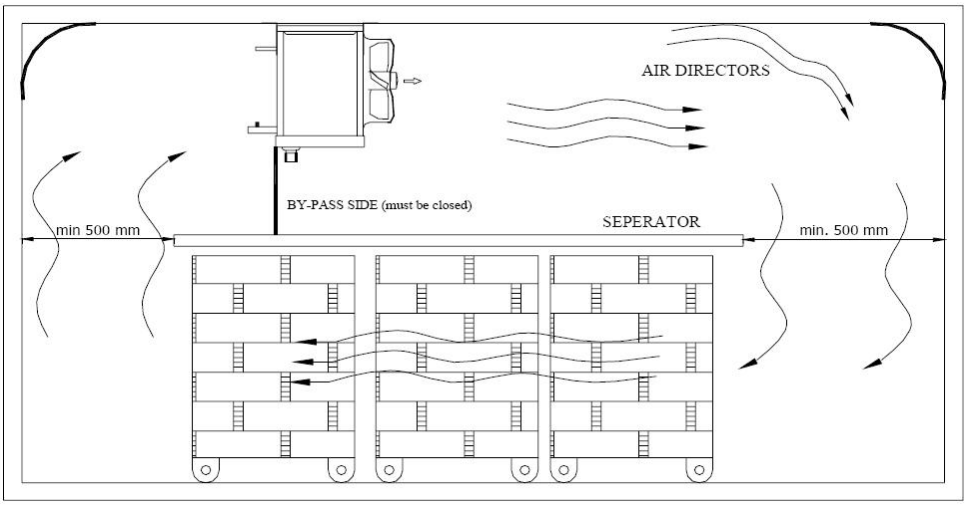

Figure 5.4 Ceiling unit mounting

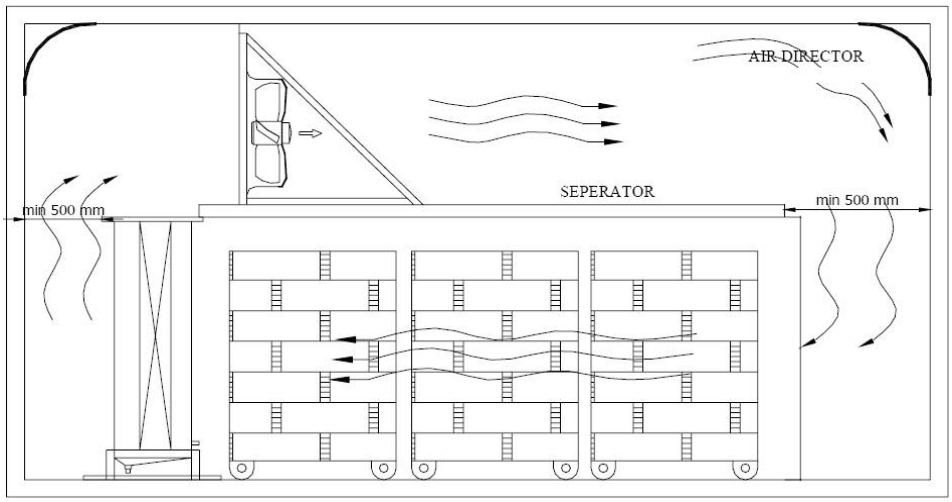

Figure 5.5 Separate fan-coil unit mounting

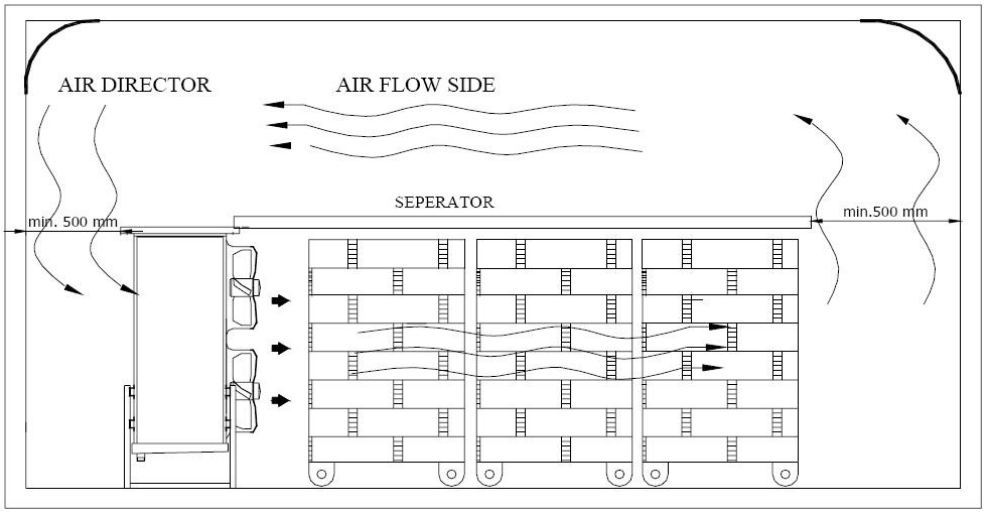

Figure 5.6 Compact unit mounting

Evaporator must be located in short edge of the cold room; by this method intended air velocity can be obtained by less fan power. The same amount of product can be frozen with two applications both: one of them is the narrow edge, needs 8.5 kW fan power; the other one is the wide edge, needs 12.8 kW fan power. Extra cooling load and extra expenses occurs for the second application. Two diagrammatic arrangements for freezing 1 ton of fish in four pallets are shown in Figure 5.7.

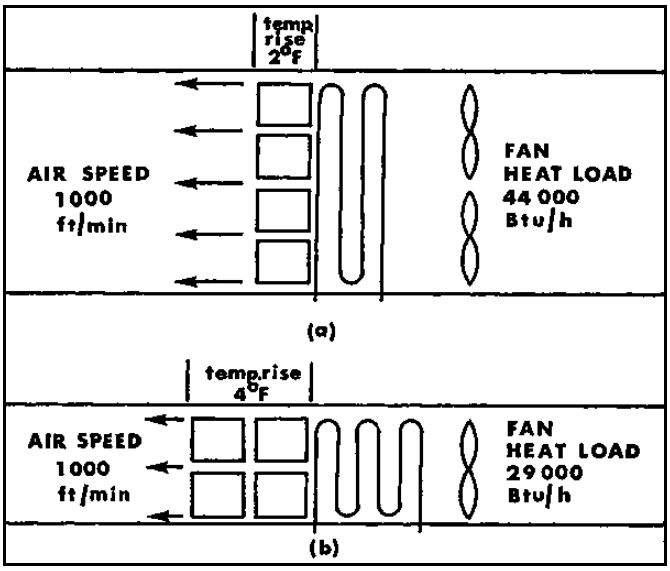

Figure 5.7 Two diagrammatic arrangements for freezing 1 ton of fish in four pallets

a)Tunnel with large cross-section - high fan load

b)Tunnel with reduced cross-section - reduced fan load

5.4 Air Temperature

The air temperature in an air blast freezer should be low enough to freeze the fish as quickly as the code of practice recommends. In addition the air has to be cold enough to reduce the temperature of the frozen fish to that of the cold store; in Britain the accepted temperature for the storage of frozen fish is -29 °C. Therefore the air in the freezer has to be lower than -29°C and, in many commercial blast freezers, an air temperature of -35°C is found to be practicable.

The lower the air temperature, the shorter will be the freezing time, but the cost of removing the heat will be greater. A refrigeration compressor can be compared with a pump taking water from a well; the deeper the well, the greater the cost of taking out a given quantity of water. In the same way, when you lower the operating temperature of a refrigeration system, more power, and therefore more money, is needed to transfer the same amount of heat from the fish, even although it does so more quickly. Therefore, the freezer should not be run at a temperature any lower

than is necessary to give the required freezing time and final temperature of the product. Exceptionally it may be necessary to use an air temperature lower than -35°C in order to quick freeze very thick fish for example, or to shorten the freezing time to fit a particular timetable in spite of extra cost.

5.5 Freezing Time

The freezing time of all the products likely to be handled must be known before a freezer can be specified. The freezing time and the output of the freezer are the two main factors that determine the dimensions of the freezer and the capacity of the coolers and the refrigeration machinery.

There is no simple formula for estimating the freezing time of a given product. Exceptionally it is possible to predict a freezing time for an unwrapped fish product of regular shape, but in practice it is usually necessary either to measure the freezing time by running trials with the product under the desired operating conditions or to refer to known freezing times for similar products. This important piece of information must be known before attempting to design a suitable freezer.

5.6 Freezer Capacity

In an air blast freezer, the shape and size of the freezing space, the size of the coolers and the refrigeration machinery have to be matched to handle a given product load, but because the blast freezer is versatile, a range of products can be accommodated, having different shapes and sizes and different freezing times; it is therefore difficult to predict accurately the most suitable design and to avoid misuse of the freezer once it is in operation.

As an example, a blast freezer is designed to freeze two tons an hour of a product that takes four hours to freeze. Therefore the freezer must have room for eight tons of that product at a time to maintain the designed output, and the cooler and refrigeration machinery will be designed to cope with two tons an hour. But, if the same freezer is then loaded with eight tons of a differently shaped product that takes only two hours to freeze, the new freezing rate is four tons an hour and the

refrigeration equipment is greatly overloaded. On the other hand, when the freezer is loaded with eight tons of a product that takes eight hours to freeze, the freezing rate is down to one ton an hour and the refrigeration equipment is then running at very much below its design capacity. Table 5.1 shows these three different cases.

Thus a freezer designed specifically for handling product A can be misused whenever it is fully loaded with products B or C. When a freezer has to handle all three products, it should be made roomy enough to house 16 tons at a time of product C, but not more than eight tons of A or four tons of B must be put in that space at any one time. Then, and only then, would the freezing equipment be operating at its design capacity of two tons an hour for all three products, but with more frequent reloading for the faster freezing products.

Table 5.1 Loading an air blast freezer

Product	**Product weight in freezer (tons)**	**Product freezing time (hours)**	**Freezing rate demanded (tons/hour)**	**Designed freezing rate (tons/hour)**	**Remarks**
A	8	4	2	2	Freezer correctly loaded
B	8	2	4	2	Freezer overloaded
C	8	8	1	2	Freezer under loaded

Given the freezing time of a particular product, and the weight of it to be loaded into the freezer, it is then possible to work out how much heat the refrigeration plant has to remove from it in that time to freeze it quickly to the recommended storage temperature. Table 5.2 shows the heat to be removed from unprocessed white fish with various initial temperatures.

Table 5.2 Heat to be removed from fish

Initial temperature (°C)	**Storage temperature (°C)**	**Heat to be removed (kW/kg)**
1.67	-28.9	85.6
4.44	-28.9	88.2
6.67	-28.9	91.1
10.0	-28.9	94.0
12.8	-28.9	96.6
15.6	-28.9	99.5

There are slight variations in the heat to be removed from various kinds of fish and fish products but the freezer should be designed to cope with the above maximum requirement. In commercial practice, the heat allowance made for fish frozen in an air blast freezer is often taken as 129 kW/kg but this includes a safety factor allowance for peak loads at the start of freezing, unduly high product temperatures and other inefficiencies in freezer operation. An allowance is always made in calculating the refrigeration load as a safety precaution but whether this is applied to each individual item as in this instance, or to the total load, is a matter for individual interpretation.

In addition to freezing the fish, the refrigeration plant must also cope with heat from other sources, and allowance for these must be made in the design. For example, allowance must be made for heat coming in through the insulation, heat generated by the fans and the lights, and heat introduced by warm air and warm trolleys and trays; all of these are additional to the heat to be taken from the fish itself.

5.7 Incorrectly Loaded Blast Freezer

When a blast freezer is overloaded, the air temperature will rise and the freezing time will be longer; in addition the pressure in the discharge side of the refrigeration

compressor is likely to rise fairly quickly. An excessively high discharge pressure should cause a safety device to trip and stop the compressor motor; failing that, the electrical overload device should trip and again stop the motor, a bursting disc should blow, or a pressure relief valve operate but, where these devices are not fitted or are incorrectly set, the high pressure may cause serious damage to the equipment and possibly endanger the staff nearby.

The immediate effect of under loading is less serious than that of overloading, but the cumulative effects may eventually prove costly. First the air temperature will fall and the plant will thus operate at a less economic level than the one it was designed for. Very light loading of the compressor results in extra strain on its bearings due to the absence of the cushioning effect of the compressed gas; the accompanying knocking sound indicates that premature wear and possibly permanent damage to the machinery may result. A low pressure safety device will stop the motor and avoid this risk, but continual stopping and starting will in turn impose unnecessary wear and tear on both motor and starter. Some compressors have a device that compensates for low loads and thus prevents undesirable effects but nevertheless the machinery is still being operated inefficiently and therefore expensively. Two-stage compressors are usually used for air blast freezers operating at -35°C or lower; these are less likely to suffer damage due to low suction pressures when operating with low loads.

Every effort should be made, therefore, to run the blast freezer correctly loaded to give maximum output at least cost.

5.8 Design and Spacing of Freezer Trays

Many fish products are packed in trays before they are loaded into an air blast freezer. The trays should transfer heat efficiently, be easily emptied and be robust. Normally they are required to yield a frozen pack that is rectangular or nearly so. It is extremely difficult to remove a truly rectangular pack even from a strongly made tray without damaging either the tray or the pack, but a slight degree of taper on the sides of the tray makes emptying easy; a tray with a taper of one in eight can be readily emptied by turning it upside down, spraying water on it for a few seconds and then

tapping its edge gently to release the frozen pack. Inserts can also be used to make a rectangular block in a tapered tray. With many products it is suggested that a tray of the type shown in Figure 5.8 be used.

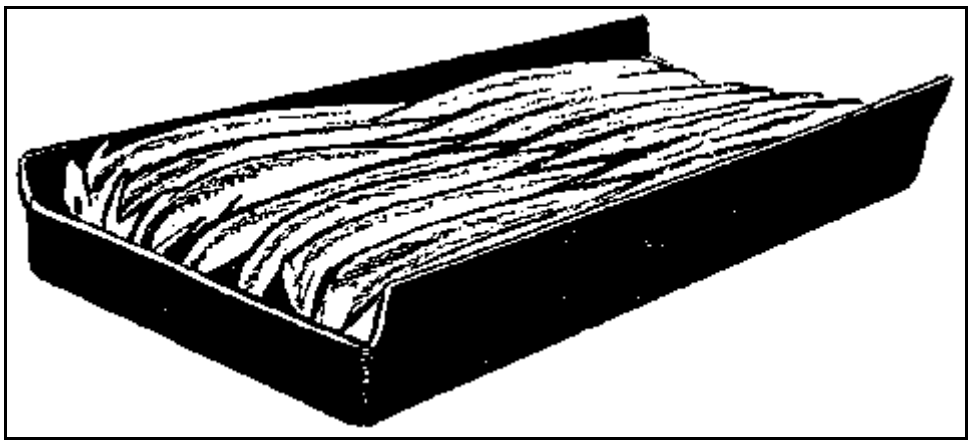

Figure 5.8 Tray for use in air blast freezers

The sides of the tray that lie across the air stream should be lower in height than the product, so that air can flow over the product in close contact with its surface. On the other hand the sides of the tray that lie along the air stream can be higher than the product to give an edge for tapping on during unloading. Aluminum of 14-16 gauges is suitable for the manufacture of blast freezer trays.

Spacing of trays in the freezer is very important; the distance between the upper surface of the product in a tray and the bottom of the tray above it should be about 2/3 of the thickness up to a maximum gap of two inches. In other words trays carrying 3-inch-thick blocks of fillets, for example, would be put on racks at 5-inch-intervals to leave an air space of two inches between them. The trays must be distributed uniformly over the whole cross-section of the tunnel so that the resistance to air flow is everywhere the same; thus the truck or pallet with its racking to support the trays must fit neatly into the tunnel, so that there are no excessive gaps anywhere outside the framework.

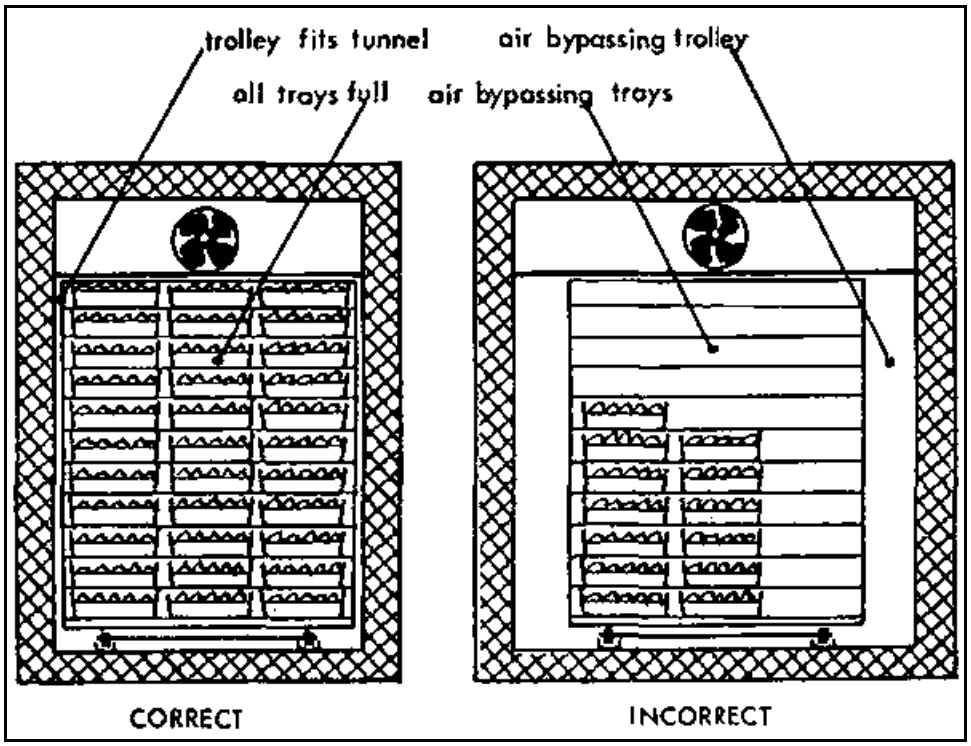

Figure 5.9 Correct and incorrect loading an air blast freezer

Where trolleys or pallets are partly loaded, the load should be evenly distributed across the tunnel to maintain an even air flow. Sometimes it may be necessary to use dummy packs alongside the real ones to prevent the air bypassing the product and thus extending the freezing time.

In some cases pallets are loaded without any shelving or spacers. This practice should be discouraged since to enable the packages to be stacked there has to be a certain amount of overlap with the packages above and below. This overlap increases the effective thickness of the package and consequently prolongs the freezing time. Many stacking arrangements also stop the free passage of air over each individual package in the stack and in these cases the freezing time will be considerably increased.

5.9 The Effect of Wrapping the Product

Any kind of wrapping or packaging will lengthen the freezing time of the product; not only does the wrapper itself have some insulating effect but also some air is often trapped between the wrapper and the product. In a blast freezer the layer of still air in

the pack is sometimes more resistant to heat flow than the wrapping. The effect of wrapping on the freezing time of a typical blast freezer product, boxed kippers, is shown in Table 5.3.

Table 5.3 Effect of wrapping on freezing time of kippers

Packing procedure	**Freezing time (hours)**
Wooden box, paper wrapping, lid on	17.9
Wooden box, foil wrapping, lid on	17.2
Wooden box, paper wrapper, no lid	16.3
Wooden box, foil wrapper, no lid	16.2
Wooden box, no wrapper, lid on	14.7
Wooden box, no wrapper, no lid	8.0

The table shows that the freezing time can be considerably reduced by leaving the lid off the box and allowing the air to blow over the unwrapped contents. The table also shows that whatever the wrapper is made of its effect mainly depends on how well it excludes the moving air from direct contact with the product. The foil wrapper, a good conductor of heat compared with the wooden lid of the box, has nevertheless a greater effect on the freezing time than the lid because it makes a more effective seal. Kippers are usually loosely packed in wood boxes, compared with say wet fish fillets, and air circulation through the pack is a big factor in the removal of heat. Therefore, the difference in freezing time between unwrapped and wrapped kippers with the lid off is probably greater than it would be for most other fish products. Often it is possible to freeze the product in an open metal tray and pack it afterwards; although this means double handling, this technique may be used to give the shortest possible freezing time.

5.10 Defrosting Blast Freezers

Frost always accumulates in air blast freezers, particularly on the upstream side of the cooler and on the structure near to the warmest fish. The frost must be removed at regular intervals; otherwise it impairs the efficiency of the freezer by reducing the transfer of heat from the air to the cooler, thus causing the air to warm up, and by restricting air flow through the tunnel.

Frost is produced from three sources; water in the product evaporates, water vapor comes in with warm air from outside, for example when the doors are open, and moisture can diffuse through cracks and openings in the freezer structure. About 1-2% of the weight of the unwrapped product will evaporate into the air stream during freezing, and the moisture will eventually be deposited as frost on the cooler.

Tunnels should be made so that they can be readily inspected. Loose, powdery frost can be removed from accessible parts by brushing. Commercial freezers are often defrosted simply by shutting off the refrigerant, throwing open the doors and allowing the whole freezer to warm; natural defrosting in this way can be a slow and messy business and the heavy condensation can damage the insulation and the structure of the tunnel. Controlled heating with the freezer doors closed is much better.

The cooler can be defrosted by circulating hot gas through the coils or, where a secondary refrigerant is used, by circulating hot liquid from a reservoir. The coils can be defrosted externally by spraying water, brine or some other suitable liquid over the coils or by electrical heaters in the cooling unit.

Hot gas defrosting is efficient only when the compressor has some refrigeration work to do; therefore wherever a compressor supplies more than one cooler, only one cooler should be defrosted at a time.

In each of the above methods of defrosting the process can be speeded up if refrigerant is emptied from the coils before defrosting begins.

5.11 Frozen Fishery Products

Blast freezers for fishery products are generally small rooms or tunnels in which cold air is circulated by one or more fans over an evaporator and around the product to be frozen, which is on racks or shelves. A refrigerant such as ammonia, a halocarbon, or brine flowing through a pipe coil evaporator furnishes the necessary refrigeration effect (ASHRAE, 2002).

Static pressure in these rooms is considerable, and air velocities average between 2.5 and 7.5 m/s, with 6 m/s being common. Air velocities between 2.5 and 5 m/s give the most economical freezing. Lower air velocities slow down product freezing, and higher velocities increase unit freezing costs considerably.

Some factories have blast freezers in which conveyors move fish continuously through a blast room or tunnel. These freezers are built in several configurations, including (1) a single pass through the tunnel, (2) multiple passes, (3) spiral belts, and (4) moving trays or carpets. The configuration and type of conveyor belt or freezing surface depend on the type and quantity of the product to be frozen, the space available to install the equipment, and the capital and operating costs of the freezer.

In Figure 5.10, a spiral belt freezer tunnel is shown. The product flow directions are shown in Figure 5.11. Fish freezing is shown in Figure 5.12. Freezing food in a spiral belt freezing tunnel is shown in Figure 5.13.

Figure 5.10 Spiral belt freezer tunnel

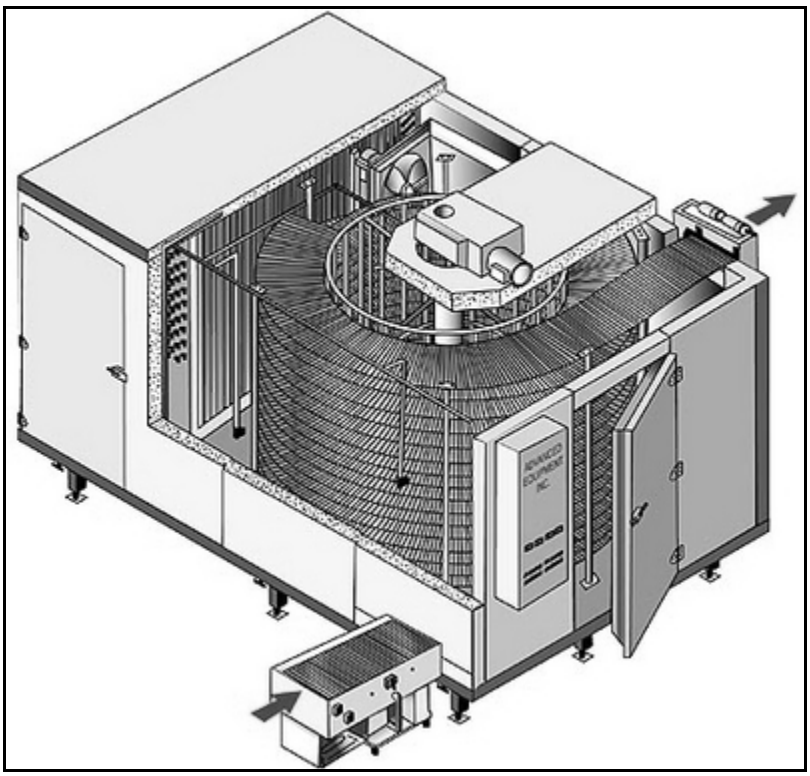

Figure 5.11 Spiral belt freezer tunnel flow directions

Figure 5.12 Freezing fish in a spiral belt freezer tunnel

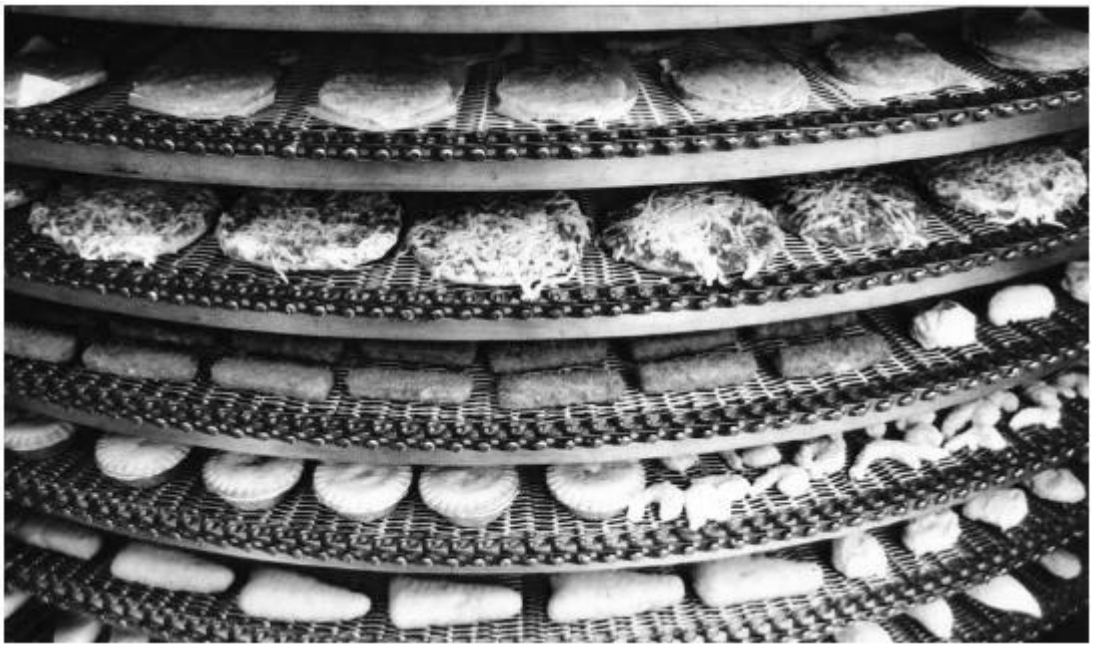

Figure 5.13 Freezing food in a spiral belt freezer tunnel

CHAPTER SIX
THEORETICAL STUDY

6.1 Problem Definition

In this chapter, the heat transfer and pressure drop of a blast freezer evaporator calculated, theoretically. The blast freezer evaporator (similar to the evaporator in Figure 6.1) is used in fish freezing at -25°C in a spiral belt freezer tunnel. Freezing capacity is 250 kg/h. Dimensions of evaporator are shown in Fig. 6.2. There are 6 suction fans to suck ambient air at -25°C and pass through the tubes and fins which have a surface temperature of -30°C and blow again to the ambient. R404A is used as refrigerant. Air inlet view and fin geometry are shown in Figure 6.3 and 6.4. Geometrical data, air-side data, and refrigerant-side data are given in Table 6.1, 6.2, and 6.3, respectively.

Figure 6.1 Blast freezer type evaporator

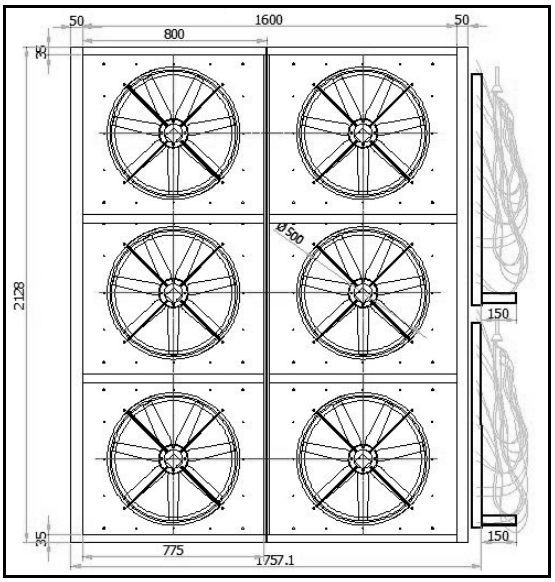

Figure 6.2 Evaporator dimensions

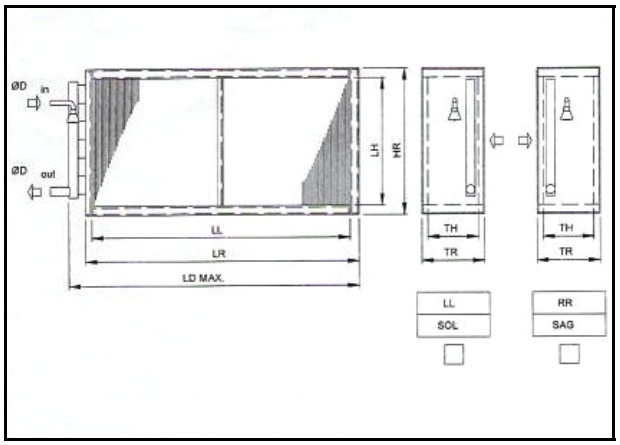

Figure 6.3 Air inlet view

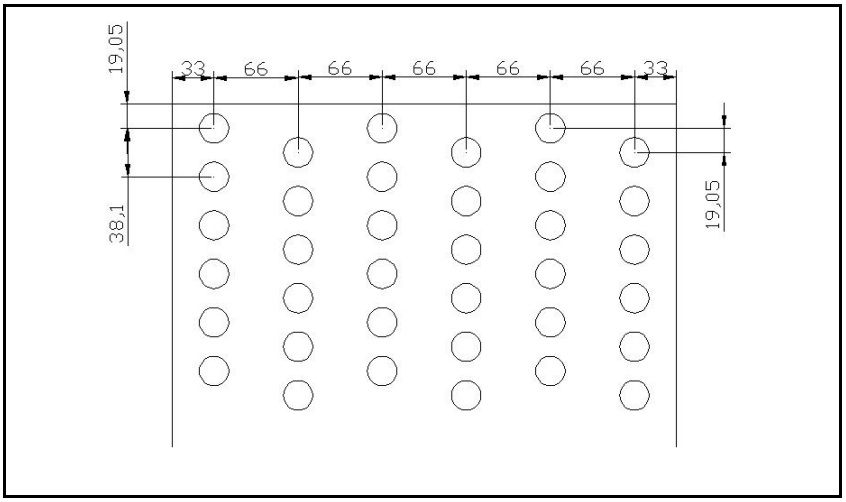

Figure 6.4 Fin geometry

Table 6.1 Geometrical data

Transverse pitch (S_T)	38.1 mm
Longitudinal pitch (S_L)	66 mm
Tube diameter	5/8”
Freezing process	F
Staggered tube arrangement	S
Number of tubes in one row	54T
Number of tube rows	6R
Total fin length	1600A
Fin pitch	8.00P
Number of circuit	27 NC
Fin material	Aluminum
Tube material	Copper
Tube outer diameter	16.65 mm
Tube inner diameter	15.85 mm

Table 6.2 Air-side data

Mass flow rate	28597 m^3/h
Velocity	2.41 m/s
Inlet temperature	-25°C
Inlet relative humidity	95%
Outlet temperature	-27.31°C
Outlet relative humidity	100%

Table 6.3 Refrigerant-side data

Refrigerant	R404A
Mass flow rate	1114 kg/h
Velocity (gas phase)	5.39 m/s
Velocity (liquid phase)	0.0463 m/s
Evaporation temperature	-30 °C
Condensation temperature	40°C

6.2 Heat Transfer Calculations

Since the evaporator is a heat exchanger, one of the heat transfer and pressure drop calculation methods, LMTD (Logarithmic Mean Temperature Difference) method is used in this study. Total heat transfer capacity is calculated from Eq. 6.1 (Kakaç, 1998),

$$Q = U_o A_o \Delta T_{lm} = U_o A_o F \Delta T_{lm,cf} \quad \ldots (6.1)$$

Q : Heat transfer capacity (W)
U_o : Overall heat transfer coefficient (W/m²K)
A_o : Total outside heat transfer area (m²)
F : Correction factor for cross flow
$\Delta T_{lm,cf}$: Average logarithmic temperature difference for cross flow (°C)
ΔT_{lm}: Average logarithmic temperature difference for counter flow (°C)

Because of the number of passes, the cross flow approaches to counter flow, so F is taken as 1. Average logarithmic temperature difference is calculated from Eq. 6.2 (Kakaç, 1998),

$$\Delta T_{lm} = \frac{T_{ai} - T_{ao}}{\ln \dfrac{T_{ai} - T_r}{T_{ao} - T_r}} \quad \ldots (6.2)$$

T_{ai} : Air inlet temperature (°C)
T_{ao} : Air outlet temperature (°C)
T_r : Refrigerant temperature (°C)

Overall heat transfer coefficient is calculated from Eq. 6.3 (Kays & London, 1984),

$$U_o = \left[\frac{A_o}{h_i A_i} + \frac{t_w A_o}{k_w A_{pm}} + \frac{A_o}{h_o \left(A_{to} + \eta_f A_f \right)} \right]^{-1} \quad \ldots (6.3)$$

A_i : Tube inside surface area (m²)

h_i : Refrigerant side heat transfer coefficient (W/m²K)

t_w : Tube thickness (m)

k_w : Tube conduction coefficient (W/mK)

A_{pm} : Tube heat transfer area depending on average tube diameter (m²)

h_o : Air side heat transfer coefficient (W/m²K)

A_{to} : Tube outside surface area (m²)

A_f : Finned heat transfer area (m²)

η_f : Fin efficiency

Since the evaporator geometry is known; h_i, and h_o must be found in order to calculate U_o.

6.2.1 Air Side Heat Transfer Coefficient (h_o)

Air-side Nusselt number is calculated from Eq. 6.4 (VDI-Heat Atlas, 1993),

$$Nu = 0.38\,\mathrm{Re}^{0.6}\,\mathrm{Pr}^{1/3}\left(\frac{A_o}{A_{to}}\right)^{-0.15} \quad \ldots (6.4)$$

Reynolds number is calculated for collar diameter and mass velocity in minimum flow area from the Eq. 6.5. Air flows over collar diameter between fins. Mass velocity in minimum area is represented as G_{max}.

$$Re = \frac{G_{\max}.d_{co}}{\mu_a} \quad \ldots (6.5)$$

$$G_{\max} = \rho_a.u_{\max} \quad \ldots (6.6)$$

$$u_{\max} = \frac{V}{A_{\min}} \quad \ldots (6.7)$$

$$d_{co} = d_o + 2t_k \quad \ldots (6.8)$$

G_{max} : Mass velocity in minimum area (kg/m²s)

u_{max} : Air velocity in minimum flow area (m/s)

V : Air volume flow rate (m³/s)

A_{min} : Minimum flow area (m²)

d_{co} : Collar diameter (m)

t_k : Fin thickness (m)

ρ_a : Air density at average temperature (kg/m³)

μ_a : Air dynamic viscosity at average temperature (N.s/m²)

$$Pr = \frac{\mu_a c_{pa}}{k_a} \quad \ldots (6.9)$$

$$A_{to} = N_t.\pi.d_o.L \quad \ldots (6.10)$$

$$A_f = 2.N_f.[(H.W) - (N_t.\pi.\frac{d_o^{\,2}}{4})] \quad \ldots (6.11)$$

$$A_o = A_{to} + A_f \quad \ldots (6.12)$$

Air side heat transfer coefficient is calculated from Eq. 6.13 (Kakaç, 1998),

$$h_o = \frac{Nu.k_a}{d_o} \quad \ldots (6.13)$$

h_o = 60.43 W/m²K

6.2.2 Refrigerant Side Heat Transfer Coefficient (h_i)

Refrigerant-side heat transfer coefficient is calculated from Eq. 6.14 (Kakaç, 1991),

$$\frac{h_{tp}}{h_l} = C_1 (Co)^{C_2} \left(25 Fr_l\right)^{C_5} + C_3 (Bo)^{C_4} F_{fl} \quad \ldots (6.14)$$

Convection number is calculated from Eq. 6.15 (Kakaç, 1991),

$$Co = \left(\frac{1-x}{x}\right)^{0.8} \left(\frac{\rho_g}{\rho_l}\right)^{0.5} \quad \ldots (6.15)$$

x : Vapor quality of the refrigerant

ρ_g : Density of saturated vapor refrigerant (kg/m³)

ρ_l : Density of saturated liquid refrigerant (kg/m³)

Coefficients depending on the Co number are shown in Table 6.4,

Table 6.4 Coefficients depending on the Co number

Coefficients	Co < 0.65	Co > 0.65
C_1	1.136	0.6683
C_2	-0.9	-0.2
C_3	667.2	1058
C_4	0.7	0.7
C_5	0.3	0.3

Froude number is calculated from Eq. 6.16 (Kakaç, 1991),

$$Fr = \frac{G^2}{\rho_l^{\,2}.g.d_i} \quad \ldots (6.16)$$

$$G = \rho_l . u_l \quad \ldots (6.17)$$

Fr : Froude number

G : Mass flux (kg/m²s)

u_l : Velocity of saturated liquid refrigerant

Boiling number is calculated from Eq. 6.18 (Kakaç, 1991),

$$Bo = \frac{q}{G.h_{fg}} \quad \ldots (6.18)$$

Bo : Boiling number

q : Heat flux

h_{fg} : Enthalpy of vaporization

Assuming refrigerant is saturated liquid only, heat transfer coefficient is calculated from Eq. 6.19 (Kakaç, 1991),

$$h_l = 0.023\left(\frac{G(1-x)d_i}{\mu_l}\right)^{0.8} \frac{\mathrm{Pr}^{0.4}\, k_l}{d_i} \quad \ldots (6.19)$$

$$Pr = \frac{\mu_l . c_{p\,l}}{k_l} \quad \ldots (6.20)$$

Pr : Prandtl number

μ_l : Dynamic viscosity of saturated liquid refrigerant

c_{pl} : Specific heat of saturated liquid refrigerant

k_l : Conduction heat transfer coefficient of saturated liquid refrigerant

$h_l = 41.17 W/m^2K$

$h_i = h_{tp} = 796.8$ W/m²K

6.2.3 Overall Heat Transfer Coefficient

$$U_o = \left[\frac{A_o}{h_i A_i} + \frac{t_w A_o}{k_w A_{pm}} + \frac{A_o}{h_o \left(A_{to} + \eta_f A_f \right)} \right]^{-1}$$

$$A_i = N_t . \pi . d_i . L \quad \ldots (6.21)$$

$$A_{pm} = N_t . \pi . d_m . L \quad \ldots (6.22)$$

$$d_m = \frac{d_o + d_i}{2} \quad \ldots (6.23)$$

A_i : Total tube inside heat transfer area

A_{pm} : Total heat transfer area calculated from average tube diameter

d_m : Average tube diameter

η_f : Fin efficiency

$U_o = 23.56$ W/m^{2}K

$Q = 27.39$ kW

6.3 Pressure Drop Calculations

6.3.1 Air Side Pressure Drop

Air side pressure drop is calculated from Eq. 6.24 (Kakaç, 1998),

$$\Delta p = \frac{G^2}{2\rho i} \left[f \frac{A_t}{A_{\min}} \frac{\rho_i}{\rho} + \left(1 + \sigma^2 \right) \left(\frac{\rho_i}{\rho_o} - 1 \right) \right] \quad \ldots (6.24)$$

$$\sigma = \frac{A_{\min}}{A_{fr}} \quad \ldots (6.25)$$

$$\frac{A_t}{A_{\min}} = \frac{4L}{D_h} \rightarrow D_h = 4L\frac{A_{\min}}{A_t} \quad \ldots (6.26)$$

$$G = \frac{\rho.u}{\sigma} \quad \ldots (6.27)$$

$$Re = \frac{GD_h}{\mu} \quad \ldots (6.28)$$

Δp = 64.16 Pa

6.3.2 Refrigerant Side Pressure Drop

Refrigerant-side pressure drop is calculated from Eq. 6.29 (Kakaç, 1998),

$$f = \frac{\Delta P}{4(L/d_i)(\rho u_m{}^2/2)} \rightarrow \Delta P = 4f\frac{L}{d_i}\frac{\rho u_m{}^2}{2} \quad \ldots (6.29)$$

$$Re = \frac{u_m d_i}{\nu} \quad \ldots (6.30)$$

$$f = 0.046\,\mathrm{Re}^{-0.2} \qquad (3.10^4 < \mathrm{Re} < 10^6) \quad \ldots (6.31)$$

ΔP = 3.57 kPa

CHAPTER SEVEN
NUMERICAL STUDY

7.1 Geometry

The studied model consists of two fins with half fin thickness, two half fin tube and air between fins. Due to the symmetry, minimum segment of the fin is modeled. Symmetrical conditions and geometrical view of the model is shown in Figure 7.1. As shown in Figure 7.2, two tube row model is considered.

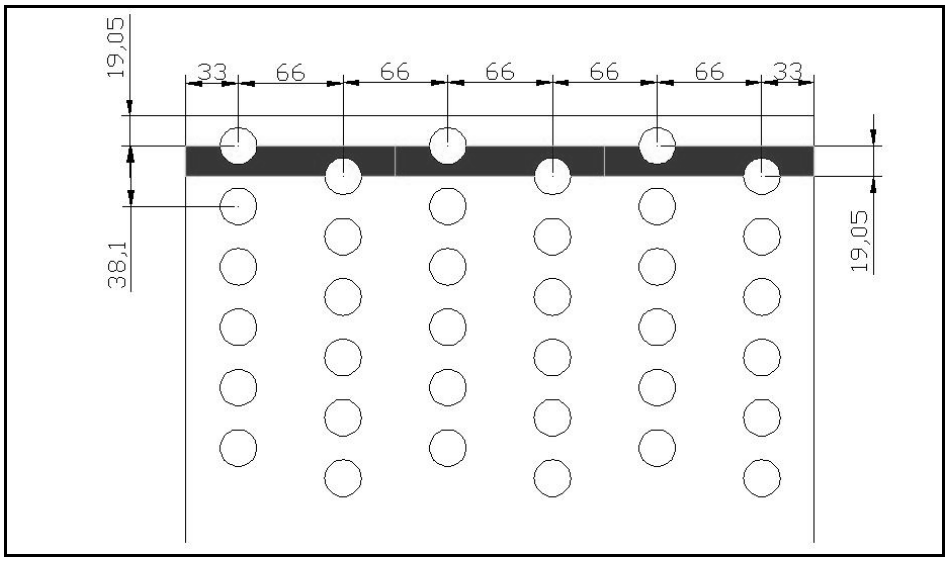

Figure 7.1 Symmetry

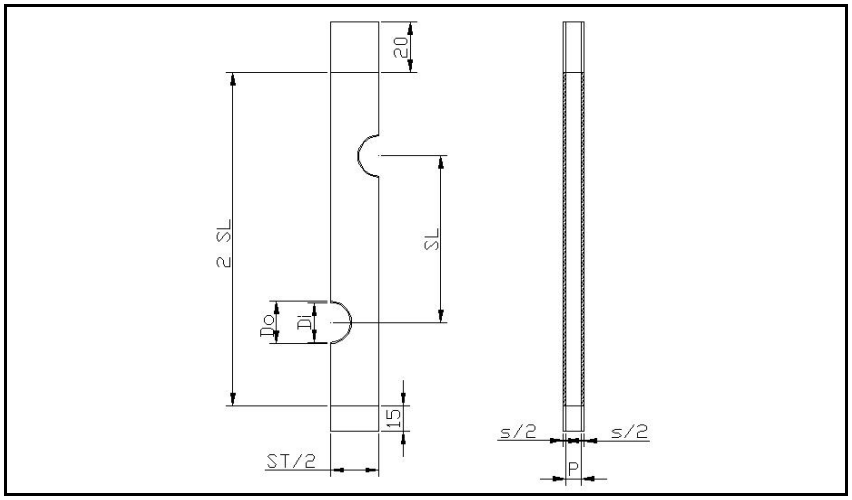

Figure 7.2 Two-row model

Creating geometry is the first step of the modeling. Vertexes, edges, faces, and volumes are created, respectively (Figure 7.3).

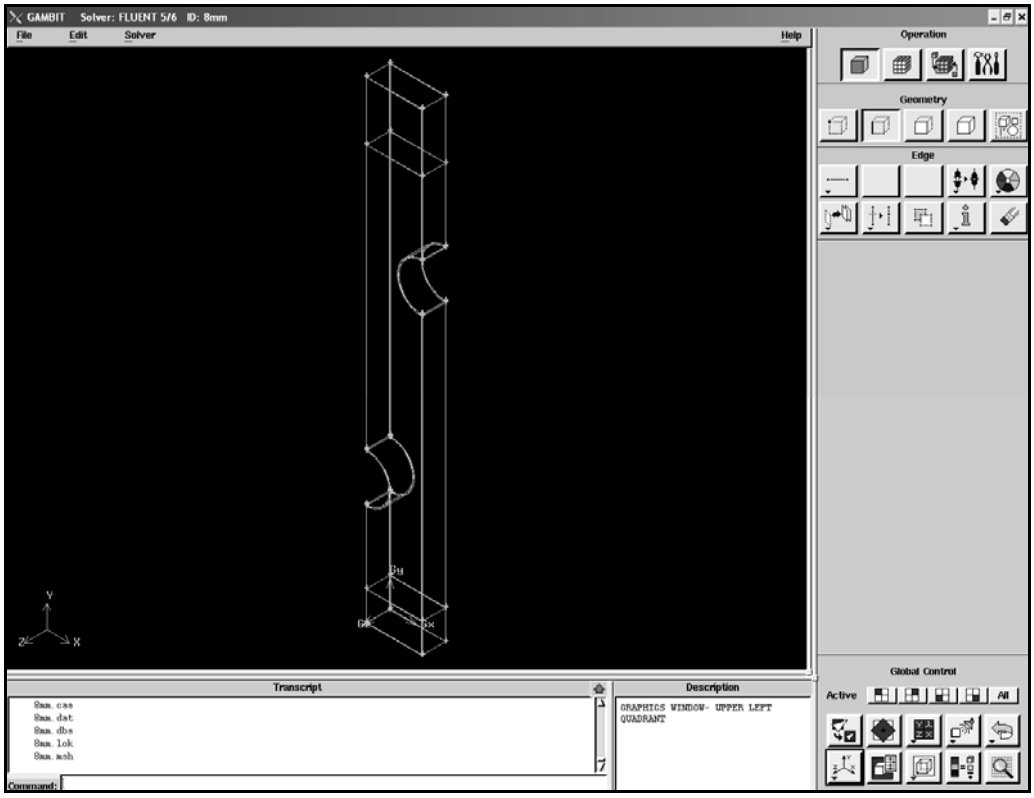

Figure 7.3 Model geometry

7.2 Mesh

Meshing the geometry is the second step of the modeling. Edges, faces, and volumes are meshed, respectively. Tube thickness is meshed in 3 elements. Tube side face is meshed for interval size of 0.3. Fin side face is meshed for interval size of 0.5. Computational faces are meshed for interval size of 1 (Figure 7.4). Four hexahedral finite volume elements along the thickness of the half fin and ten hexahedral finite volume elements along the distance between two fins are used (Figure 7.5).

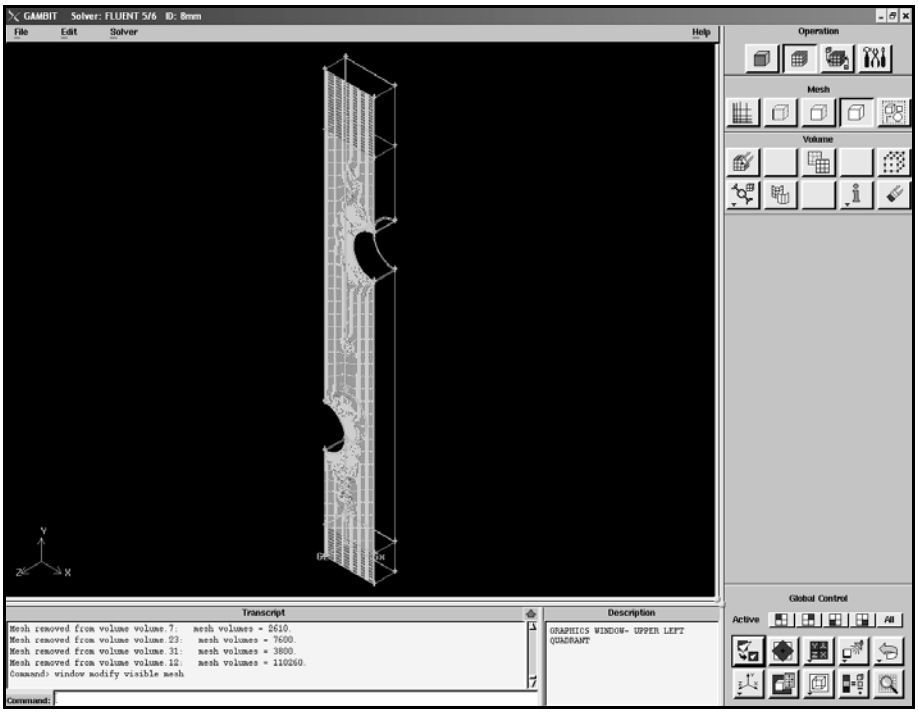

Figure 7.4 Face mesh

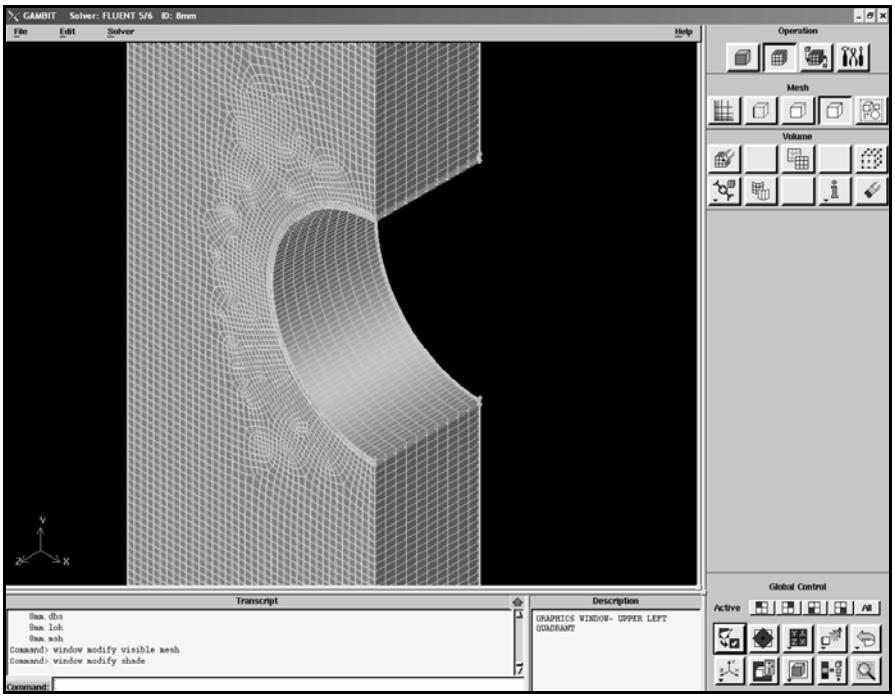

Figure 7.5 Volume mesh

7.3 Boundary Conditions

Boundary conditions are given to the meshed model. Velocity inlet boundary condition is defined for bottom surface, since air enters from that cross section. The air exits from the top side of the model. So, the outflow boundary condition is given to this surface. Symmetrical boundary conditions are given to the side, front and back surfaces of the model due to the symmetry. Tube inner surfaces are defined as wall, since convection heat transfer occurs from these surfaces. Solid and fluid volumes must be defined in order to obtain proper heat transfer results.

7.4 Thermal Analysis

3D version of the Fluent is selected in order to analyze heat transfer and pressure drop. The flow is assumed to be steady and incompressible. Standard k-epsilon turbulence model selected because of high flow velocity and Reynolds number. Aluminum is selected for fin, copper is selected for tube. Air is selected as fluid.

Boundary conditions; velocity inlet is 2.41 m/s, inlet temperature is 248 K, turbulence intensity is 10%, hydraulic diameter is 11.27 mm for 8 mm fin pitch, for other fin pitch, hydraulic diameter changes while the other conditions remain the same.

Convection heat transfer coefficient is 794.6 W/m^2K for 5/8” tubes, for other diameters, convection heat transfer coefficient changes while the other conditions remain the same. Free stream temperature of the refrigerant is taken 243 K.

After solution is converged, temperature and pressure contours, velocity vectors can be displayed for visual consideration of the results. Total heat transfer rate is calculated from flux reports. Pressure drop is calculated from surface integrals.

Some of the results are calculated manually using the Fluent results and theoretical equations:

Air-side heat transfer coefficient is calculated from Eq. 7.1 (Incropera, 2002),

$$h = \frac{Nu.k}{D_h} \quad \ldots (7.1)$$

Nu : Nusselt number, taken from the Fluent results

k : Conduction heat transfer coefficient of the air (W/mK)

D_h : Hydraulic diameter (m)

Hydraulic diameter is calculated from Eq. 7.2 (Kakaç, 1998)

$$D_h = \frac{a.b}{2(a+b)} \quad \ldots (7.2)$$

Colburn j-factor is calculated from Eq. 7.3 (Incropera, 2002),

$$j = \frac{Nu}{\mathrm{Re}.\mathrm{Pr}^{1/3}} \quad \ldots (7.3)$$

f - Friction factor is calculated from Eq. 7.4 (Kakaç, 1998),

$$f = \frac{\Delta P.D_h}{2.L.\rho.u^2} \quad \ldots (7.4)$$

ΔP : Pressure drop, taken from the Fluent results (Pa)

D_h : Hydraulic diameter (m)

L : The length of air flow (m)

ρ : Air density (kg/m³)

u : Air inlet velocity (m/s)

CHAPTER EIGHT
RESULTS AND DISCUSSIONS

The blast freezer evaporator models are analyzed for different geometrical parameters shown in Table 8.1, numerically. The geometrical parameters are taken from commercially available products. The effects of fin pitch, fin thickness, fin material, tube diameter, longitudinal and transverse tube pitch on the air side heat transfer and pressure drop of aluminum plate fin and staggered tube heat exchangers are investigated for actual boundary conditions, turbulent flow and blast freezing process.

Table 8.1 Geometrical parameters of the models

Model	P_T (mm)	t (mm)	d_o (inch)	S_L (mm)	S_T (mm)
A	8	0.15	5/8	66	38.1
B	10	0.15	5/8	66	38.1
C	12	0.15	5/8	66	38.1
D	8	0.12	5/8	66	38.1
E	8	0.15	1/2	66	38.1
F	8	0.15	3/8	66	38.1
G*	8	0.15	5/8	66	38.1
H	8	0.15	5/8	66	40
I	8	0.15	5/8	66	31.75
J	8	0.15	5/8	34.64	38.1
K	8	0.15	5/8	33	38.1
L	8	0.15	5/8	27.5	38.1
M	8	0.15	5/8	22	38.1
N**	8	0.15	5/8	66	38.1

* Aligned tube arrangement

** Fin material is copper

P_T : Fin pitch

t : Fin thickness

d_o : Tube outside diameter

S_L : Longitudinal tube pitch

S_T : Transverse tube pitch

8.1 Fin Pitch Effect

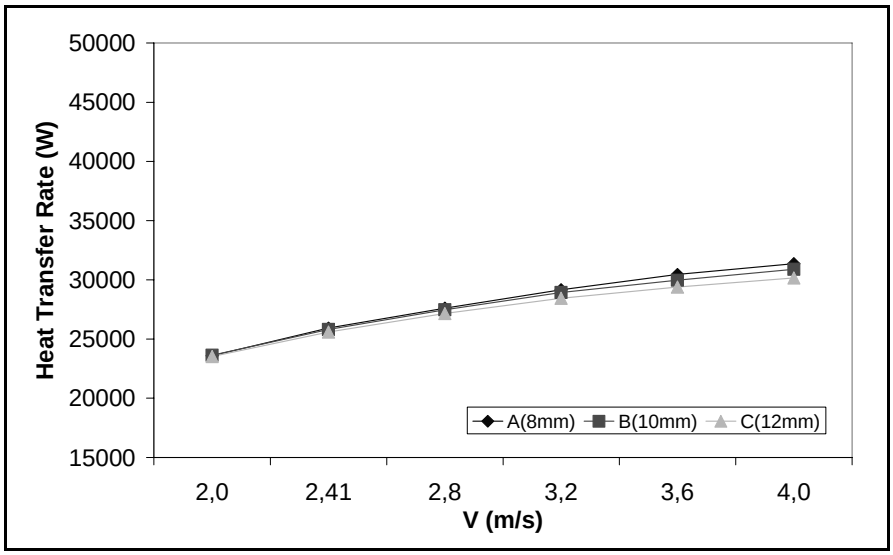

Figure 8.1 Effects of fin pitch on heat transfer rate

In Figure 8.1, the effect of fin pitch on the heat transfer rate can be clearly seen at higher air inlet velocities; the heat transfer rate is much higher for a small fin pitch than for a larger fin pitch. However, at low air inlet velocities, there is almost no effect of fin pitch on the heat transfer rate. The numerical results obtained in this study are in good agreement with the experimental results in the literature (Horuz et al., 1998).

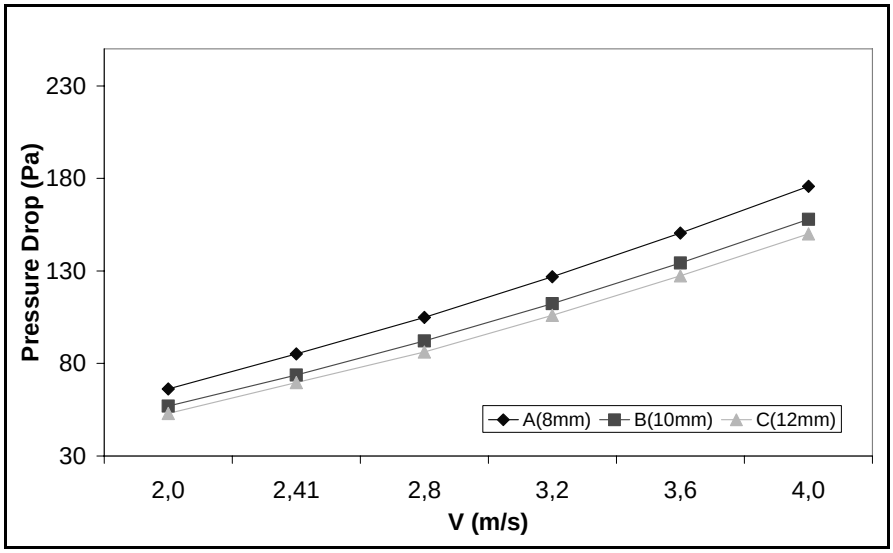

Figure 8.2 Effects of fin pitch on pressure drop

Figure 8.2 shows that the pressure drop increases with increasing air inlet velocities over the range of examined air inlet velocities. Since the turbulence intensity decreased, lower pressure drop values are obtained when the fin pitch is increased.

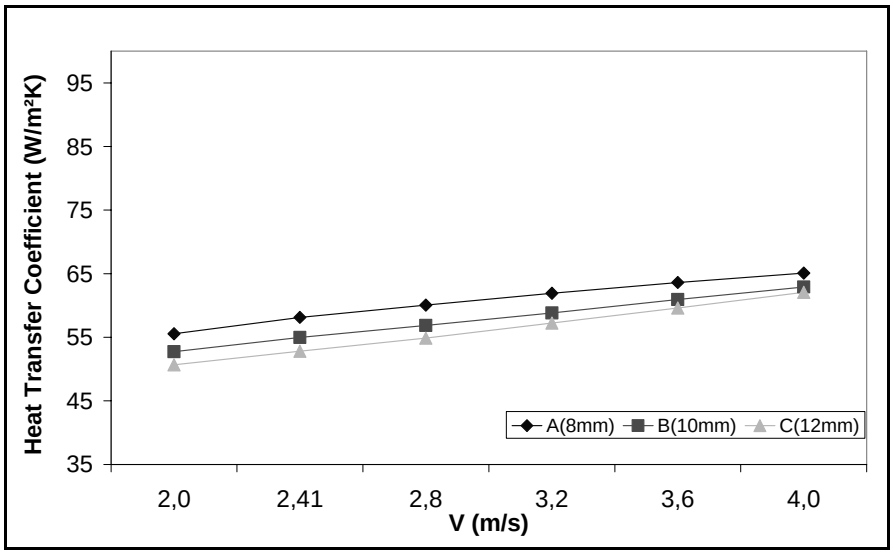

Figure 8.3 Effects of fin pitch on heat transfer coefficient

As shown in Figure 8.3, the air side heat transfer coefficient increases with a reduction of the fin pitch and increasing air inlet velocity.

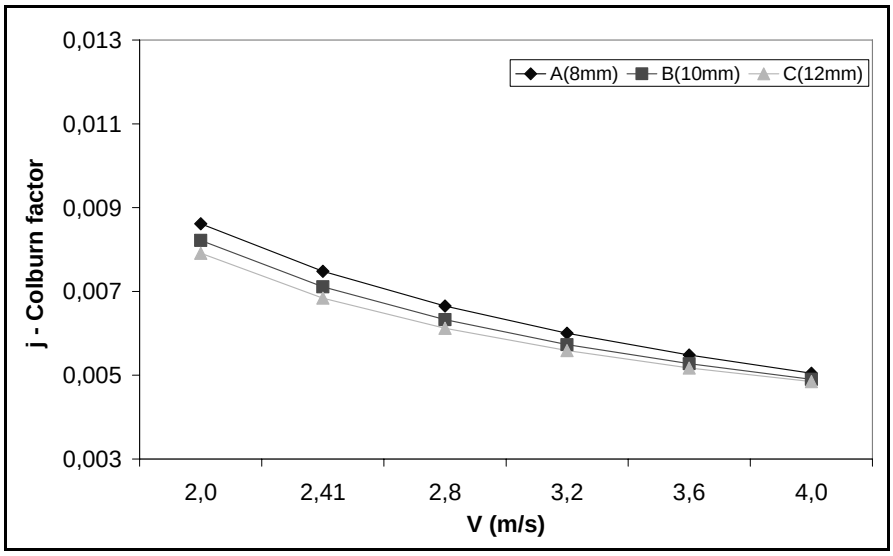

Figure 8.4 Effects of fin pitch on Colburn factor

From the Figure 8.4, it is observed that the Colburn factor increases with decrease of the fin pitch. However, the fin pitch effect diminishes as the air inlet velocity increase over 3 m/s.

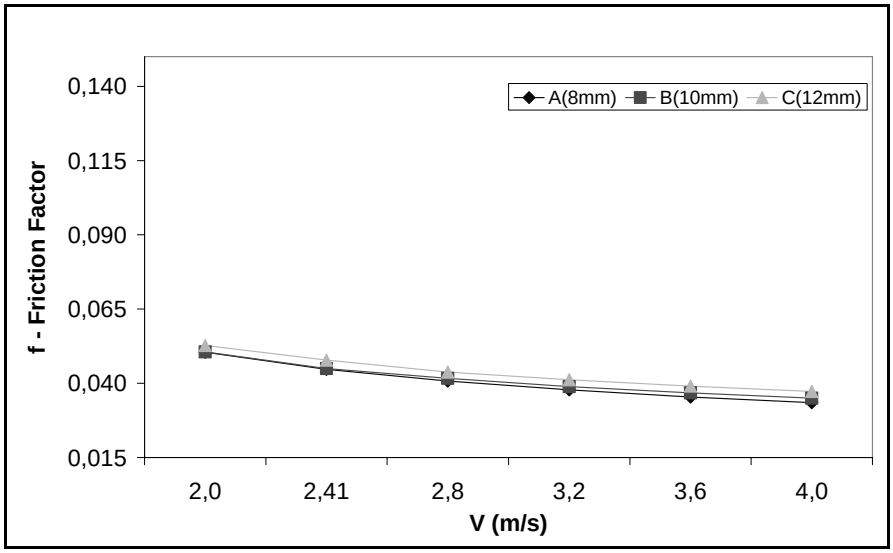

Figure 8.5 Effects of fin pitch on friction factor

Figure 8.5 shows that fin pitch has no significant effect on the friction factor whereas decreases with increasing air inlet velocity.

The effects of fin pitch on temperature contours, pressure contours, and velocity vectors are shown in Figure 8.6, 8.7, and 8.8, respectively.

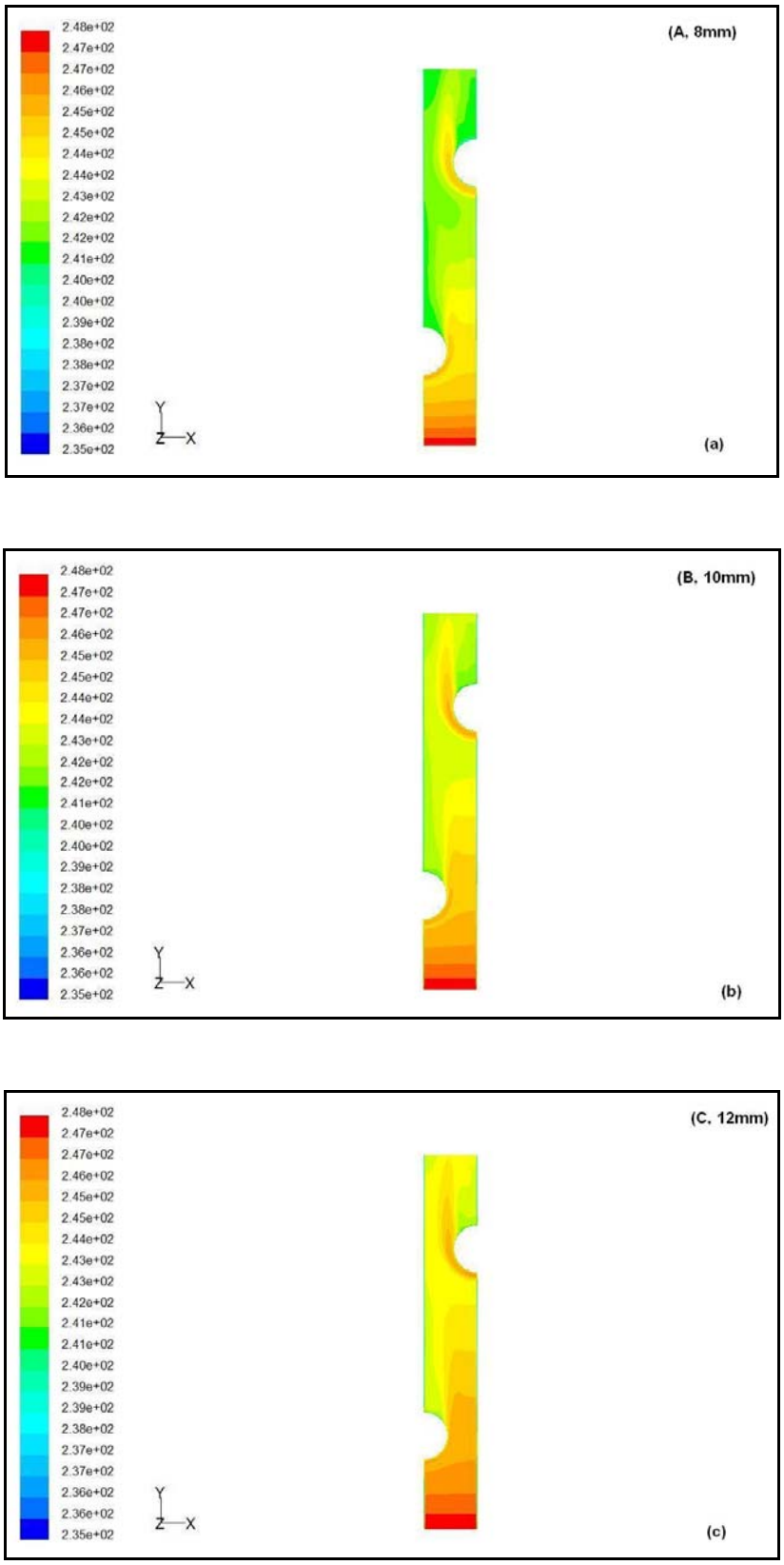

Figure 8.6 Effects of fin pitch on temperature contours

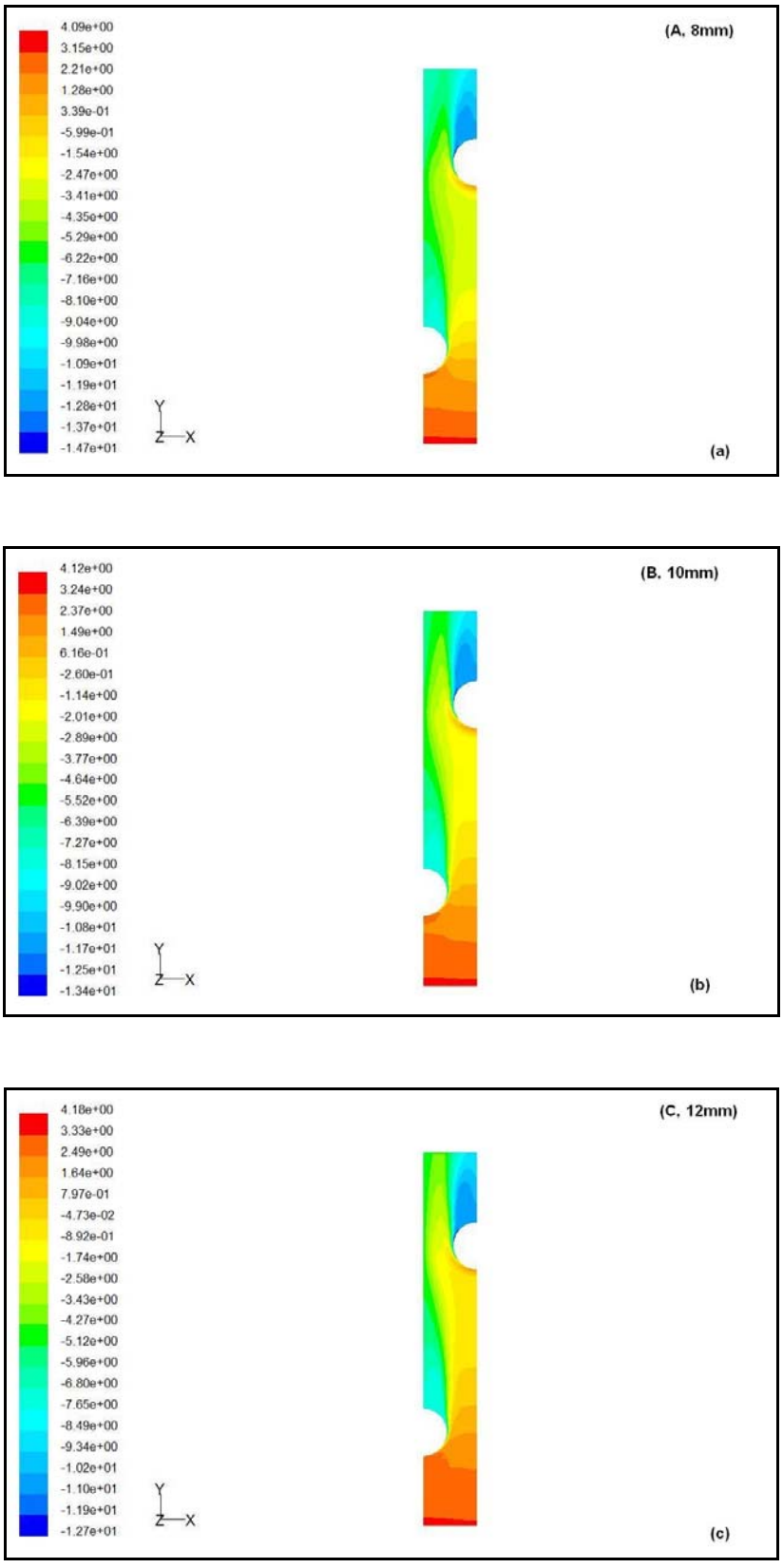

Figure 8.7 Effects of fin pitch on pressure contours

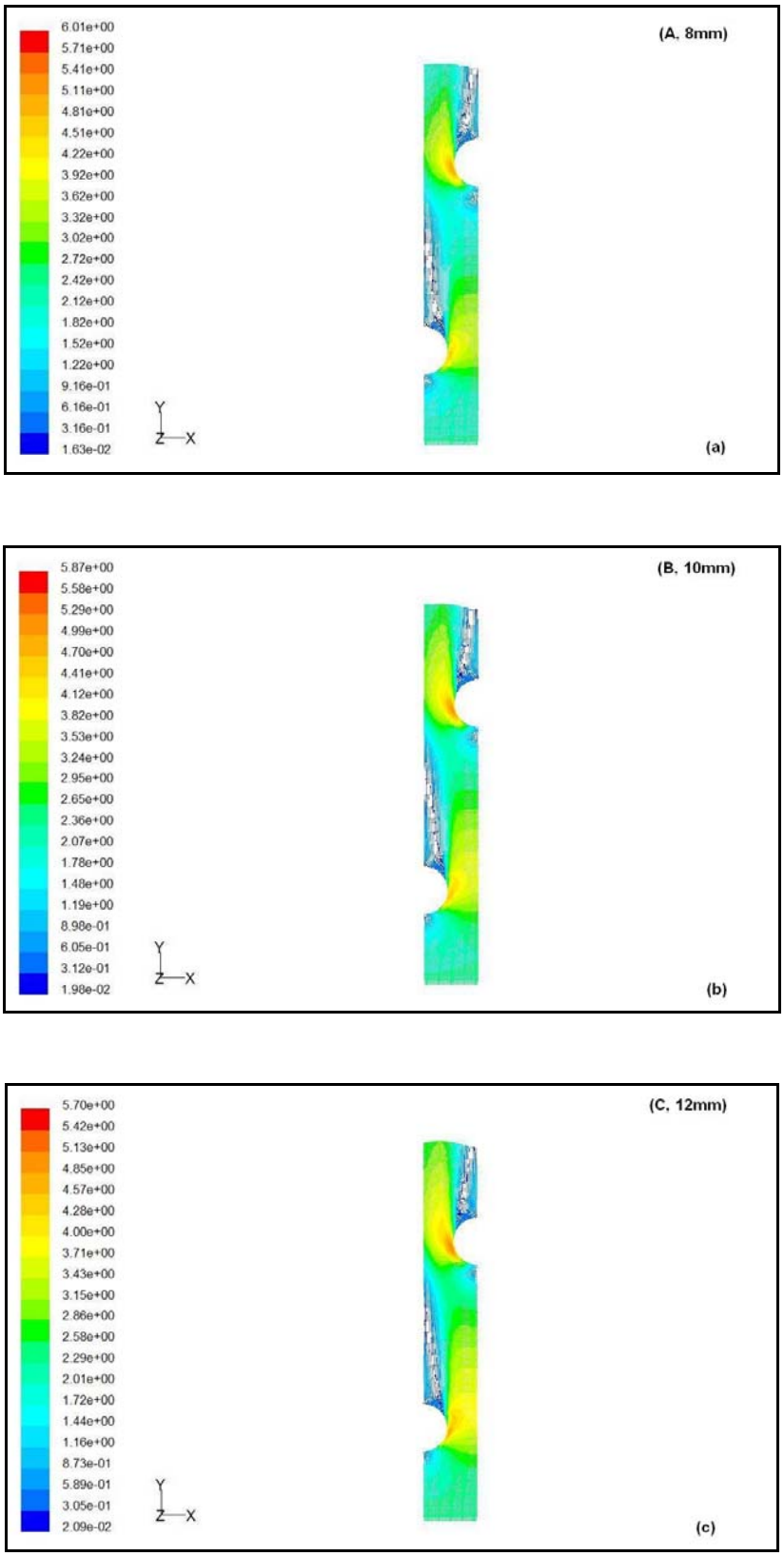

Figure 8.8 Effects of fin pitch on velocity vectors

8.2 Fin Thickness Effect

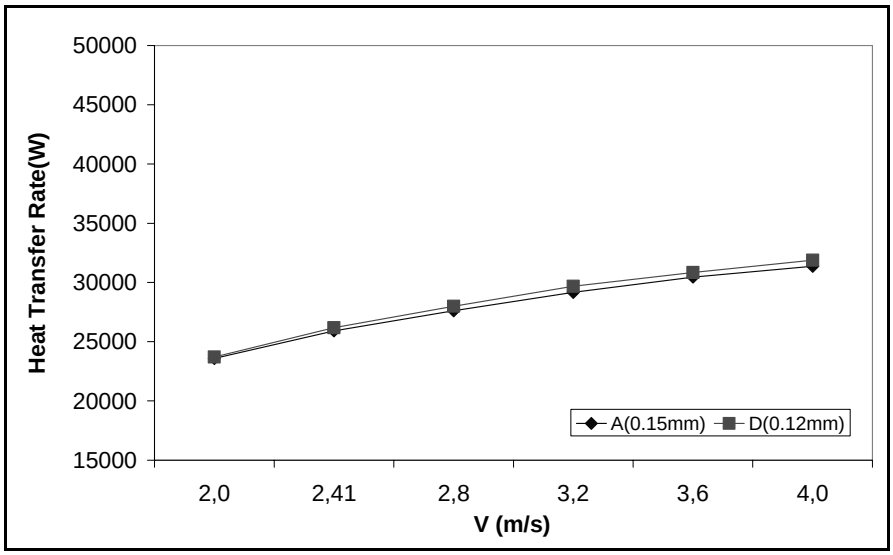

Figure 8.9 Effects of fin thickness on heat transfer rate

Figure 8.9 shows that decreasing fin thickness, as in Model D, slightly increases heat transfer rate. Heat transfer rate increases with increasing air inlet velocity.

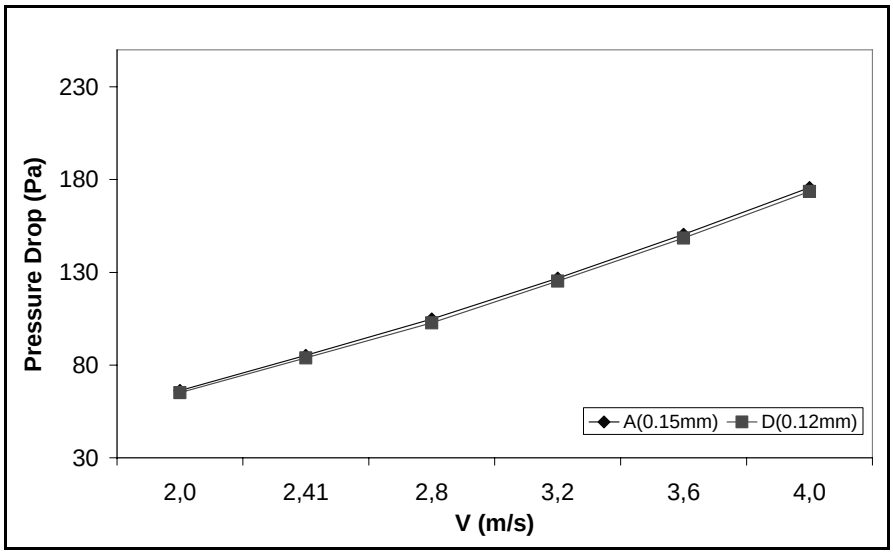

Figure 8.10 Effects of fin thickness on pressure drop

As shown in Figure 8.10, the fin thickness has no significant effect on the pressure drop. Pressure drop linearly increases when the air inlet velocity increases.

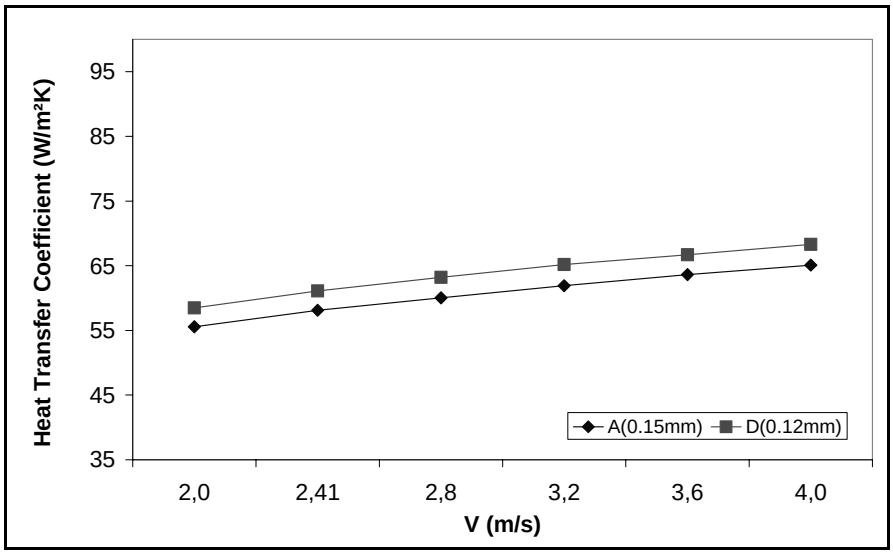

Figure 8.11 Effects of fin thickness on heat transfer coefficient

Figure 8.11 shows that the heat transfer coefficient increases with a reduction of the fin thickness and increases with air inlet velocity. The increment is about 5% for 0.12 mm fin thickness model.

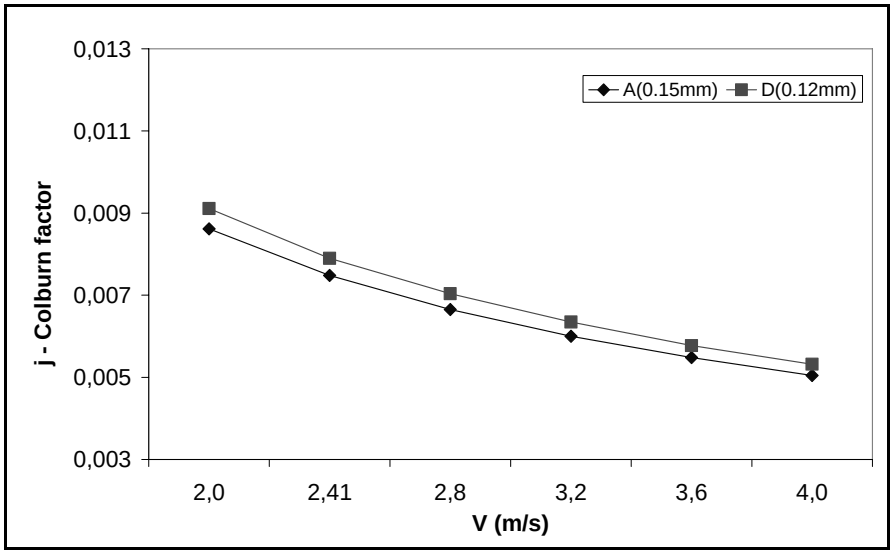

Figure 8.12 Effects of fin thickness on Colburn factor

As shown in Figure 8.12, the Colburn factor increases as the fin thickness decreases from 0.15 mm to 0.12 mm. Colburn factor decreases with increasing air inlet velocity. The numerical results obtained in this study are in good agreement with the experimental results in the literature (Abu Madi et al., 1998).

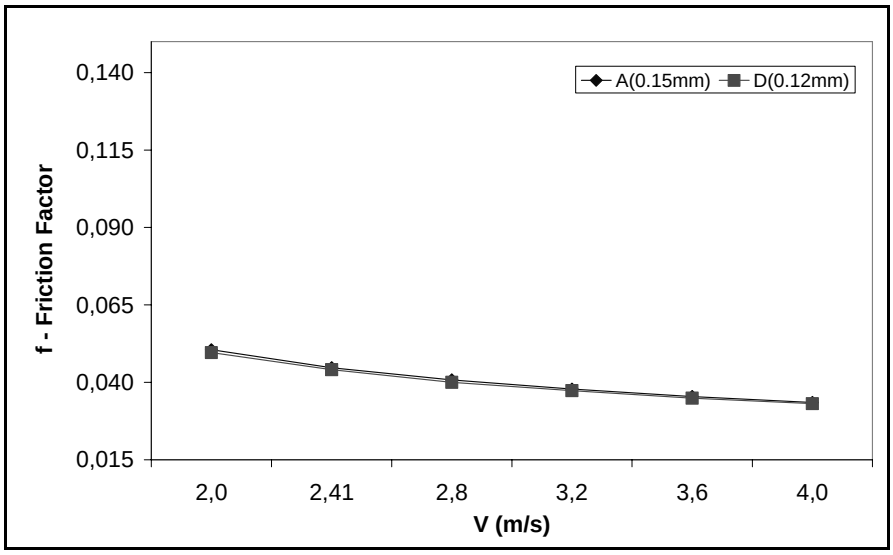

Figure 8.13 Effects of fin thickness on friction factor

Figure 8.13 shows that the effect of the fin thickness on the friction factor is negligible for two models. Friction factor decreases with increasing air inlet velocity. This numerical result is in good agreement with the experimental results in the literature (Abu Madi et al., 1998).

The effects of fin thickness on temperature contours, pressure contours, and velocity vectors are shown in Figure 8.14, 8.15, and 8.16, respectively.

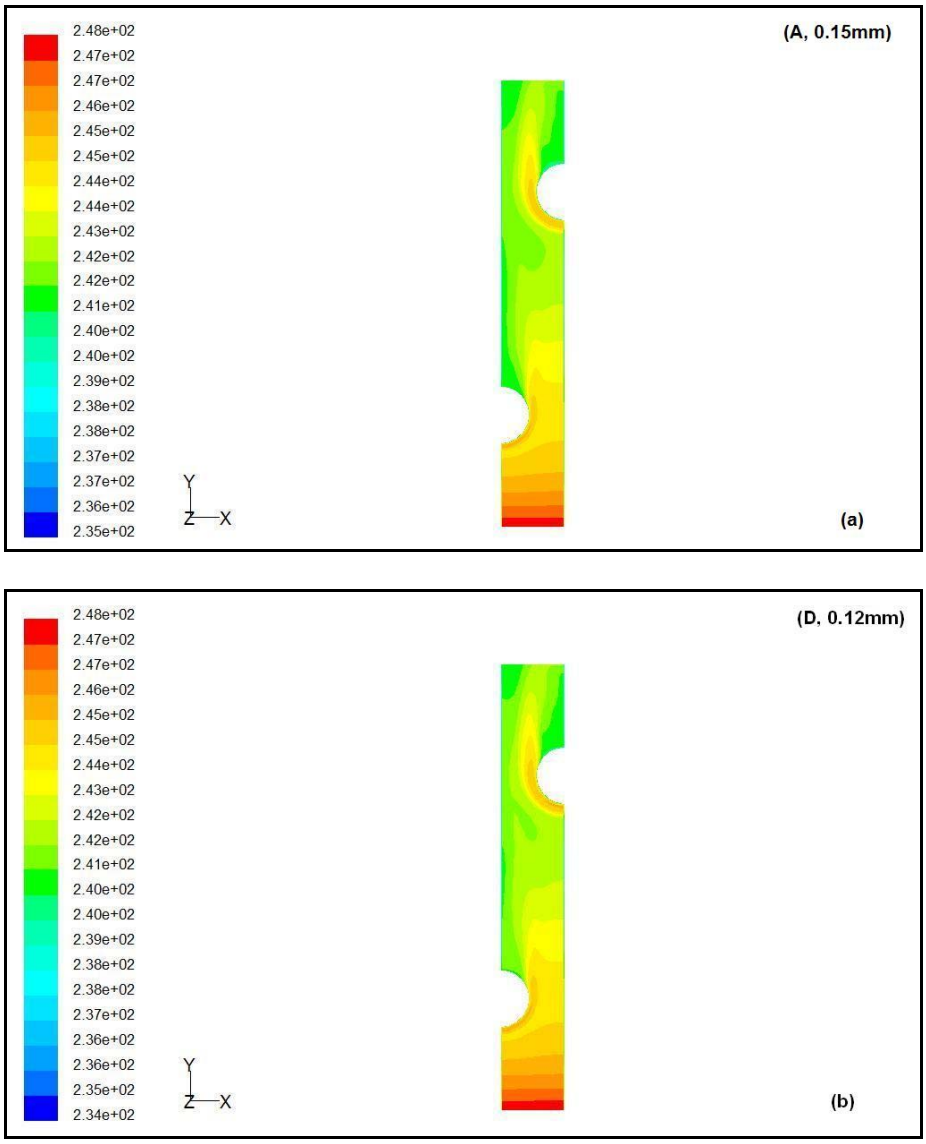

Figure 8.14 Effects of fin thickness on temperature contours

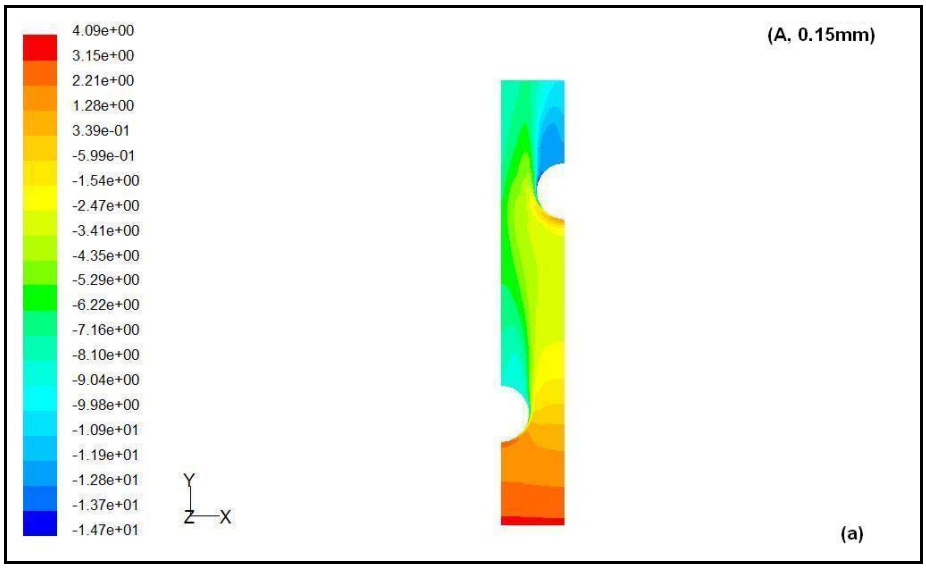

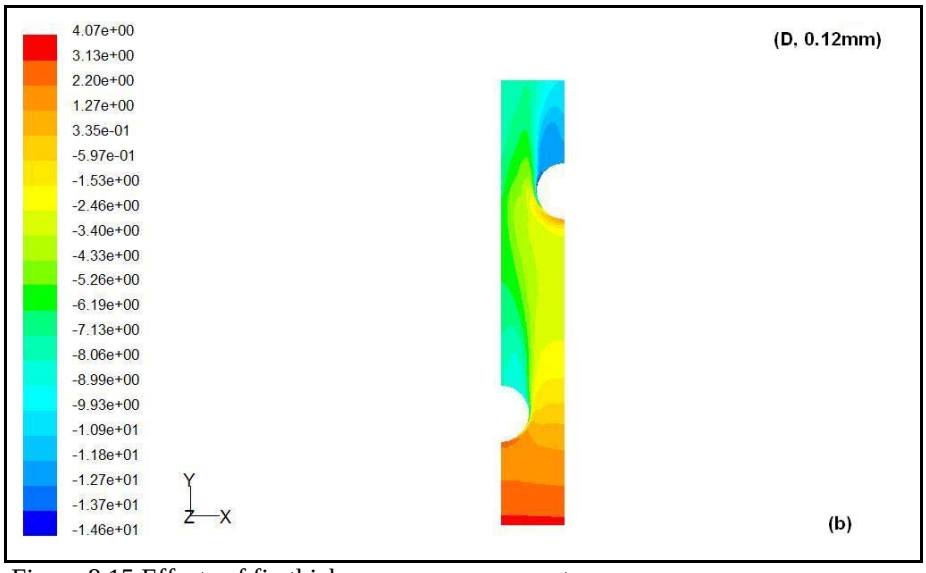

Figure 8.15 Effects of fin thickness on pressure contours

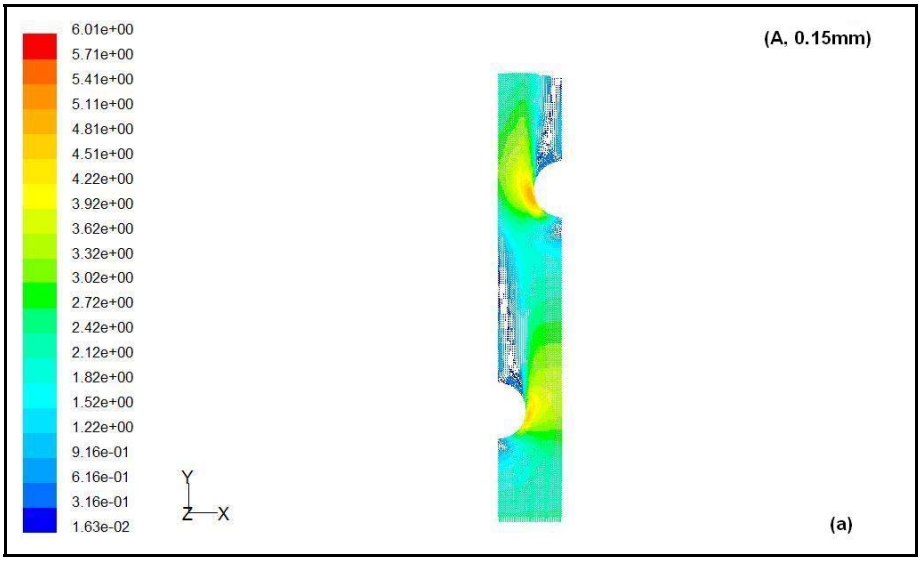

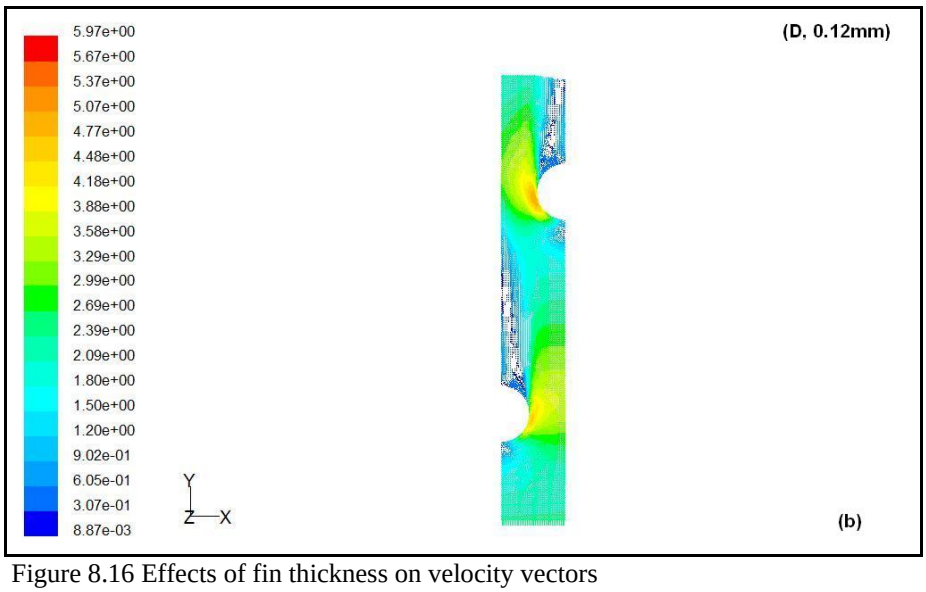

Figure 8.16 Effects of fin thickness on velocity vectors

8.3 Tube Diameter Effect

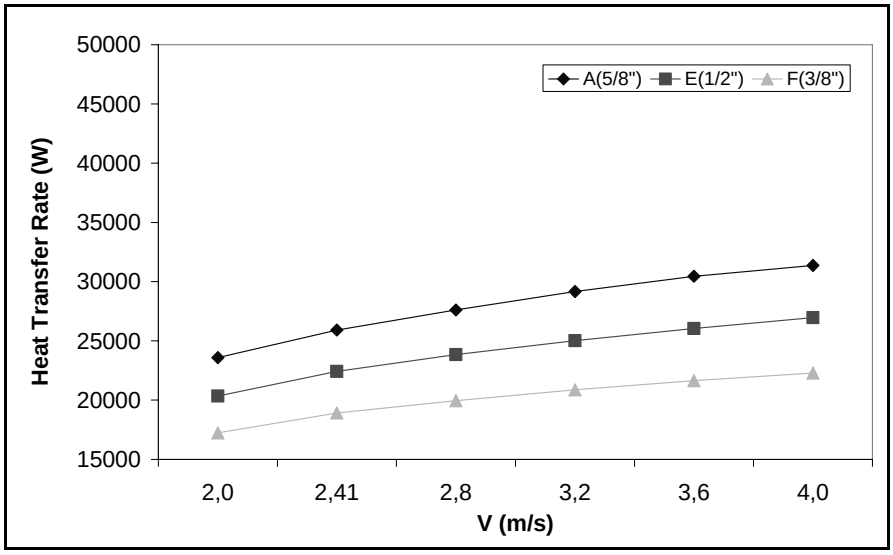

Figure 8.17 Effects of tube diameter on heat transfer rate

From the Figure 8.17, the tube diameter is found to have a considerable effect on heat transfer rate for different geometrical models. As the tube diameter increases, heat transfer increases with the air inlet velocity.

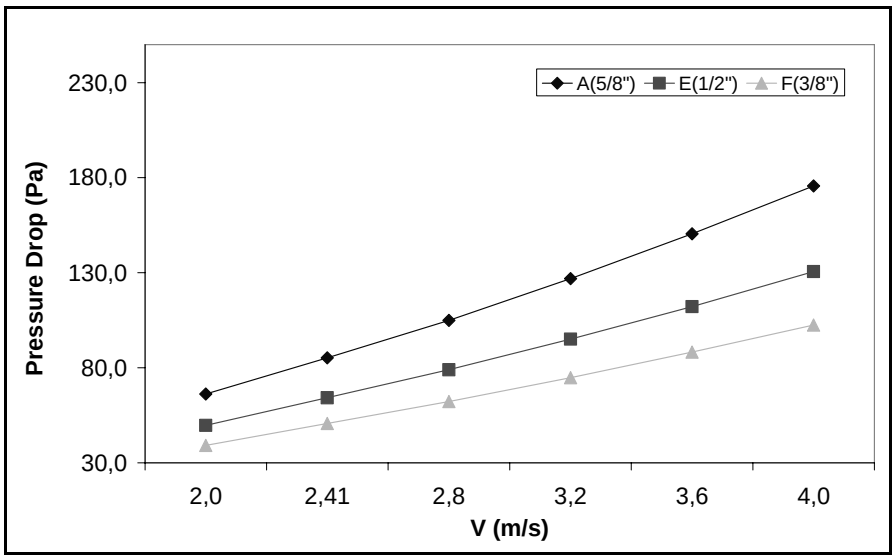

Figure 8.18 Effects of tube diameter on pressure drop

In Figure 8.18, numerical results reveal that tube diameter has a significant effect on the pressure drop. The air side pressure drop decreases with a reduction of the

tube diameter. The numerical results obtained in this study are in good agreement with the experimental results in the literature (Wang & Chi, 2000).

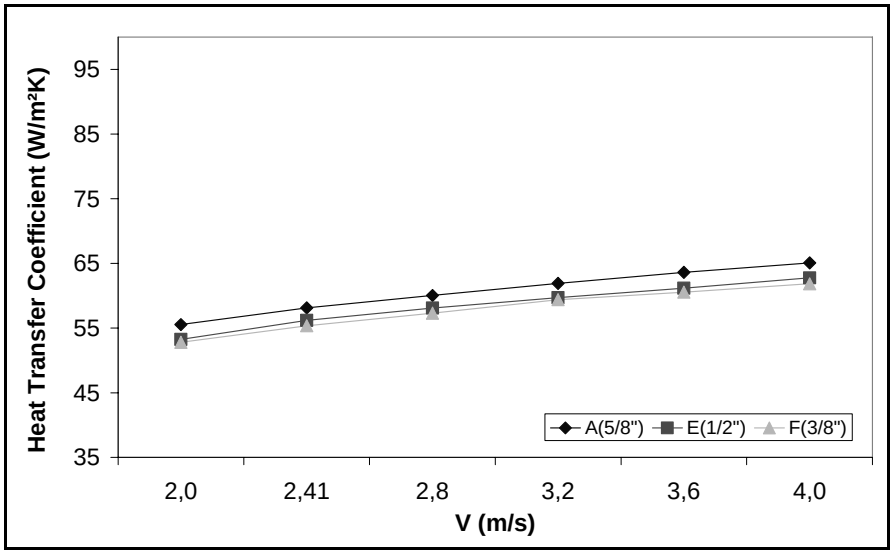

Figure 8.19 Effects of tube diameter on heat transfer coefficient

Figure 8.19 shows the effects of the tube diameter depending on the air inlet velocity on the heat transfer coefficient for different geometrical models. The air side heat transfer coefficient increases with an increase of the tube diameter. The numerical results obtained in this study are in good agreement with the experimental results in the literature (Wang & Chi, 2000).

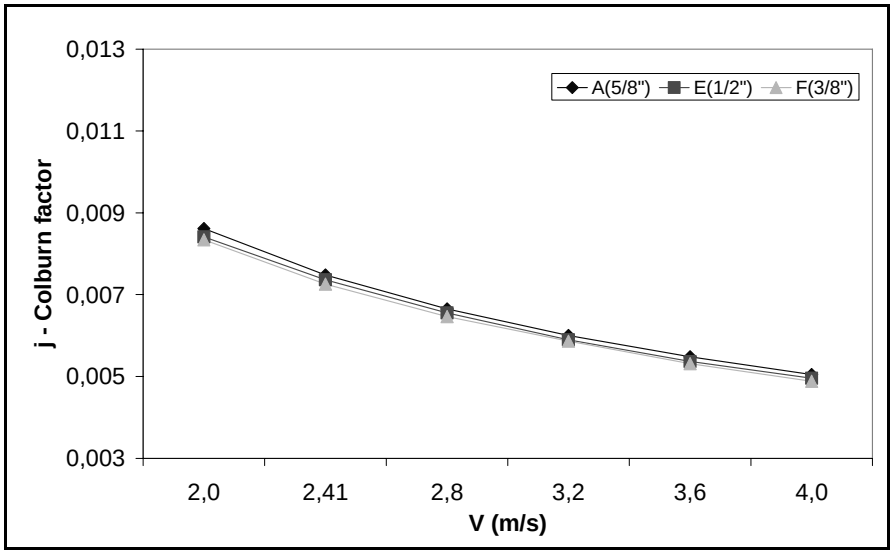

Figure 8.20 Effects of tube diameter on Colburn factor

In Figure 8.20, it can be clearly seen that at low air inlet velocities, the increase of the tube diameter results in the increase of the Colburn factor. However, when the air inlet velocity increases, the effect of tube diameter on the heat transfer characteristics tends to vanish.

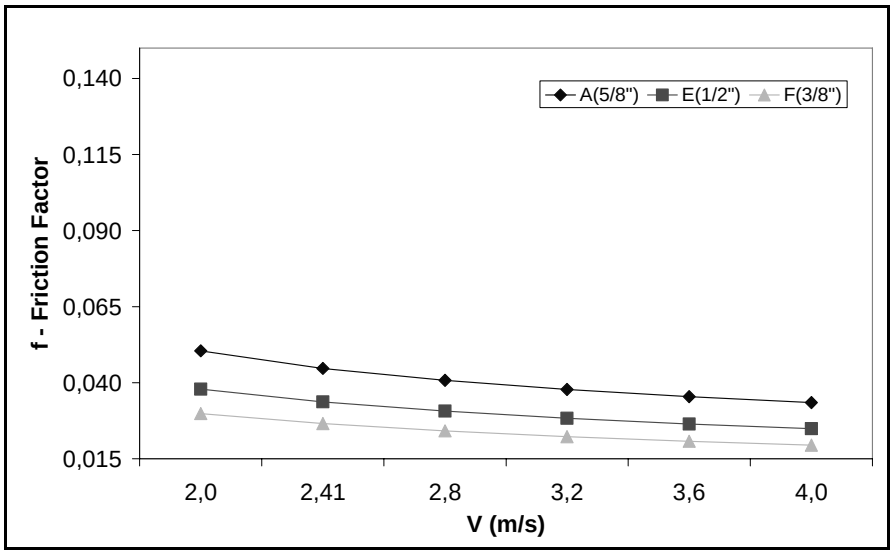

Figure 8.21 Effects of tube diameter on friction factor

The effect of tube diameter on friction factor for different models is shown in Figure 8.21. As the tube diameter decreases, the friction factor drops more severely with increasing air inlet velocity.

The effects of tube diameter on temperature contours, pressure contours, and velocity vectors are shown in Figure 8.22, 8.23, and 8.24, respectively.

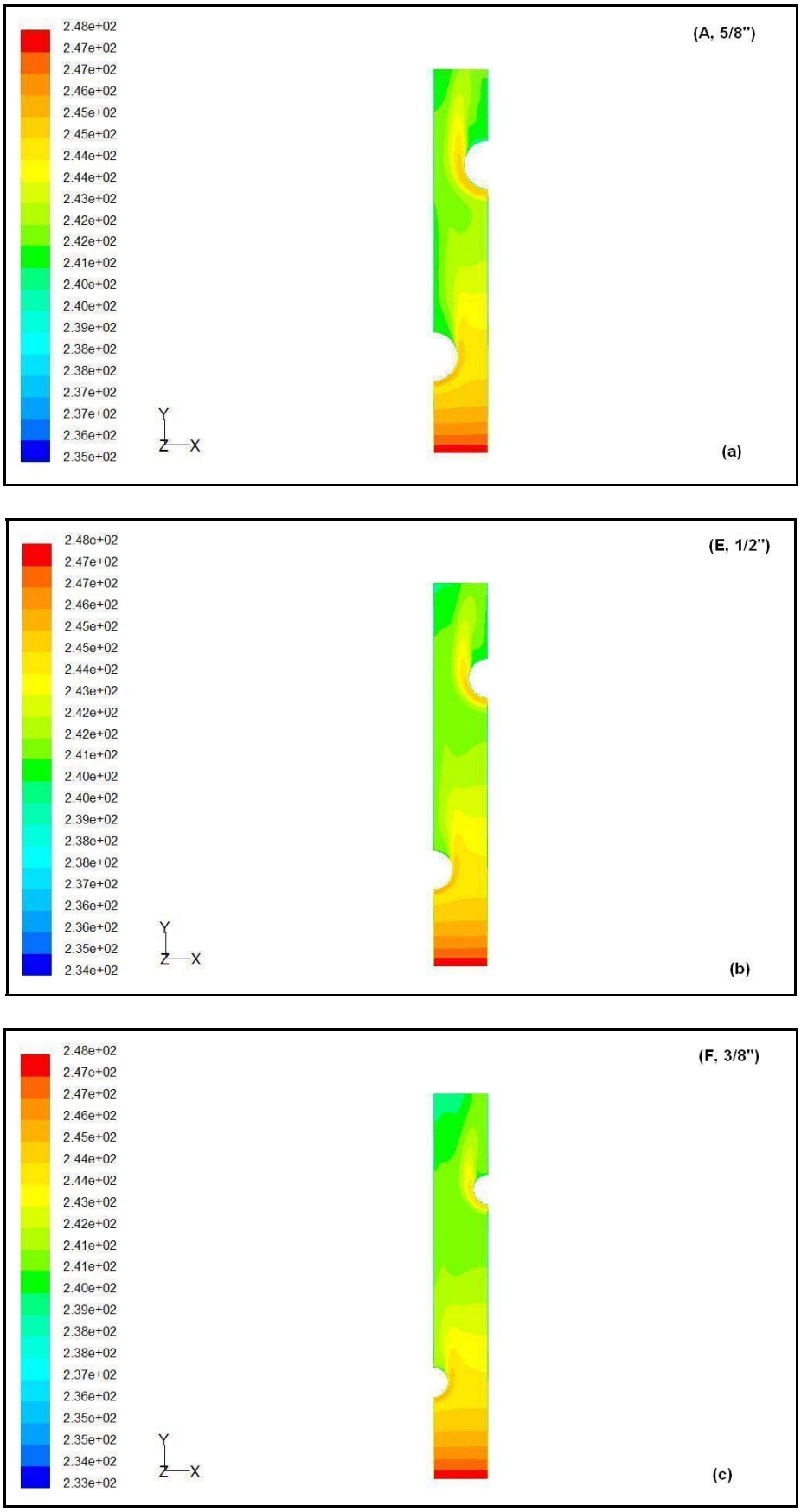

Figure 8.22 Effects of tube diameter on temperature contours

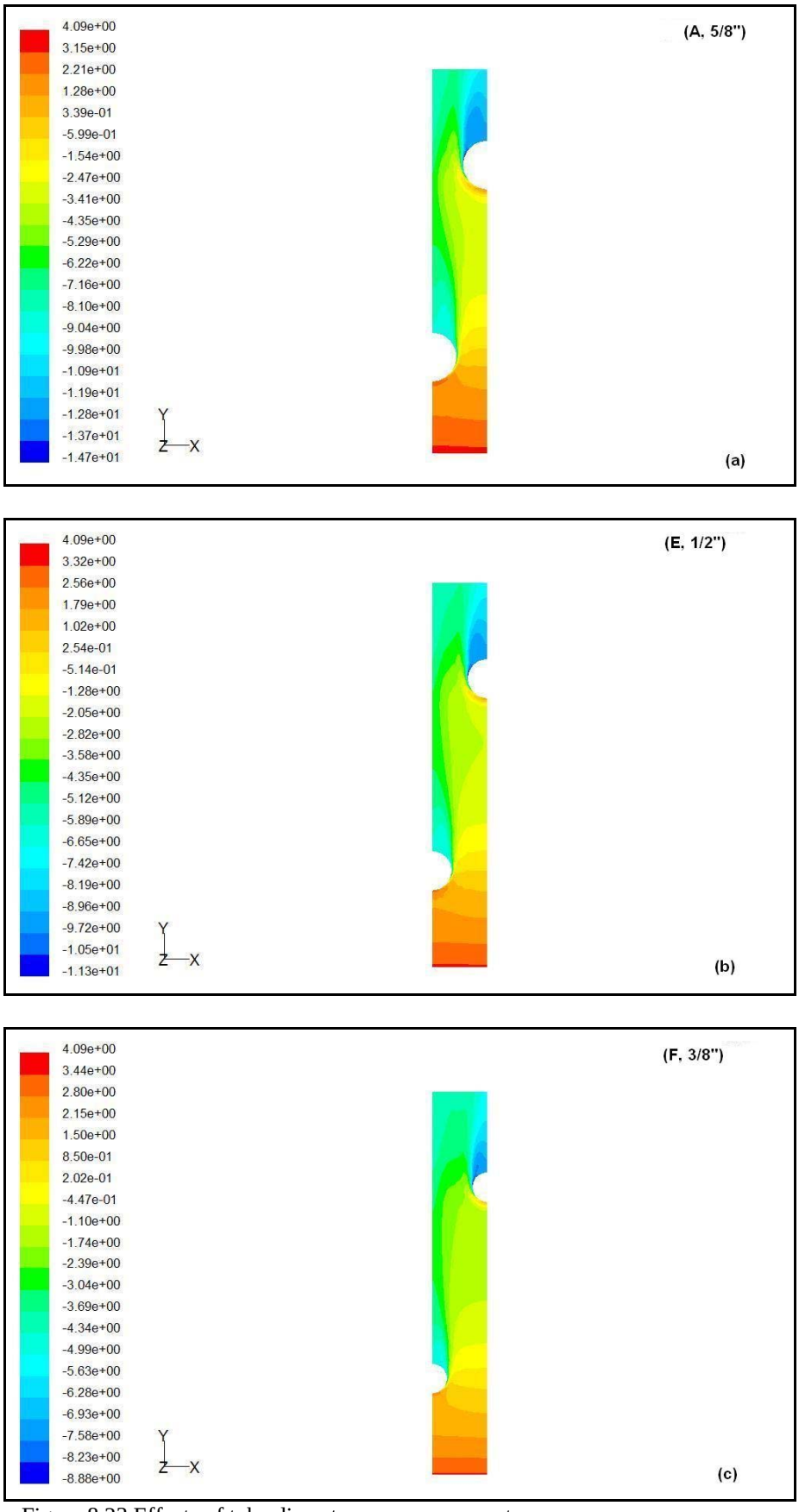

Figure 8.23 Effects of tube diameter on pressure contours

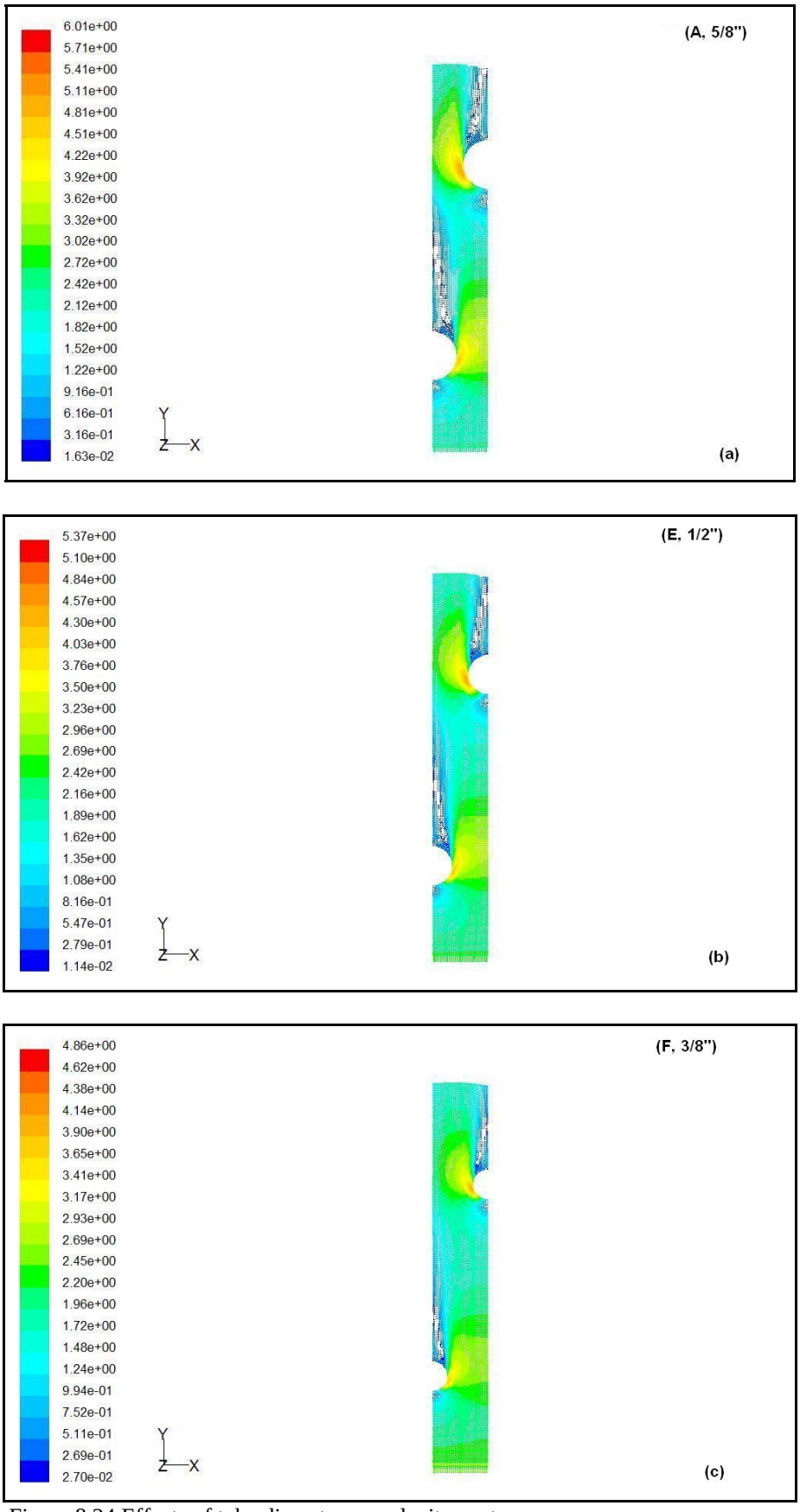

Figure 8.24 Effects of tube diameter on velocity vectors

8.4 Tube Arrangement Effect

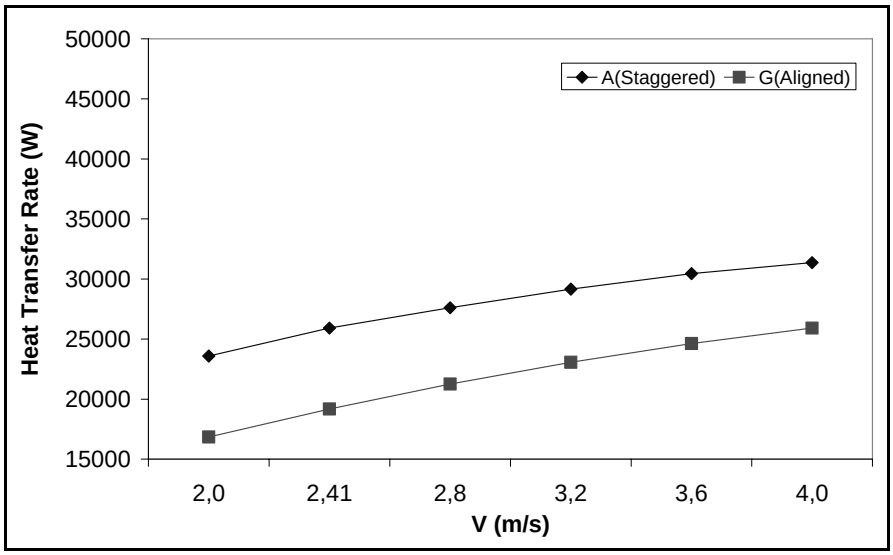

Figure 8.25 Effects of tube arrangement on heat transfer rate

As shown in Figure 8.25, the staggered tube arrangement improves heat exchanger performance more than 30% compared to the aligned tube arrangement.

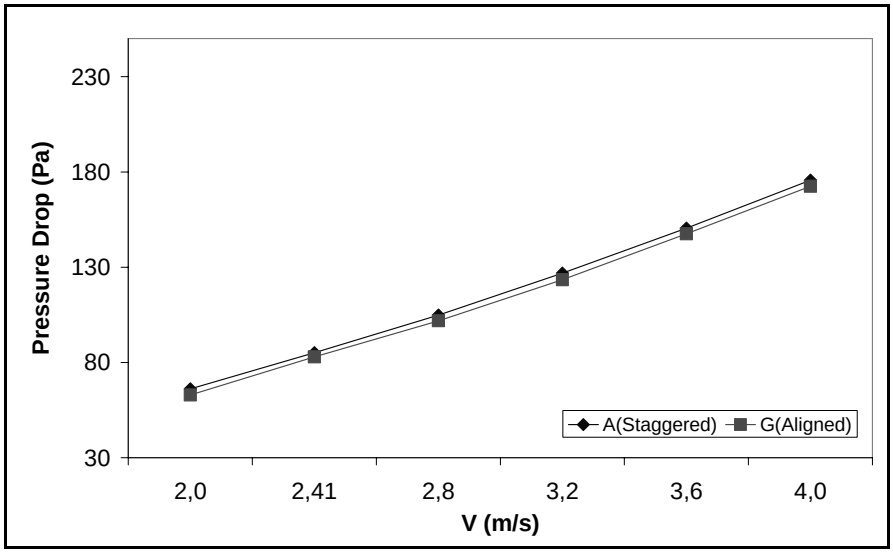

Figure 8.26 Effects of tube arrangement on pressure drop

Figure 8.26 shows that the effects of tube arrangement depending on the air inlet velocity on pressure drop. In staggered tube arrangement pressure drop is higher than aligned tube arrangement. Both of them increase with increasing air inlet velocity.

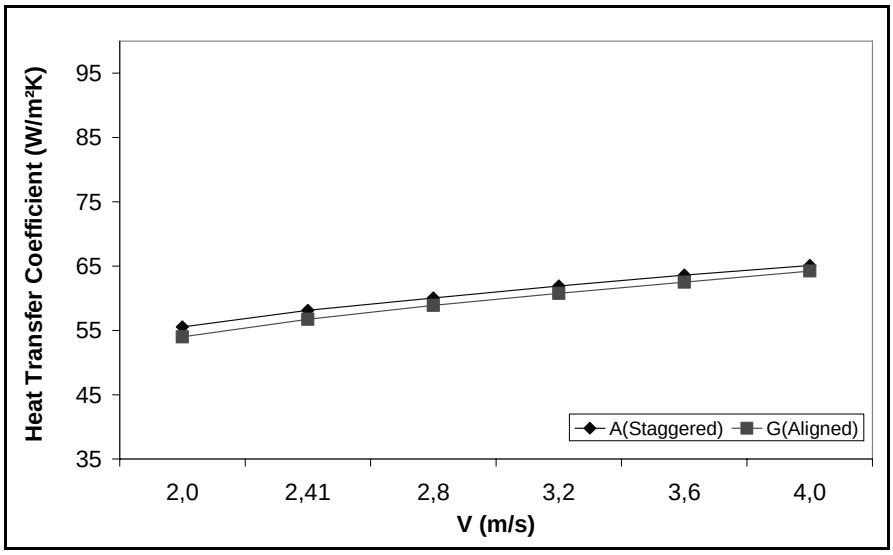

Figure 8.27 Effects of tube arrangement on heat transfer coefficient

Figure 8.27 shows the tube arrangement effect on heat transfer coefficient for two different models. Generally, the staggered tube arrangement yields higher enhancement of the heat transfer coefficient with increase intensity in turbulence.

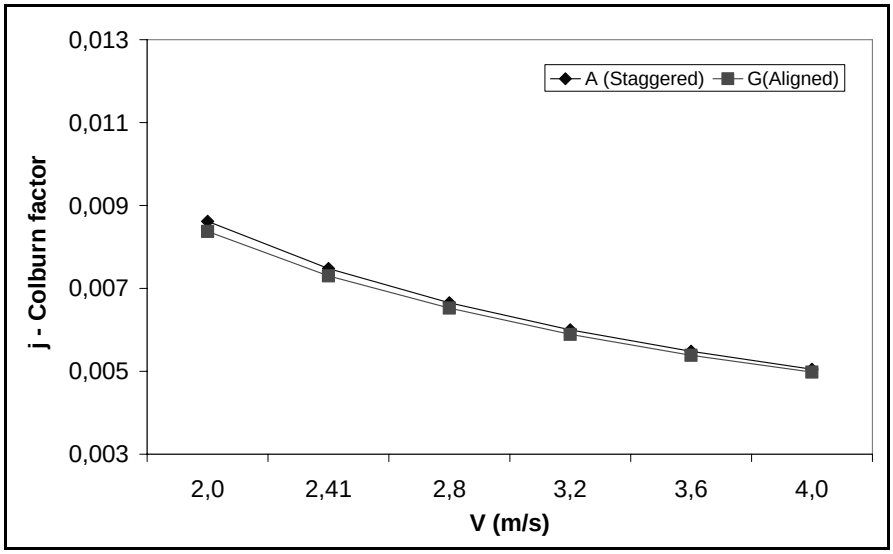

Figure 8.28 Effects of tube arrangement on Colburn factor

In Figure 8.28, the staggered tube arrangement has higher Colburn factors than aligned tube arrangement. The Colburn factors for both tube arrangements approaches the same value when the air inlet velocity increases.

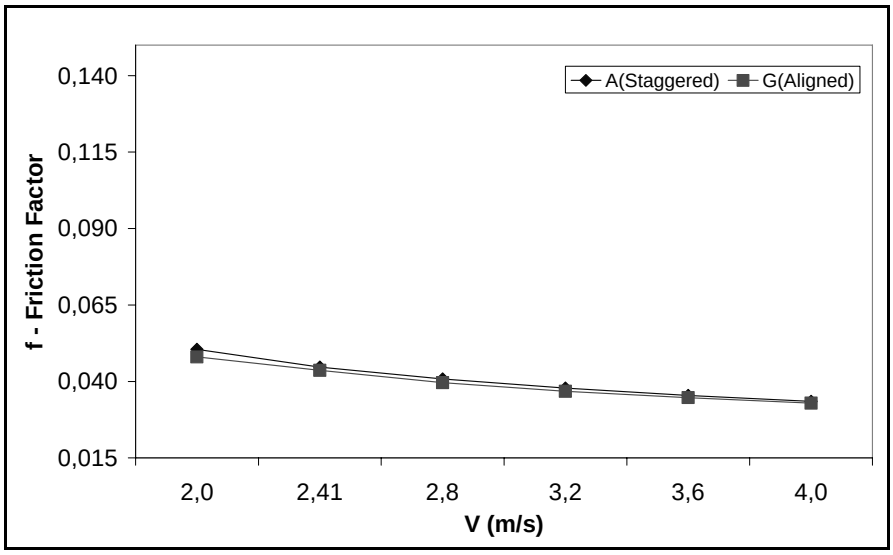

Figure 8.29 Effects of tube arrangement on friction factor

Figure 8.29 shows the effect of tube arrangement on the friction factor for two different geometries. The staggered tube arrangement has higher friction factor values. The decreasing slope of the friction factors gradually became less important for increasing air inlet velocities.

The effects of tube arrangement on temperature contours, pressure contours, and velocity vectors are shown in Figure 8.30, 8.31, and 8.32, respectively.

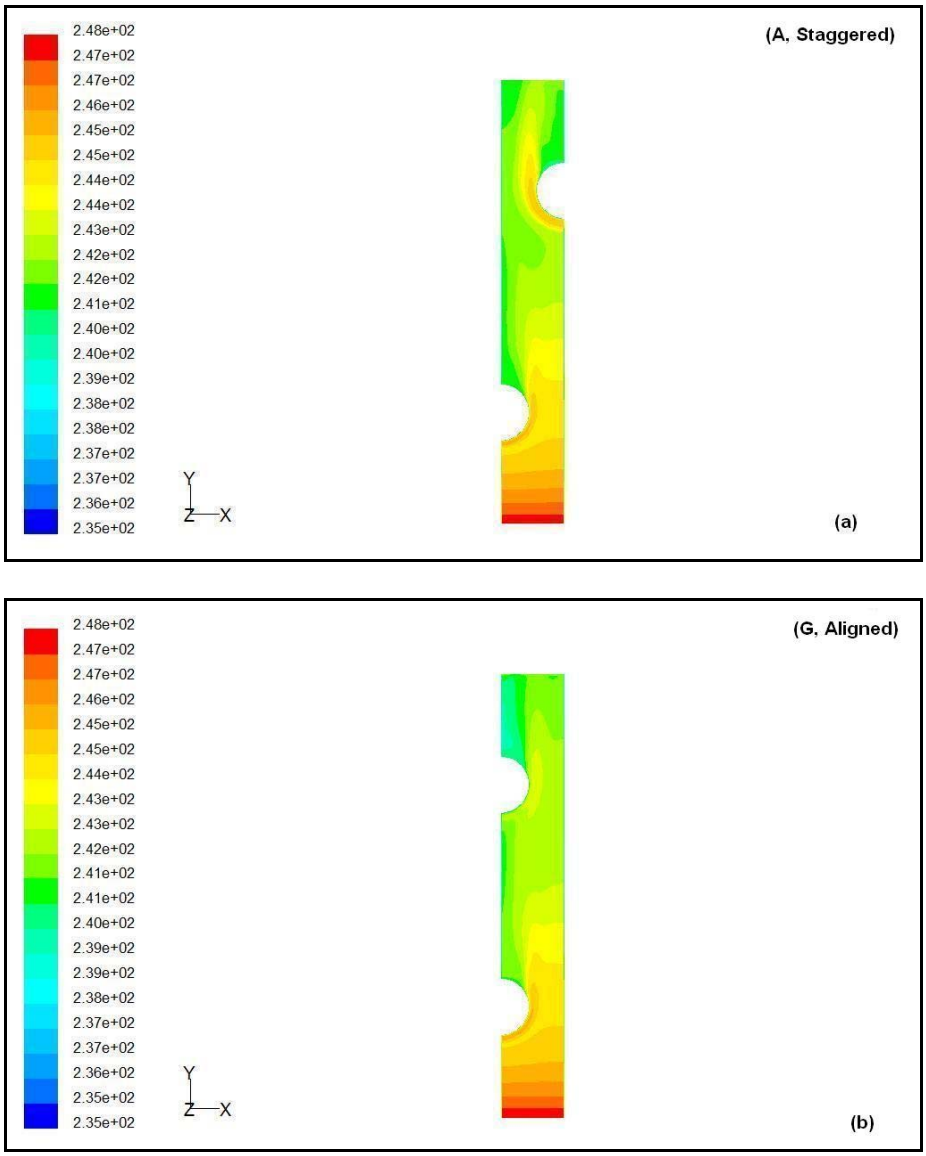

Figure 8.30 Effects of tube arrangement on temperature contours

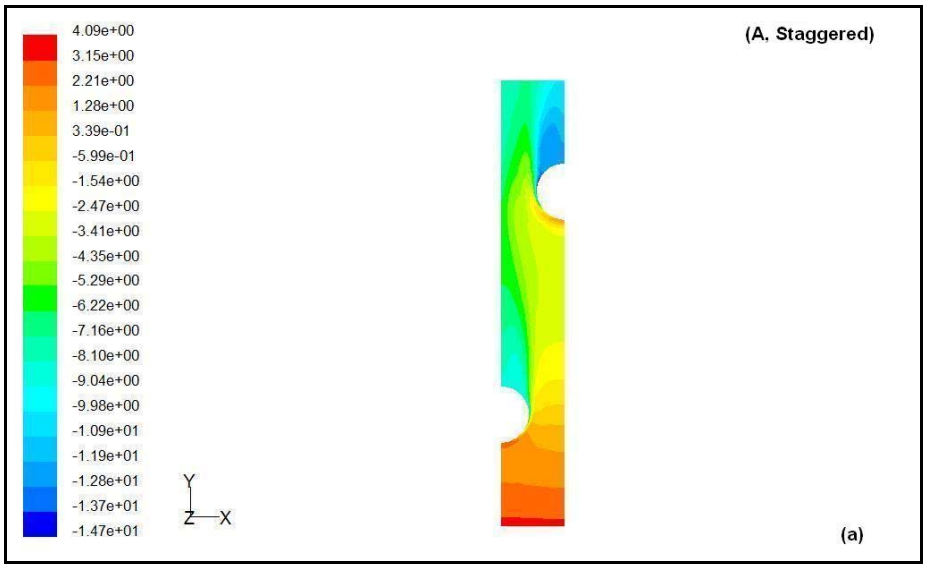

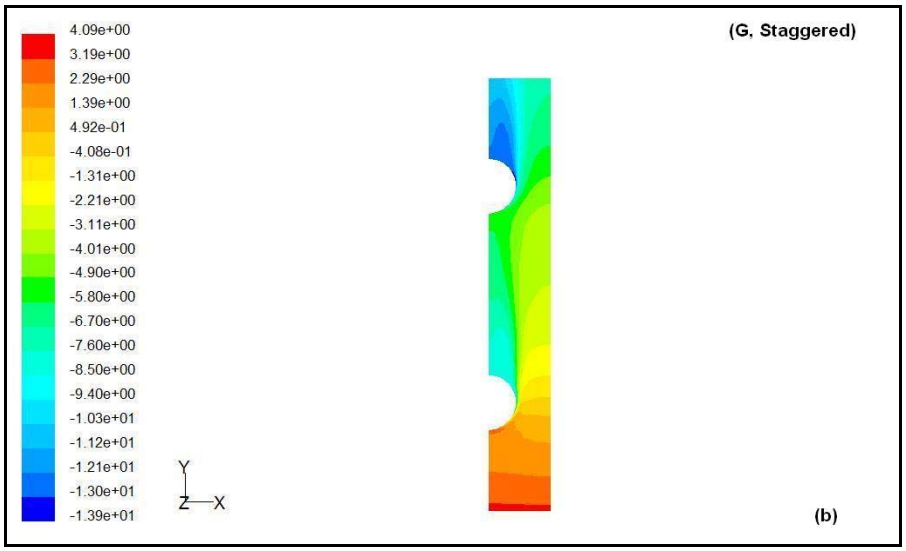

Figure 8.31 Effects of tube arrangement on pressure contours

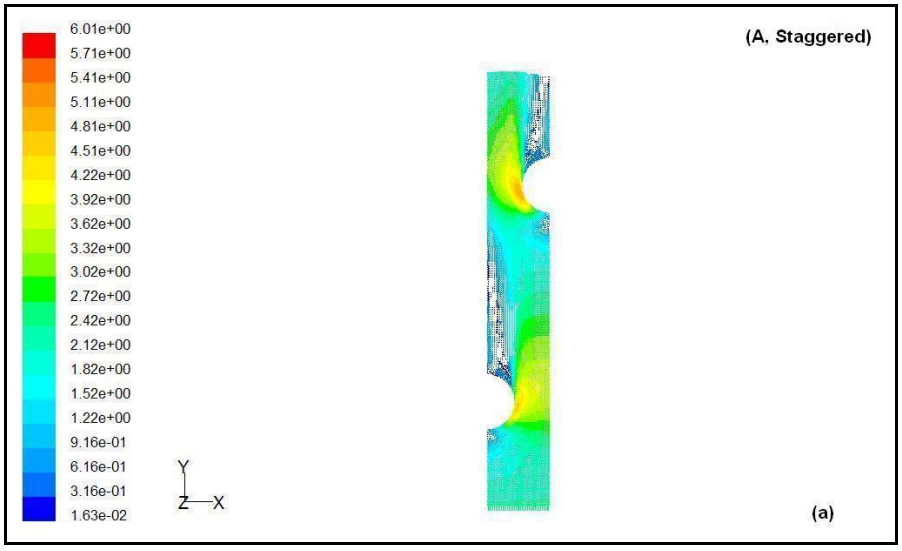

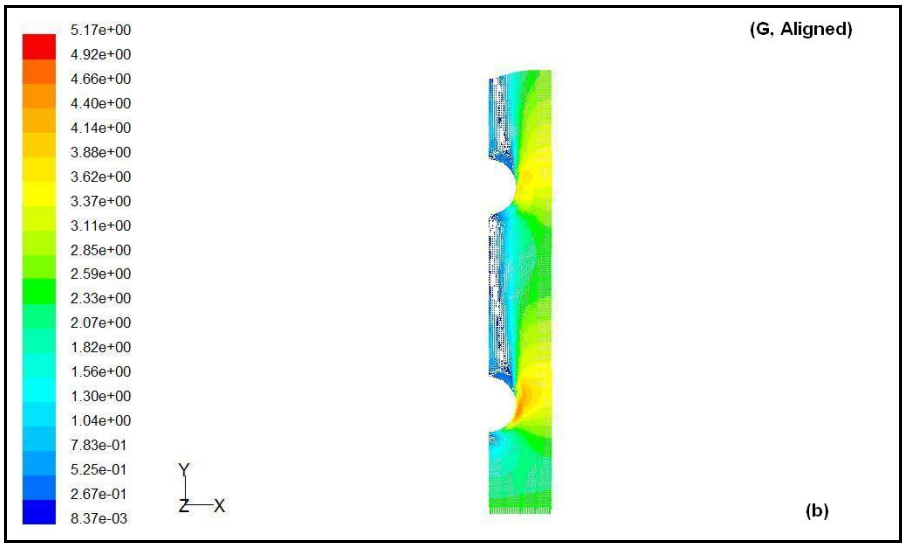

Figure 8.32 Effects of tube arrangement on velocity vectors

8.5 Transverse Tube Pitch Effect

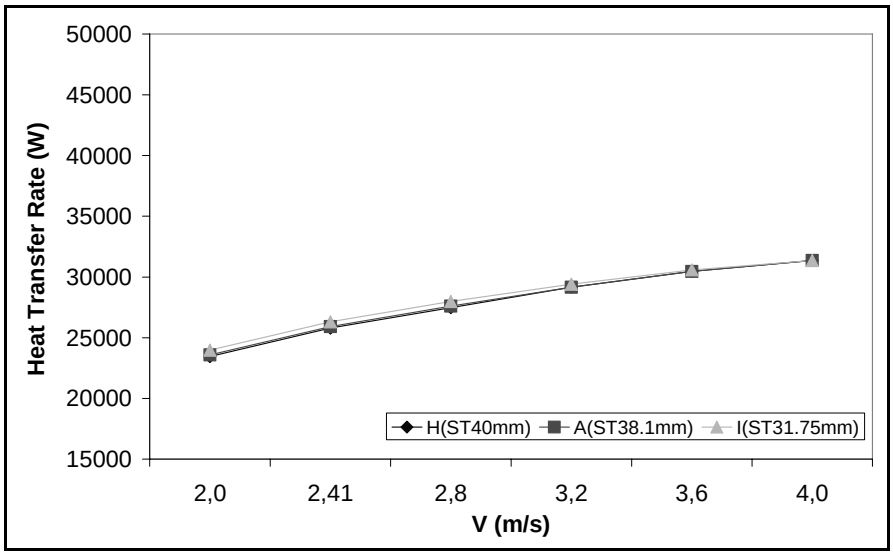

Figure 8.33 Effects of transverse tube pitch on heat transfer rate

As shown in Figure 8.33, the transverse tube pitch effect on heat transfer rate is negligible. The heat transfer rate for all transverse tube pitches approaches the same value when the air inlet velocity increases.

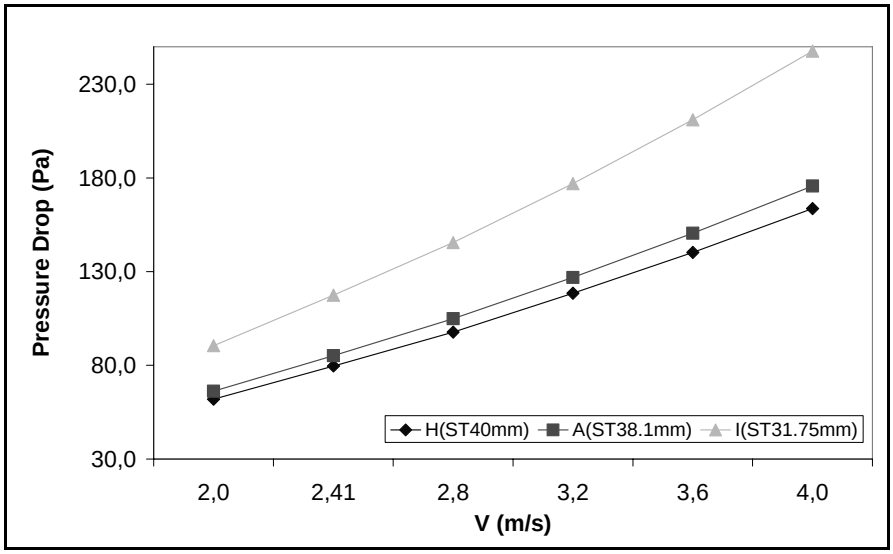

Figure 8.34 Effects of transverse tube pitch on pressure drop

The tube pitch effect on pressure drop for different geometrical models is shown in Figure 8.34. The pressure drop increases when the transverse tube pitch decreases.

The dependency of the transverse tube pitch on pressure drop is reduced with an increase in the air inlet velocity. Model I has a different slope because of the higher turbulence intensity.

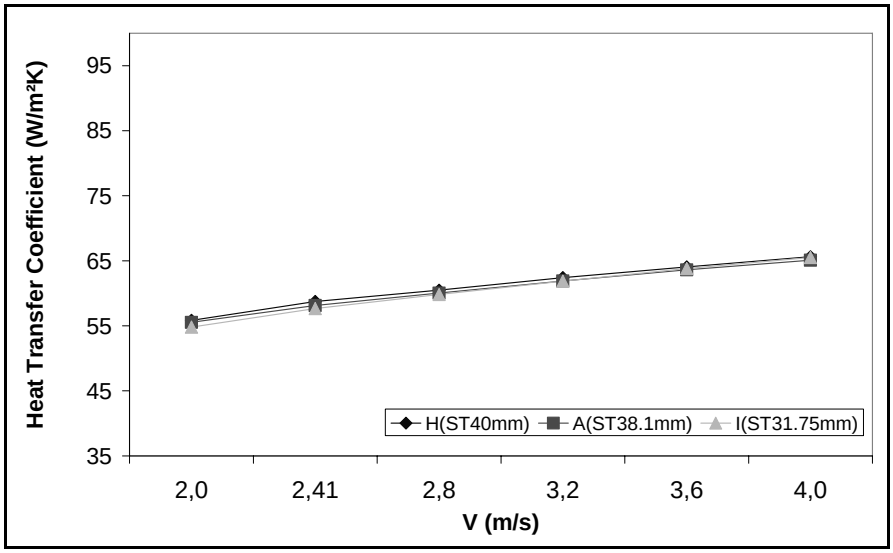

Figure 8.35 Effects of transverse tube pitch on heat transfer coefficient

Figure 8.35 shows that the effect of transverse tube pitch on heat transfer coefficient is negligible. The air side heat transfer coefficient increases with increasing air inlet velocity.

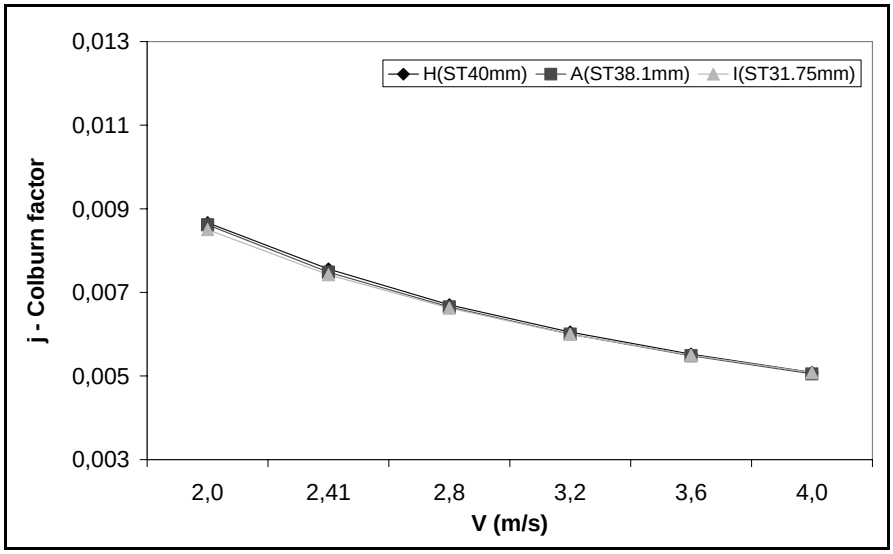

Figure 8.36 Effects of transverse tube pitch on Colburn factor

As shown in Figure 8.36, the effect of transverse tube pitch on the Colburn factor is negligible for different geometrical models. Increasing air inlet velocity decreases Colburn factor.

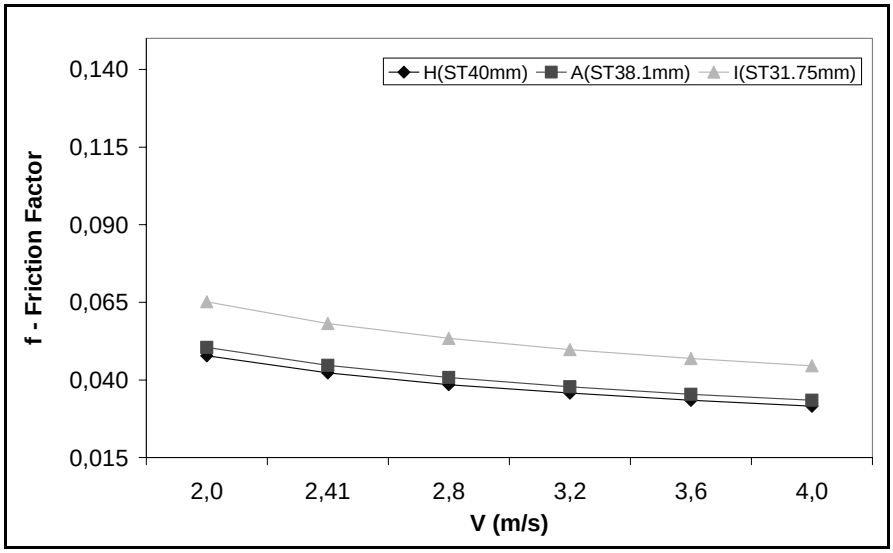

Figure 8.37 Effects of transverse tube pitch on friction factor

Figure 8.37 shows the effect of transverse tube pitch depending on the air inlet velocity on friction factor for different geometrical models. Two different models except Model I has similar slopes and both of them has lower friction factors. Model I has higher friction factor because of the higher turbulence intensity.

The effects of transverse tube pitch on temperature contours, pressure contours, and velocity vectors are shown in Figure 8.38, 8.39, and 8.40, respectively.

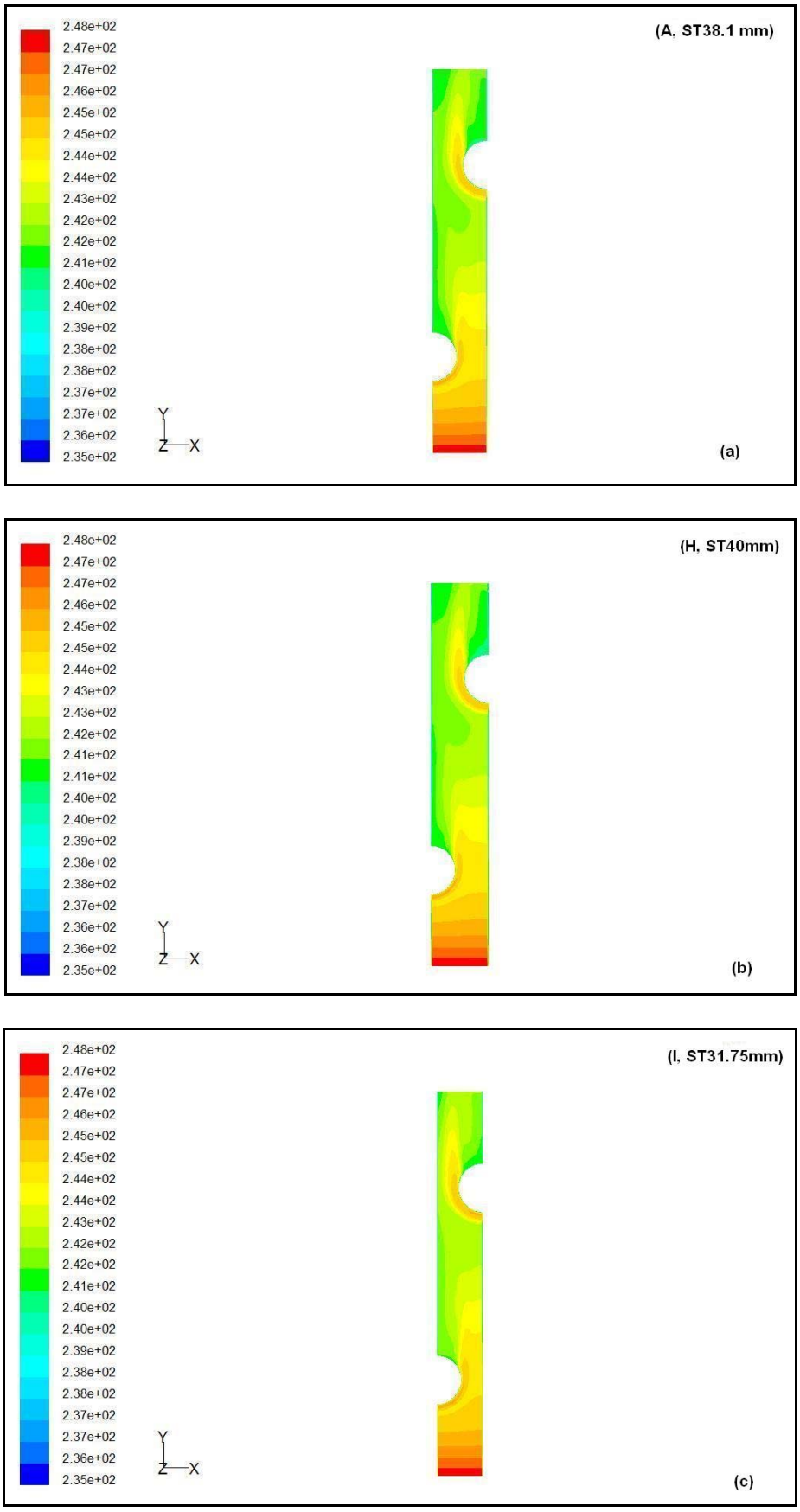

Figure 8.38 Effects of transverse tube pitch on temperature contours

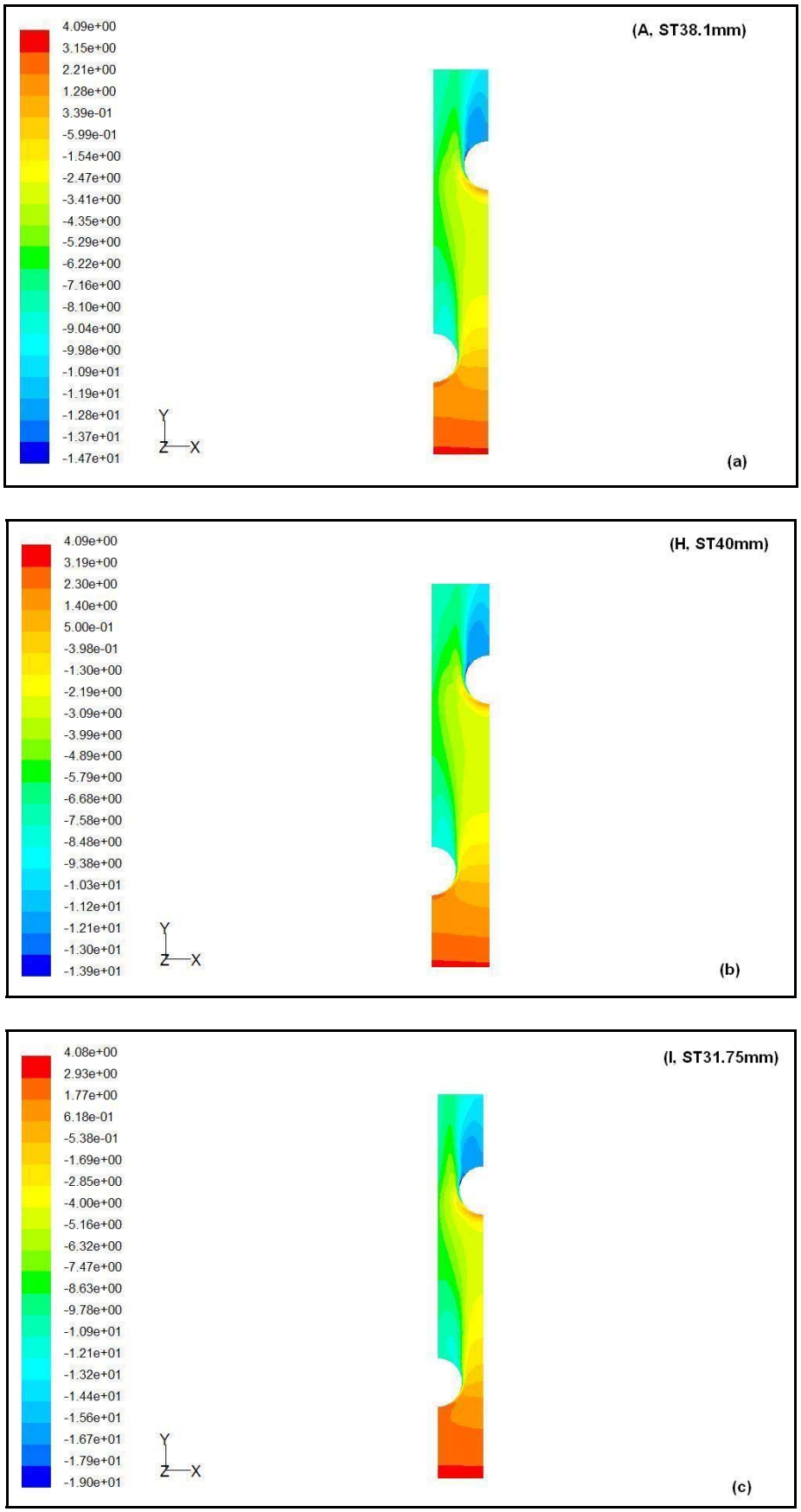

Figure 8.39 Effects of transverse tube pitch on pressure contours

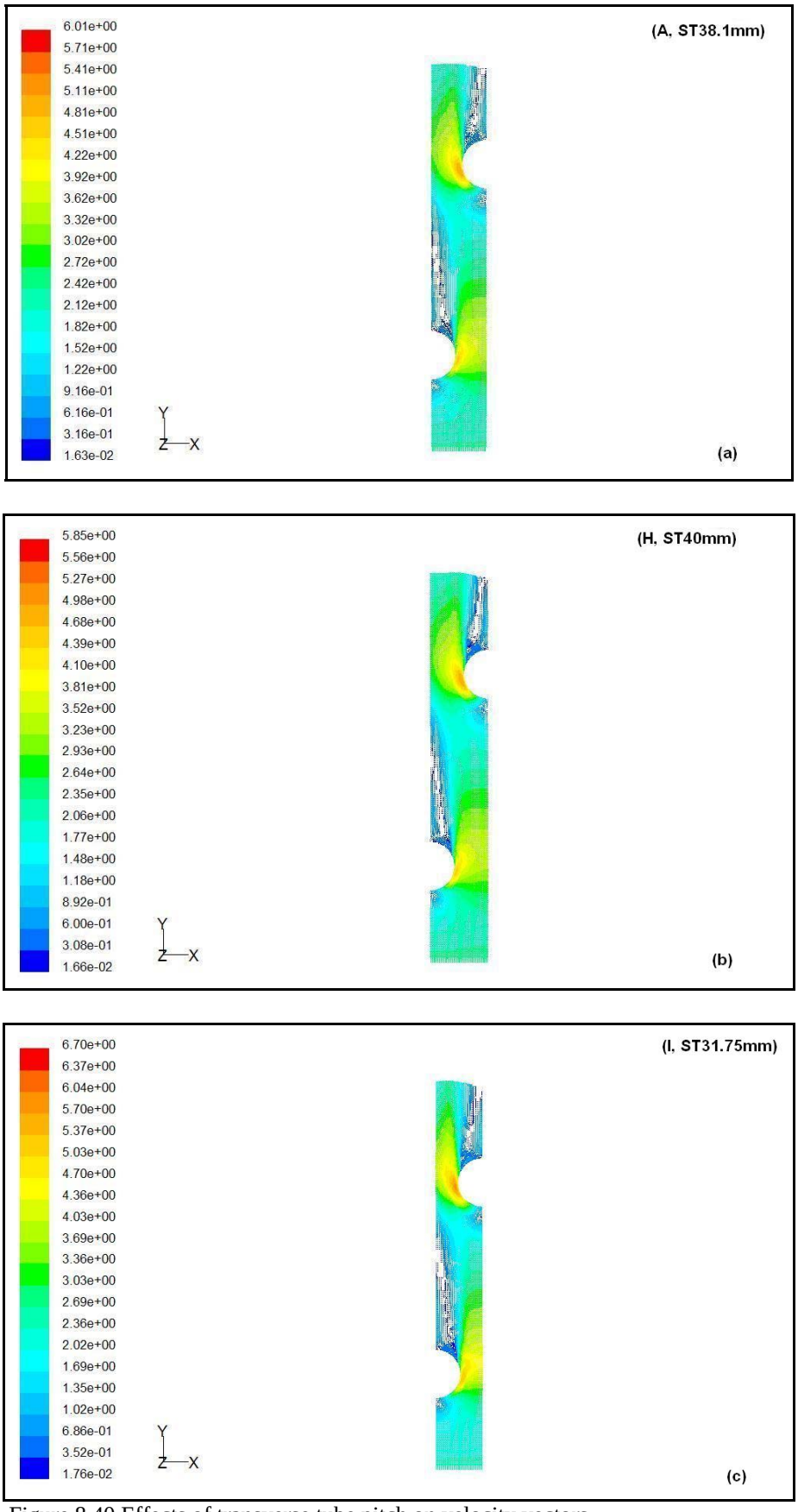

Figure 8.40 Effects of transverse tube pitch on velocity vectors

8.6 Longitudinal Tube Pitch Effect

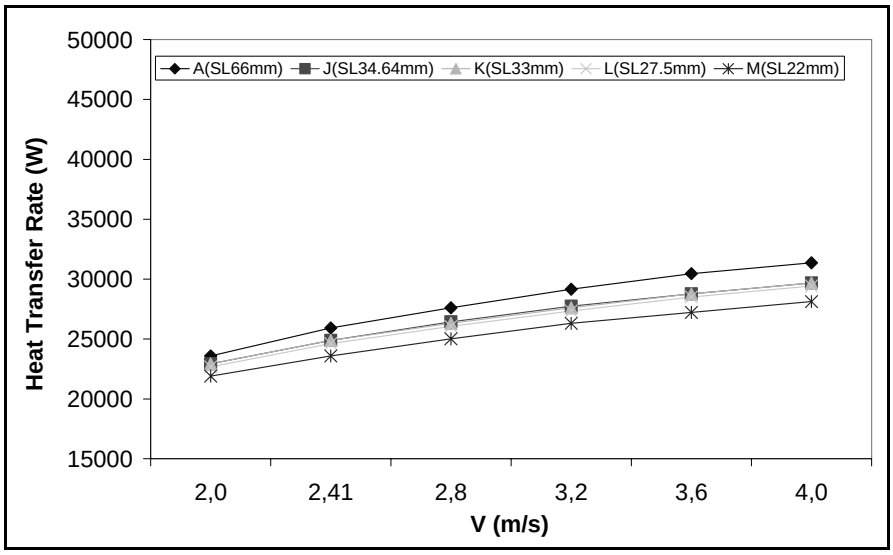

Figure 8.41 Effects of longitudinal tube pitch on heat transfer rate

Figure 8.41 shows that greater heat transfer rates are obtained as the longitudinal tube pitch increases, due to the increased heat transfer area.

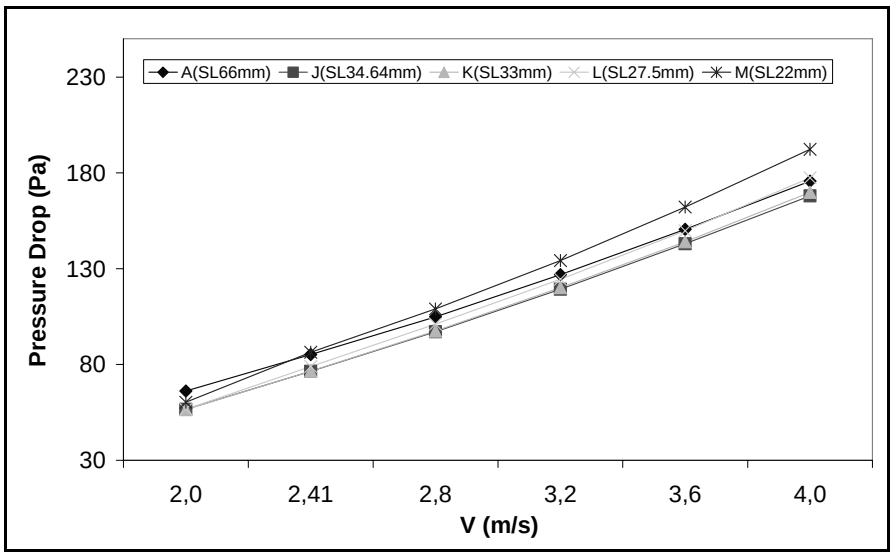

Figure 8.42 Effects of longitudinal tube pitch on pressure drop

As shown in Figure 8.42, the pressure drop increases with a reduction of longitudinal tube pitches.

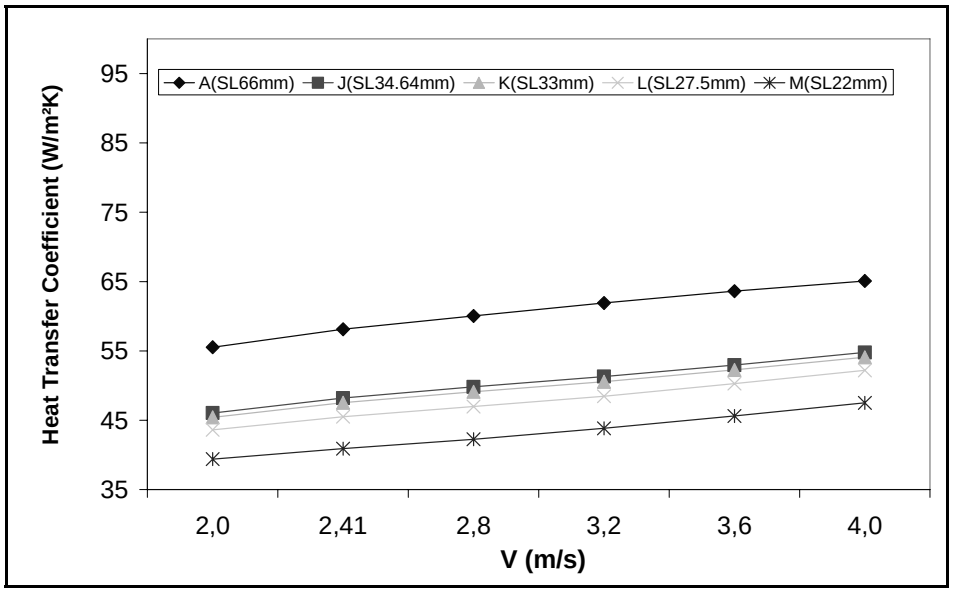

Figure 8.43 Effects of longitudinal tube pitch on heat transfer coefficient

Figure 8.43 shows the effect of longitudinal tube pitch with increasing air inlet velocity on heat transfer coefficient. The air side heat transfer coefficient increases with an increase of the longitudinal tube pitch. All slopes are separated from each other. Model A and M are different from the others because of the very large and very small longitudinal tube pitches.

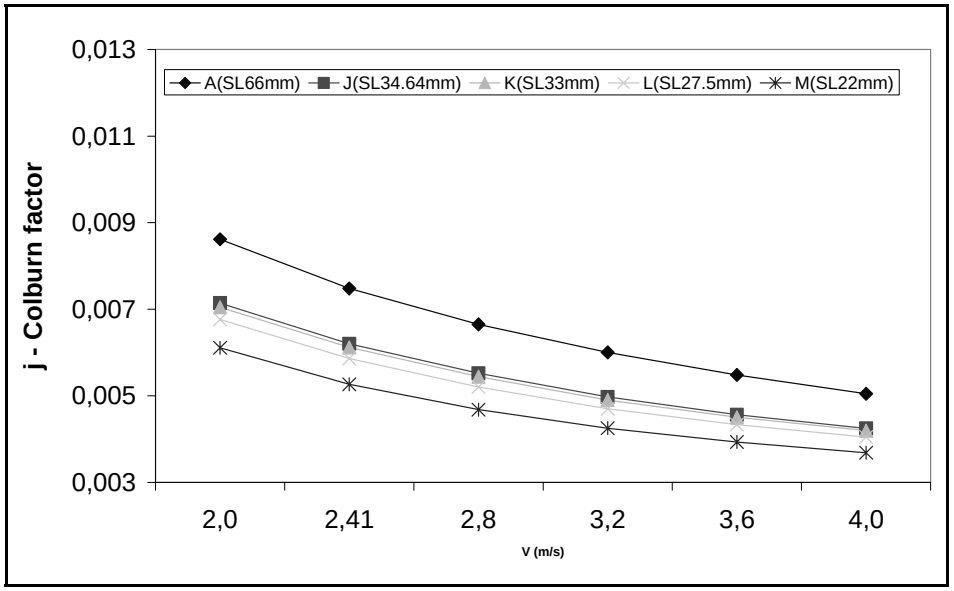

Figure 8.44 Effects of longitudinal tube pitch on Colburn factor

As shown in Figure 8.44, the longitudinal tube pitch has an important effect on Colburn factor. As the longitudinal tube pitch decreases from 66 mm to 22 mm, the Colburn factor decreases by 33% and 20% for air inlet velocity of 2 m/s and 4 m/s, respectively.

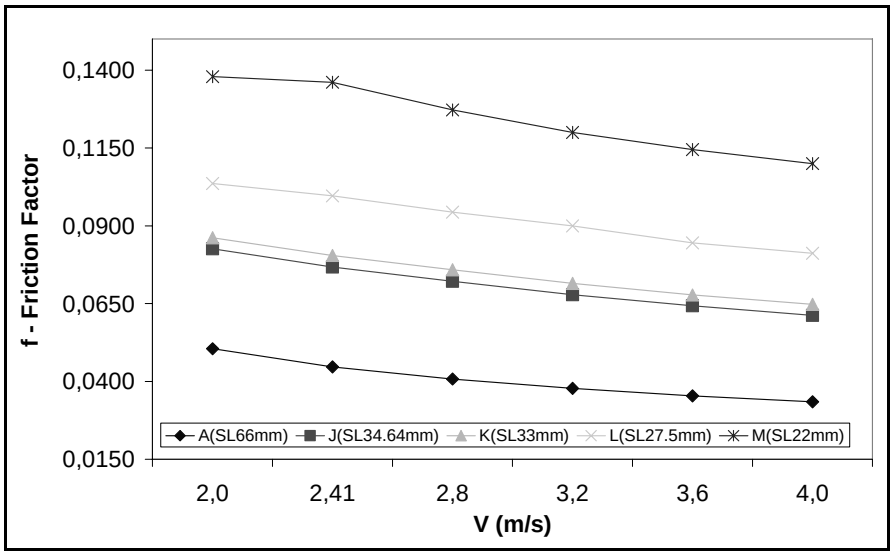

Figure 8.45 Effects of longitudinal tube pitch on friction factor

Figure 8.45 shows the effect of longitudinal tube pitch on friction factor for different geometrical models. Generally, the friction factor increases with a reduction of longitudinal tube pitches.

The effects of transverse tube pitch on temperature contours, pressure contours, and velocity vectors are shown in Figure 8.46, 8.47, and 8.48, respectively.

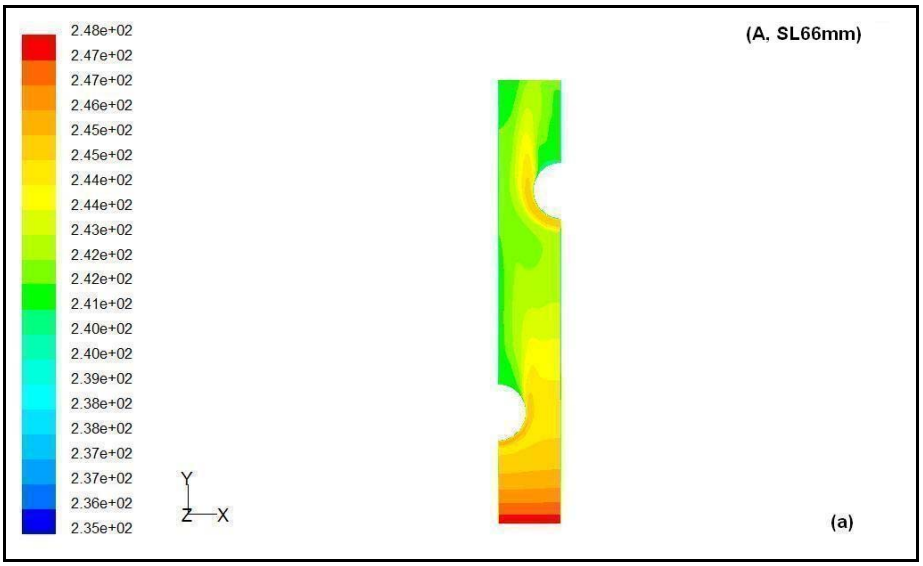
2.48e+02
2.47e+02
2.47e+02
2.46e+02
2.45e+02
2.45e+02
2.44e+02
2.44e+02
2.43e+02
2.42e+02
2.42e+02
2.41e+02
2.40e+02
2.40e+02
2.39e+02
2.38e+02
2.38e+02
2.37e+02
2.37e+02
2.36e+02
2.35e+02
Y
Z
X
(A, SL66mm)
(a)

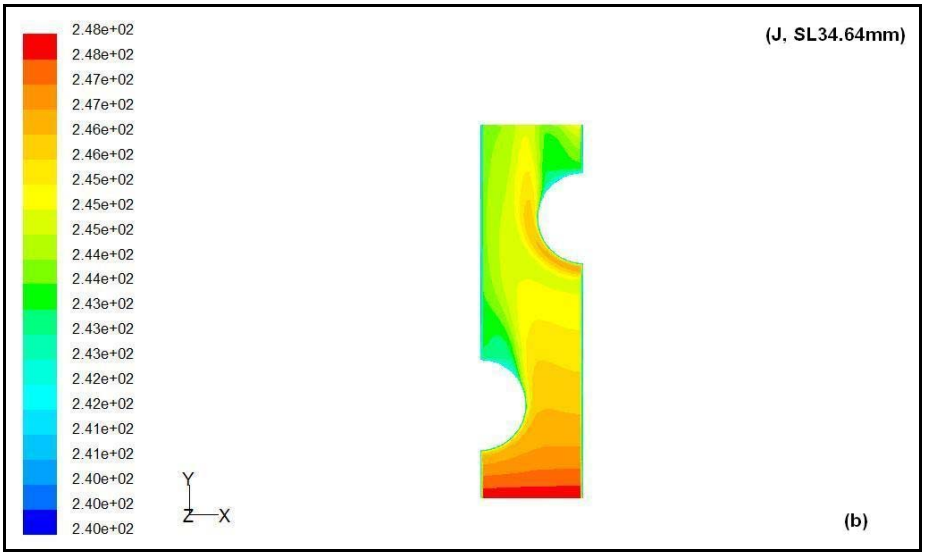
2.48e+02
2.48e+02
2.47e+02
2.47e+02
2.46e+02
2.46e+02
2.45e+02
2.45e+02
2.45e+02
2.44e+02
2.44e+02
2.43e+02
2.43e+02
2.43e+02
2.42e+02
2.42e+02
2.41e+02
2.41e+02
2.40e+02
2.40e+02
2.40e+02
Y
Z
X
(J, SL34.64mm)
(b)

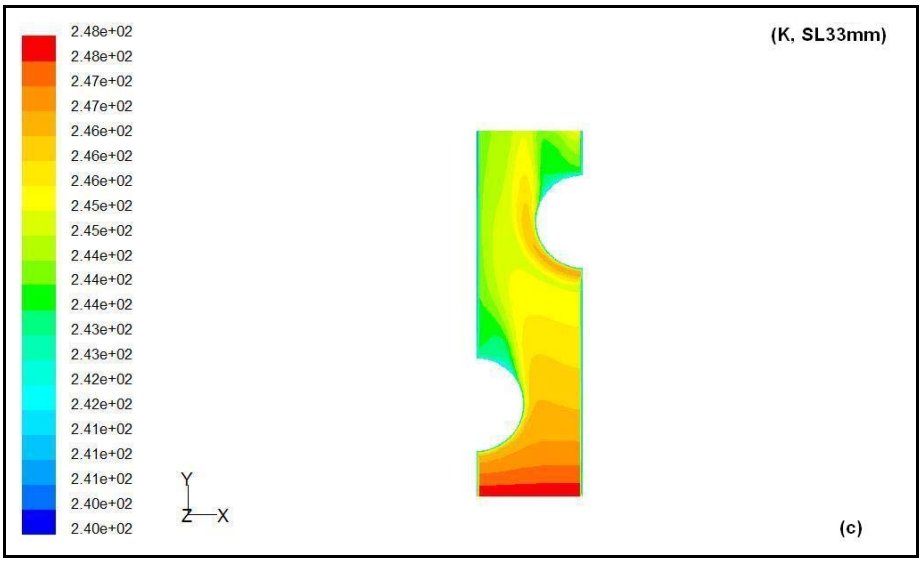
2.48e+02
2.48e+02
2.47e+02
2.47e+02
2.46e+02
2.46e+02
2.46e+02
2.45e+02
2.45e+02
2.44e+02
2.44e+02
2.44e+02
2.43e+02
2.43e+02
2.42e+02
2.42e+02
2.41e+02
2.41e+02
2.41e+02
2.40e+02
2.40e+02
Y
Z
X
(K, SL33mm)
(c)

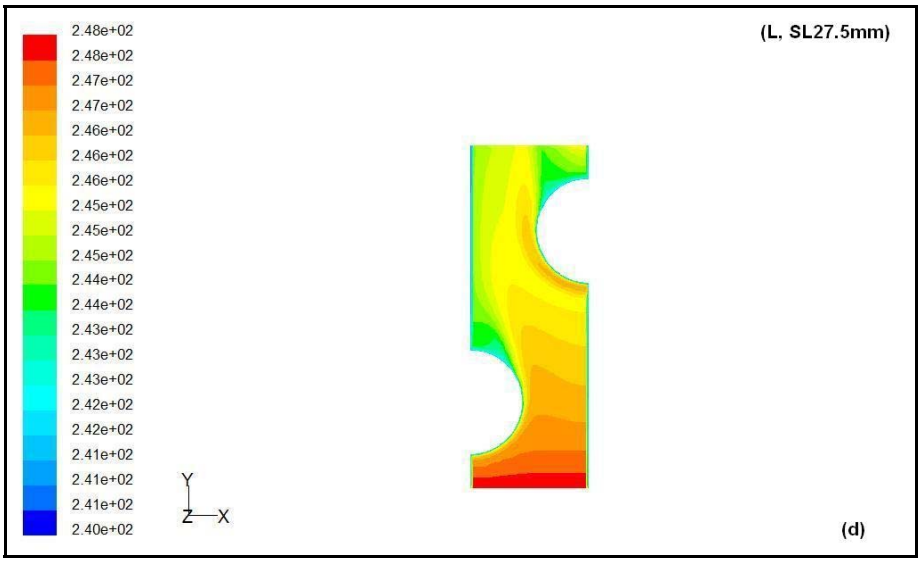

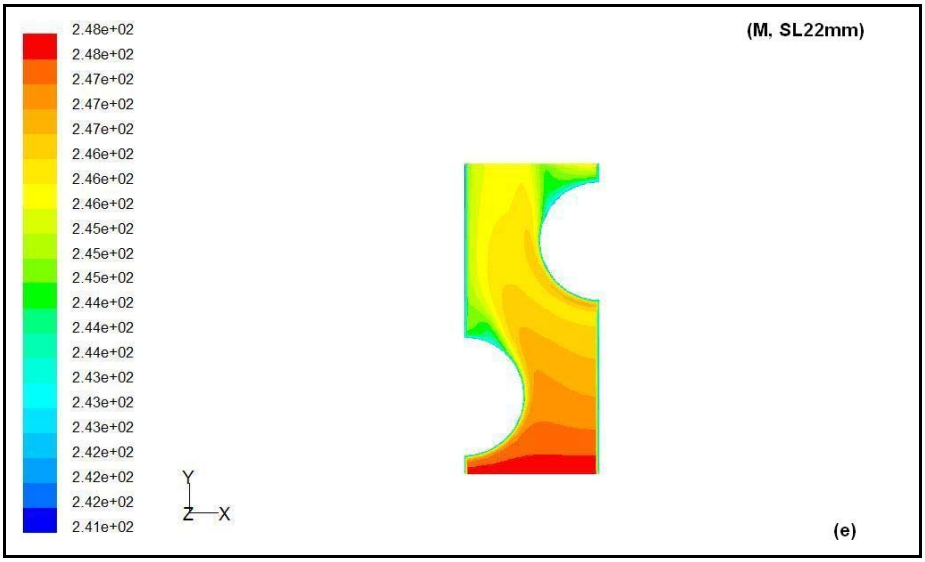

Figure 8.46 Effects of longitudinal tube pitch on temperature contours

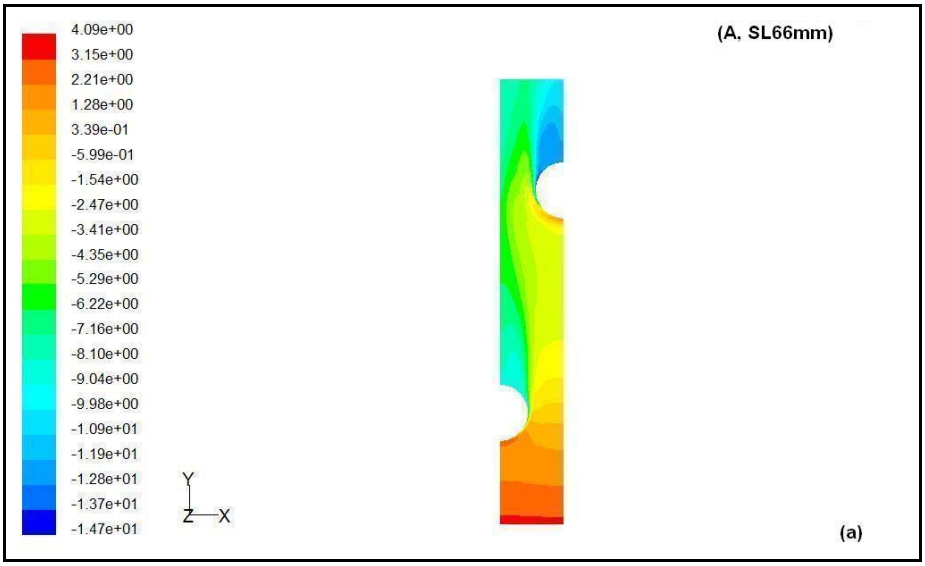

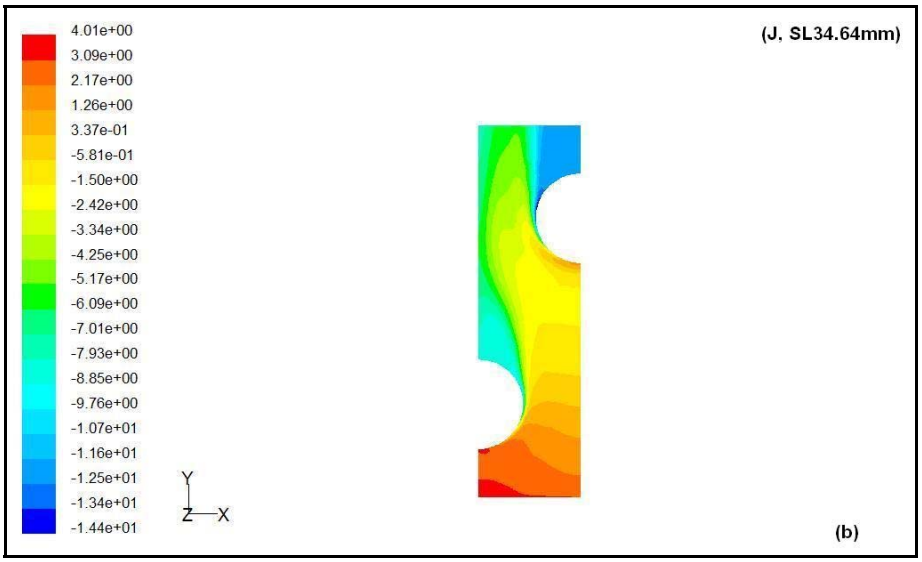
4.01e+00
3.09e+00
2.17e+00
1.26e+00
3.37e-01
-5.81e-01
-1.50e+00
-2.42e+00
-3.34e+00
-4.25e+00
-5.17e+00
-6.09e+00
-7.01e+00
-7.93e+00
-8.85e+00
-9.76e+00
-1.07e+01
-1.16e+01
-1.25e+01
-1.34e+01
-1.44e+01
Y
Z
X
(J, SL34.64mm)
(b)

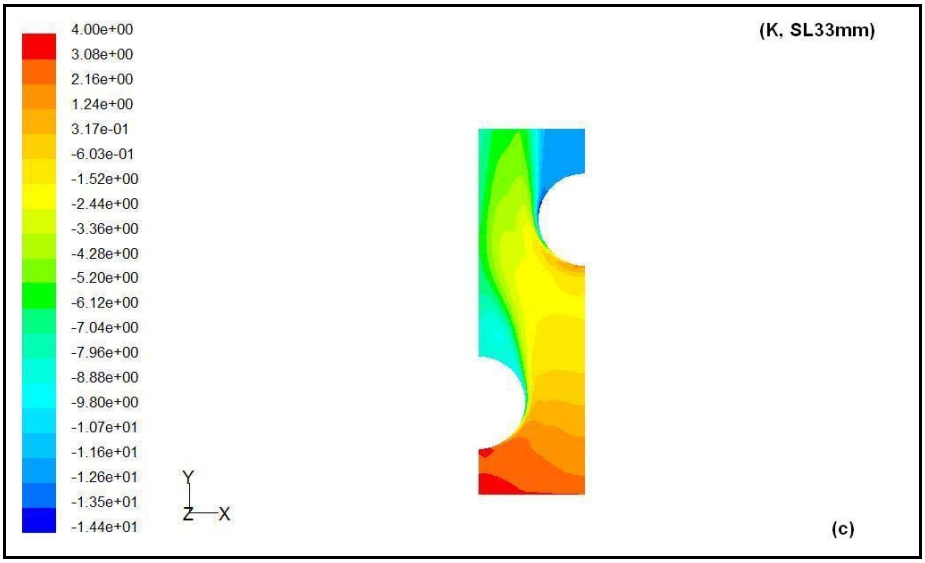
4.00e+00
3.08e+00
2.16e+00
1.24e+00
3.17e-01
-6.03e-01
-1.52e+00
-2.44e+00
-3.36e+00
-4.28e+00
-5.20e+00
-6.12e+00
-7.04e+00
-7.96e+00
-8.88e+00
-9.80e+00
-1.07e+01
-1.16e+01
-1.26e+01
-1.35e+01
-1.44e+01
Y
Z
X
(K, SL33mm)
(c)

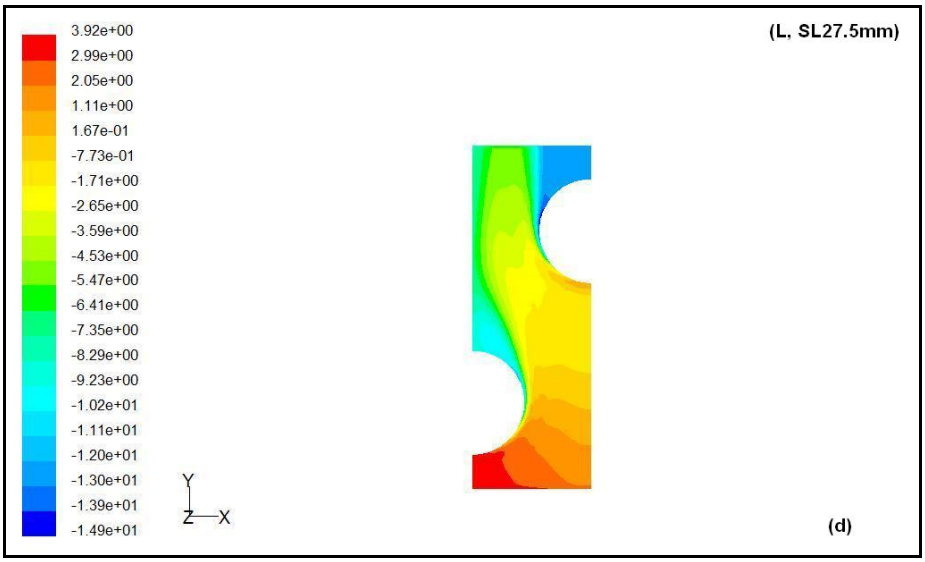
3.92e+00
2.99e+00
2.05e+00
1.11e+00
1.67e-01
-7.73e-01
-1.71e+00
-2.65e+00
-3.59e+00
-4.53e+00
-5.47e+00
-6.41e+00
-7.35e+00
-8.29e+00
-9.23e+00
-1.02e+01
-1.11e+01
-1.20e+01
-1.30e+01
-1.39e+01
-1.49e+01
Y
Z
X
(L, SL27.5mm)
(d)

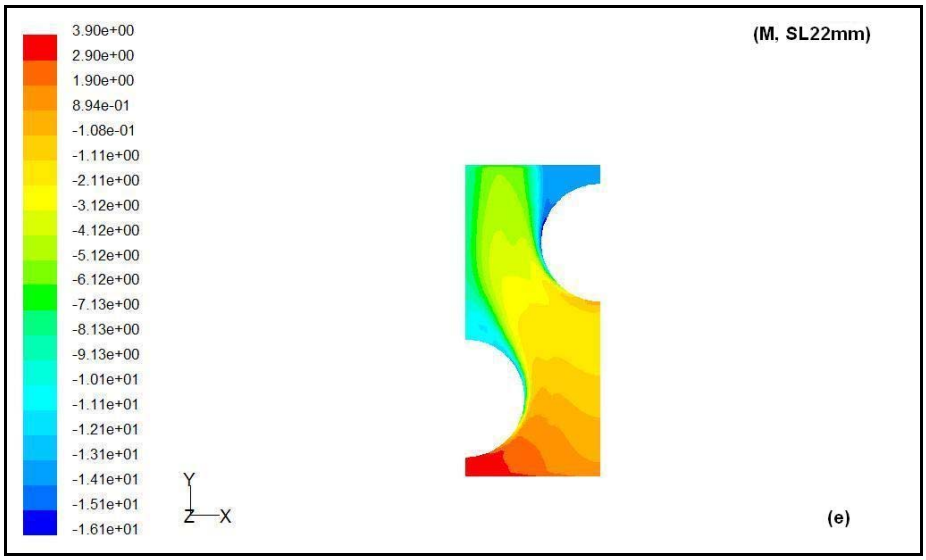

Figure 8.47 Effects of longitudinal tube pitch on pressure contours

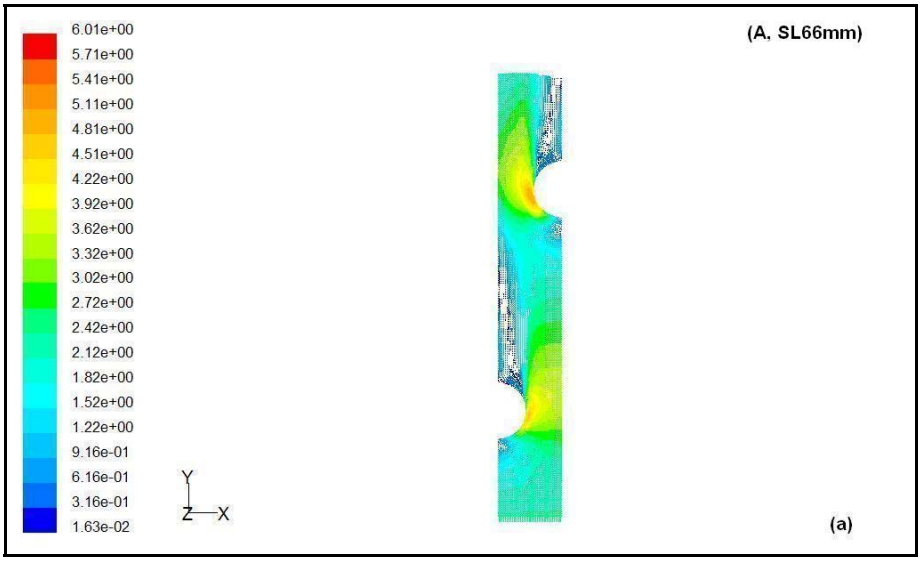

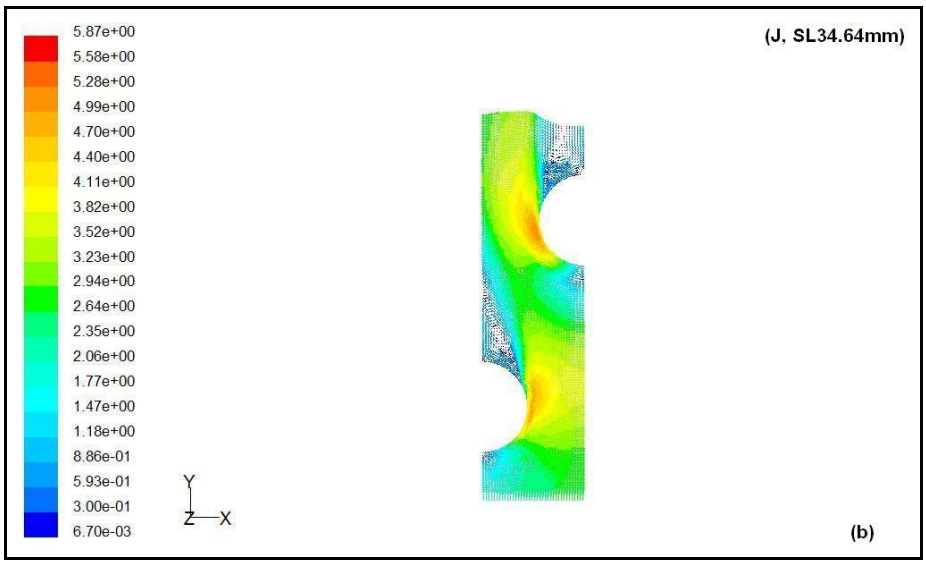

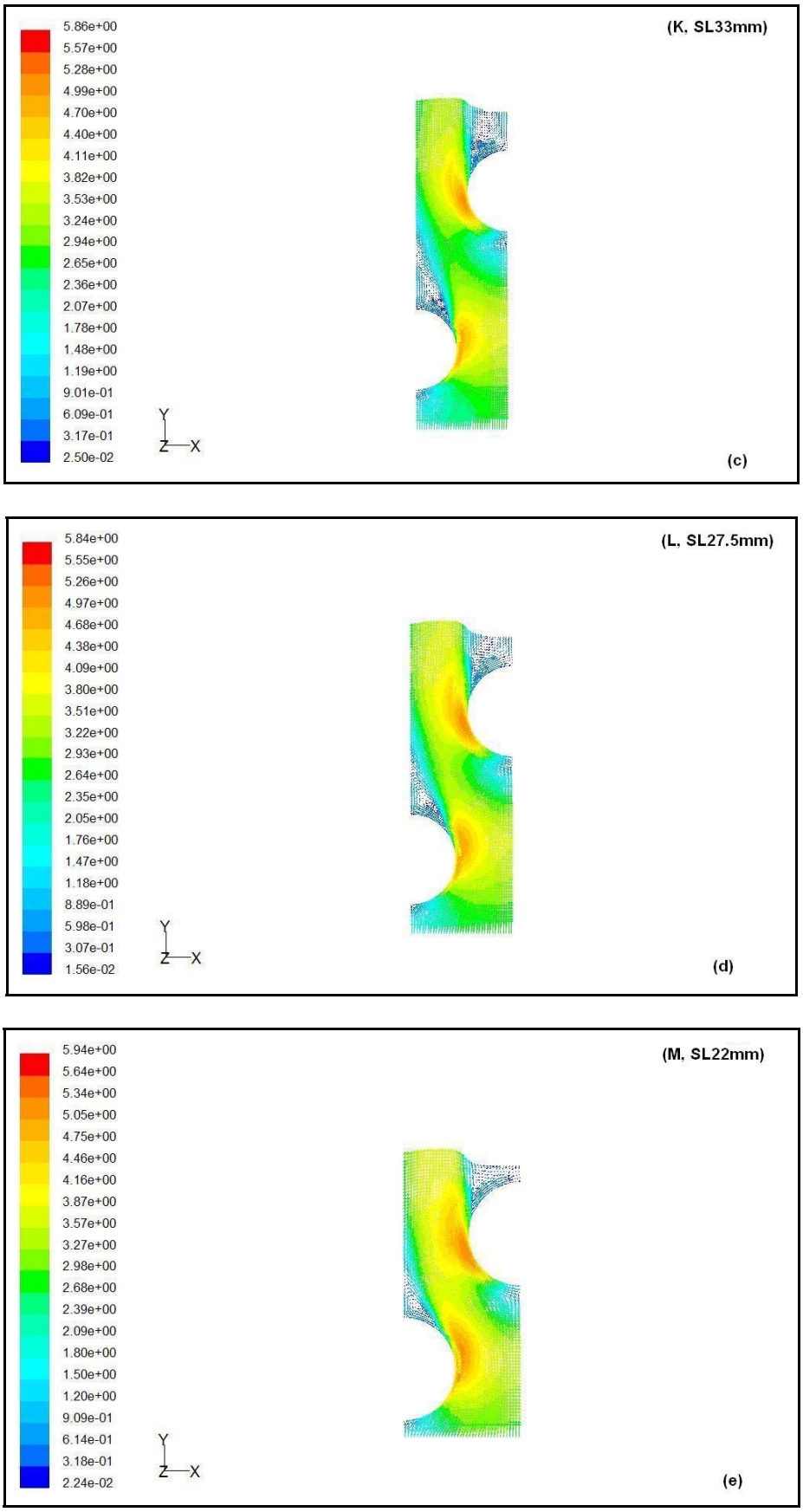

Figure 8.48 Effects of longitudinal tube pitch on velocity vectors

8.7 Fin Material Effect

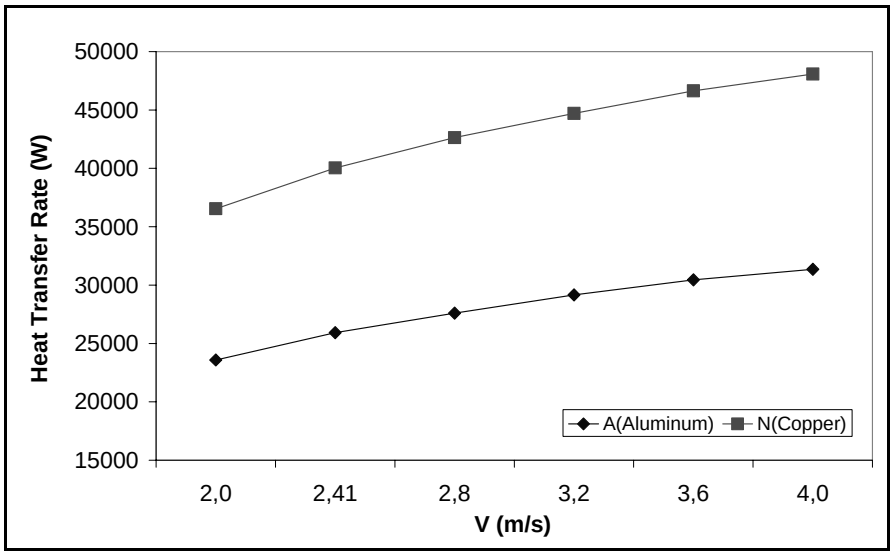

Figure 8.49 Effects of fin material on heat transfer rate

As shown in Figure 8.49, greater heat transfer rates are obtained as the copper fin is selected. Heat transfer increases with increasing air inlet velocity.

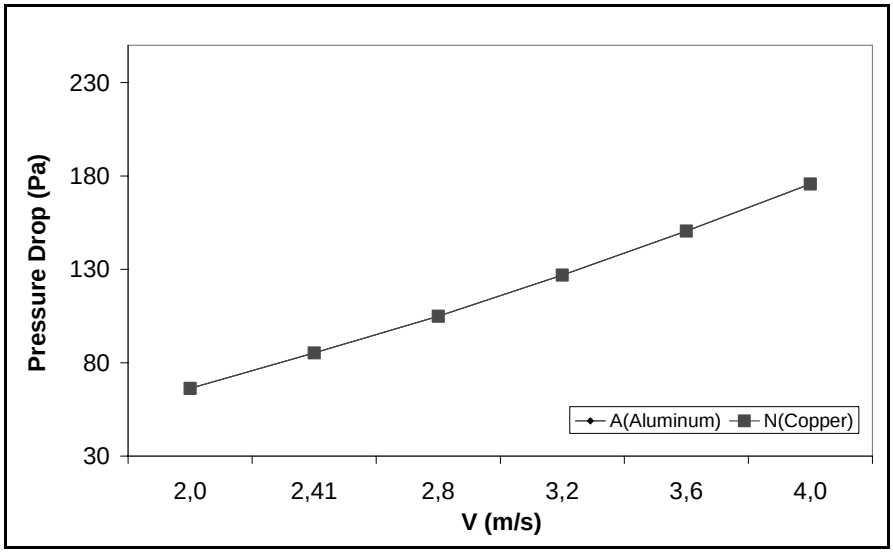

Figure 8.50 Effects of fin material on pressure drop

Figure 8.50 shows that the fin material has no change on pressure drop. The pressure drop increases with the increasing air inlet velocity.

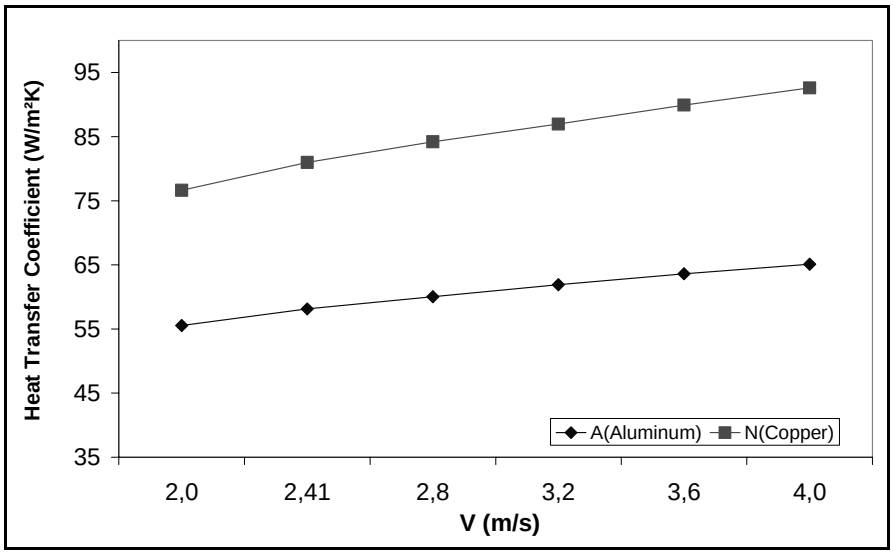

Figure 8.51 Effects of fin material on heat transfer coefficient

As shown in Figure 8.51, fin material has a considerable effect on heat transfer coefficient. Copper fins have greater heat transfer coefficients.

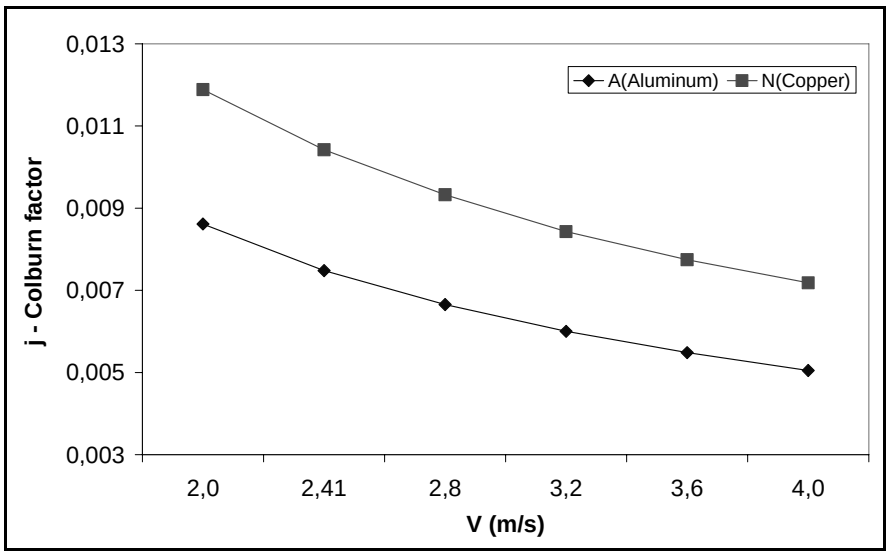

Figure 8.52 Effects of fin material on Colburn factor

Figure 8.52 shows that greater Colburn factors are obtained when the copper is selected as fin material.

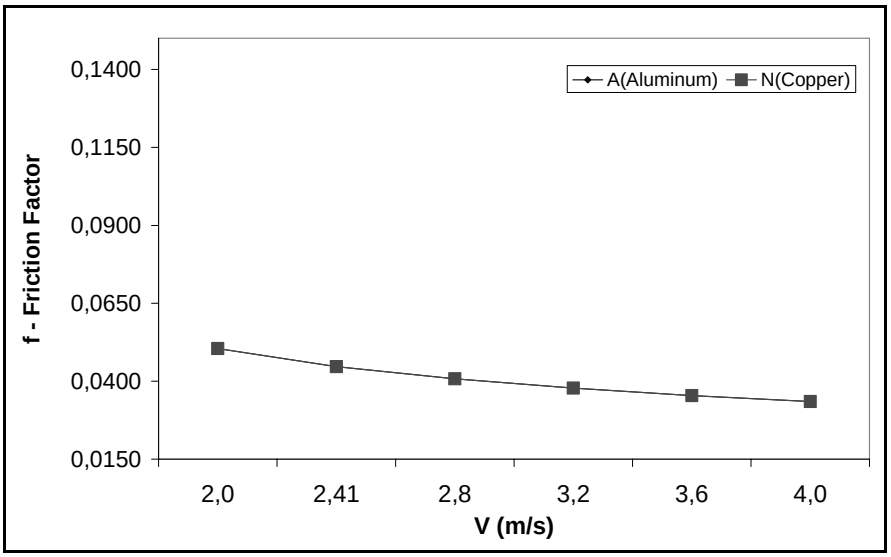

Figure 8.53 Effects of fin material on friction factor

Figure 8.53 shows that when the copper is selected as fin material, the friction factor has no change. Friction factor decreases with increasing air inlet velocity.

The effects of fin material on temperature contours, pressure contours, and velocity vectors are shown in Figure 8.54, 8.55, and 8.56, respectively.

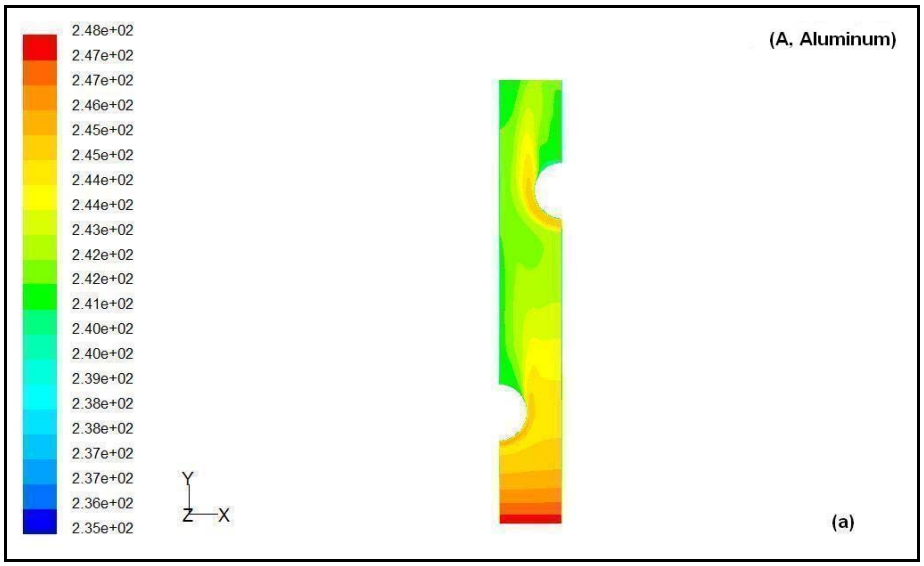

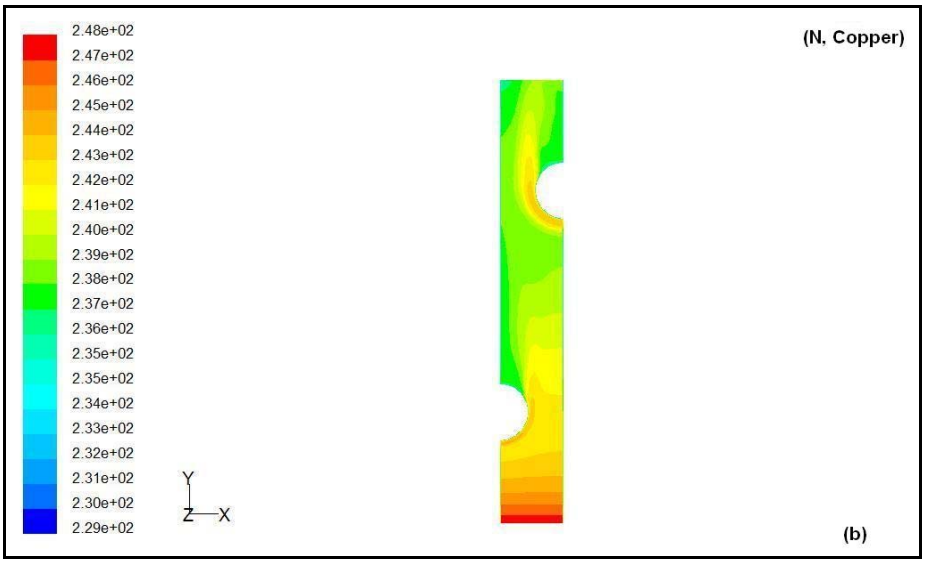

Figure 8.54 Effects of fin material on temperature contours

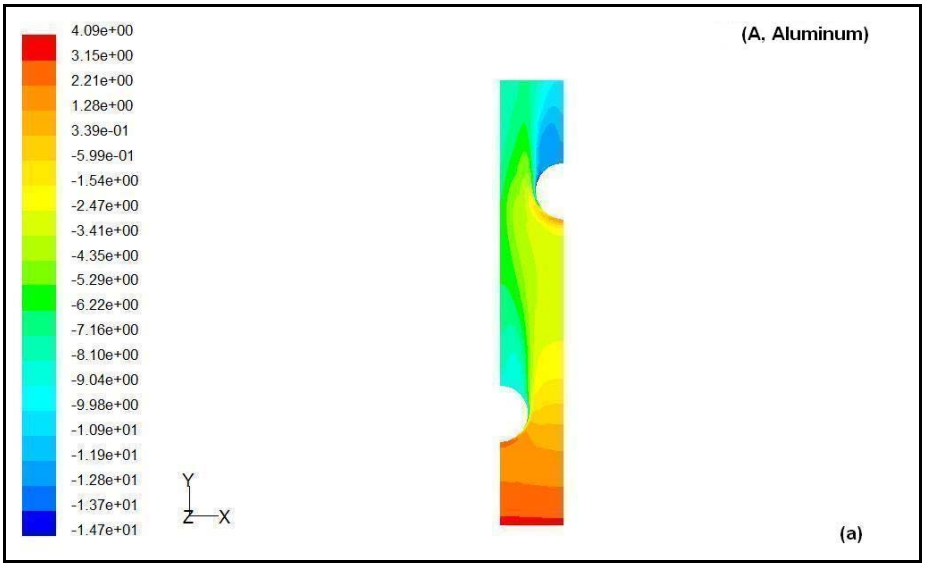

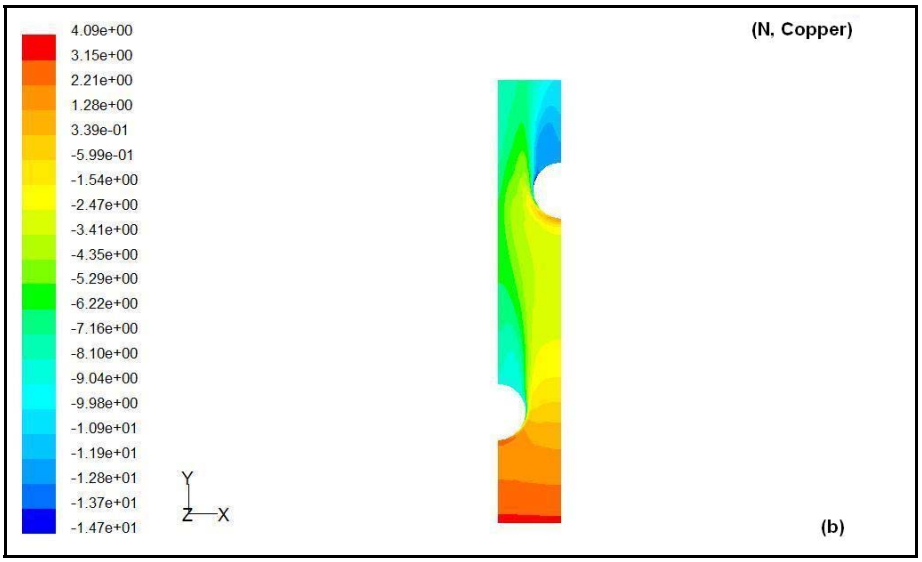

Figure 8.55 Effects of fin material on pressure contours

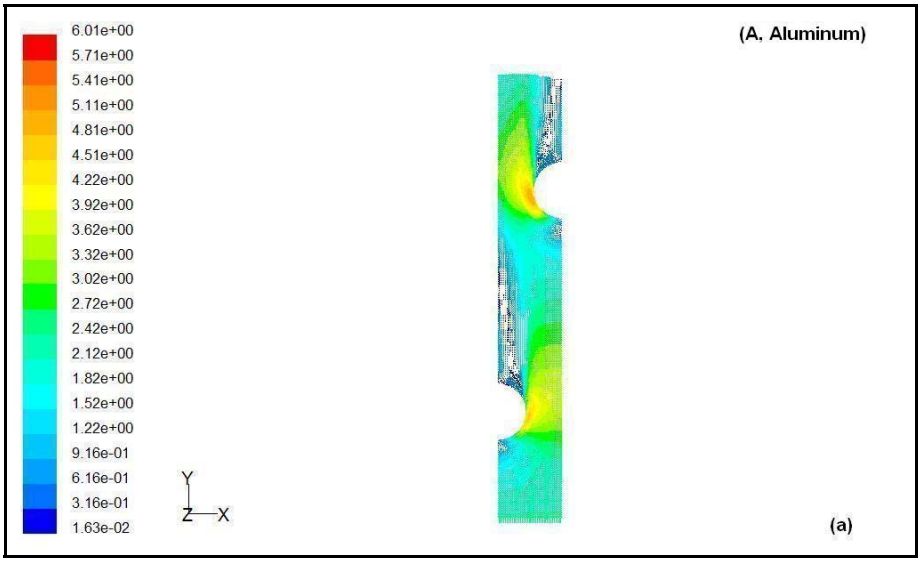

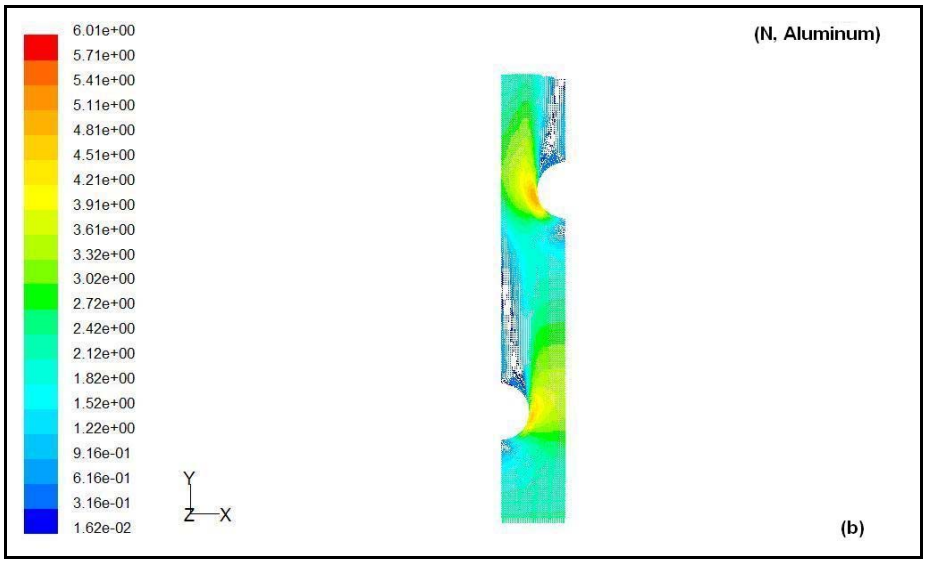

Figure 8.56 Effects of fin material on velocity vectors

8.8 Overall Results

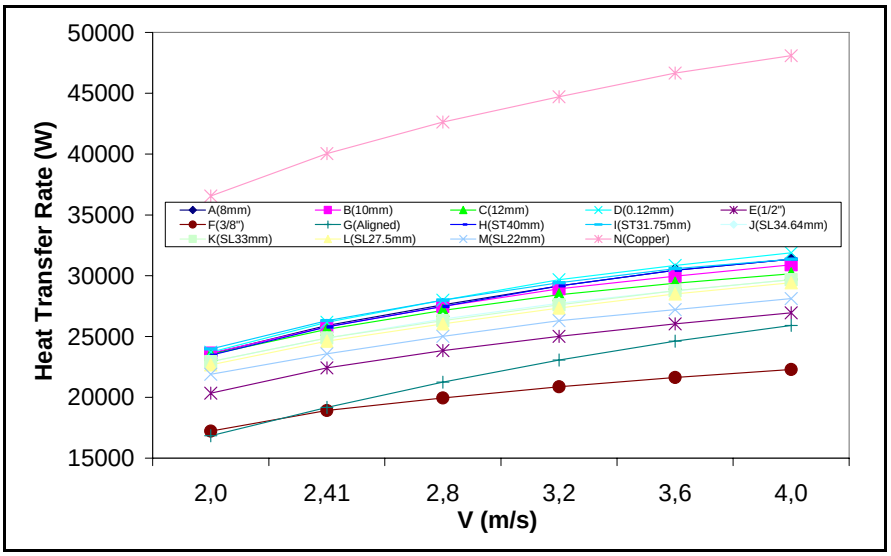

Figure 8.57 Heat transfer rate

Figure 8.57 shows the heat transfer rate results for all geometrical models. Selecting copper as fin material increases heat transfer too much. Heat transfer also increases when the fin thickness decreases. The important result of this study is that the fin material must be selected as copper.

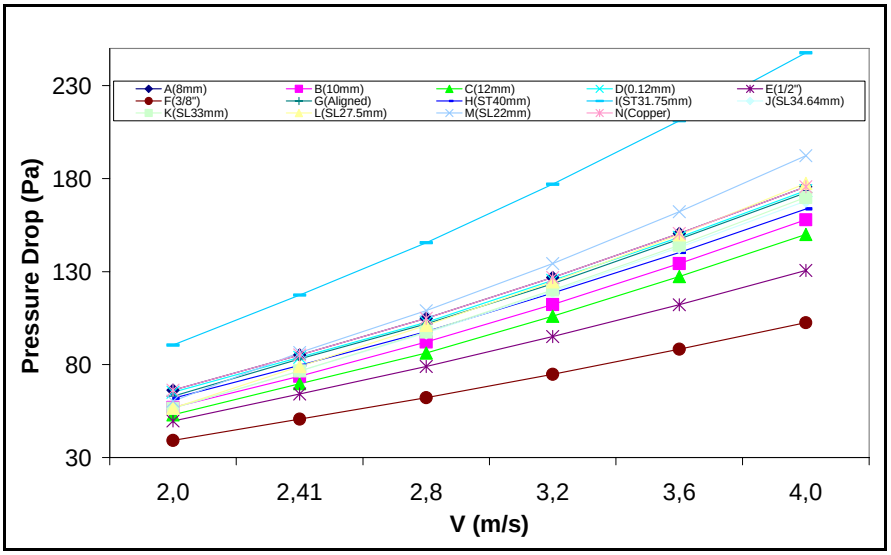

Figure 8.58 Pressure drop

As shown in Figure 8.58, the biggest pressure drop values are obtained in Model I, which is related with transverse tube pitch. The smallest pressure drop values are

obtained in Model F, which has a tube diameter of 3/8”. The important parameter of this study is transverse tube pitch. The transverse tube pitch must be wide enough to prevent higher pressure drops.

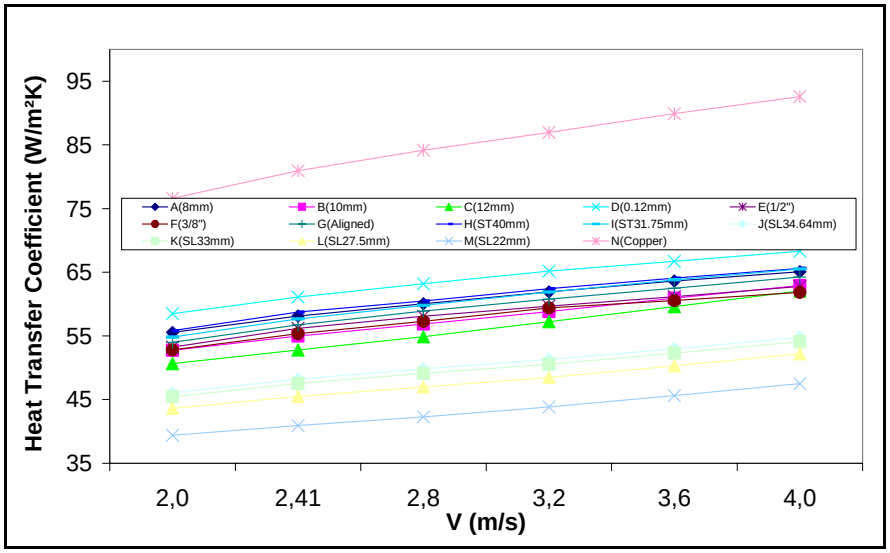

Figure 8.59 Heat transfer coefficient

In Figure 8.59, model N has the highest heat transfer coefficient, means copper fins have better heat transfer coefficients. Fin thickness is another important parameter in heat transfer coefficient. As a result of this study, copper must be selected as fin material. Decreasing fin thickness is another solution to increase heat transfer coefficient.

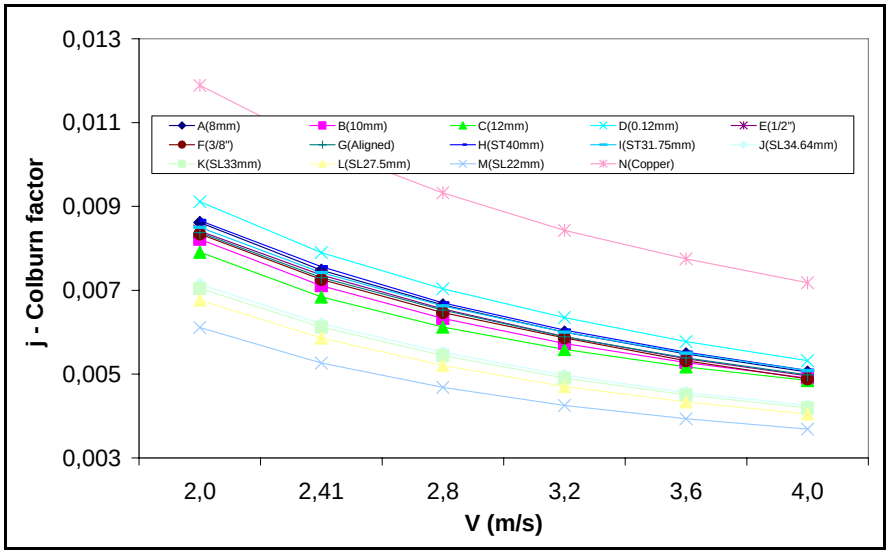

Figure 8.60 Colburn factor

Figure 8.60 shows the Colburn factor results depending on the air inlet velocities. The most important result of the study is that Model N has the highest Colburn factor. Selecting copper as fin material increases Colburn factor. Fin thickness also has an important effect on Colburn factor. The fin material must be selected as copper, or the fin must be decreased in order to obtain great heat transfer values.

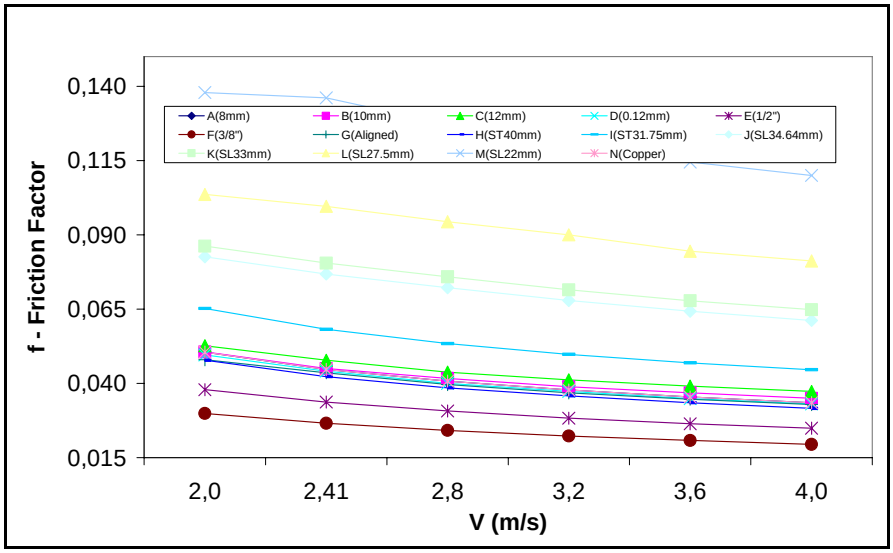

Figure 8.61 Friction factor

As shown in Figure 8.61, the friction factor increases when the longitudinal tube pitch decreases. The smallest friction factor is obtained for 3/8” tube diameter. The important result of this study is the longitudinal tube pitch must be wide enough to prevent high pressure drops.

CHAPTER NINE
CONCLUSIONS

In this study, a literature survey about the heat transfer and pressure drop characteristics of heat exchangers are performed. Heat exchanger types are mentioned, shortly. Evaporators, especially blast freezer evaporators are analyzed in freezing process. Industrial food freezing systems are investigated. Heat transfer and pressure drops are calculated, theoretically. A Computational Fluid Dynamics (CFD) software, Fluent is used in numerical study for real conditions of a blast freezer evaporator used in a spiral belt freezer tunnel fish freezing at -25°C. Theoretical study is compared with the numerical study.

In numerical study, a two-row blast freezer evaporator is analyzed for different geometrical parameters. The effects of the fin pitch, fin thickness, fin material, tube diameter, longitudinal and transverse tube pitch on heat transfer and pressure drop characteristics of the evaporator are investigated in 14 different models for actual boundary conditions and blast freezing process. Geometric parameters of the models are shown in Table 8.1. Because of the air inlet velocity ranges between 2 and 4 m/s, the flow assumed to be turbulent.

- The fin pitch has a considerable effect on heat transfer and pressure drop. From Figure 8.1 to 8.5 shows the fin pitch effect depending on air inlet velocity. Figures 8.6 and 8.7 shows the temperature and pressure contours of analyzed fin pitch. Figure 8.8 shows the velocity vectors. As the fin pitch decreases, heat transfer rate and pressure drop increases. Heat transfer and pressure drop increases with the increasing air inlet velocity. It is observed that increasing fin pitch decreases Colburn factor. Generally, the friction factor increases with a rise of fin pitch. Increasing air velocity decreases both of them.

- The fin thickness has an insignificant effect on heat transfer and pressure drop. From Figure 8.9 to 8.13 shows the fin thickness effect depending on air

inlet velocity. Figures 8.14 and 8.15 shows the temperature and pressure contours. Figure 8.16 shows the velocity vectors. The effect of fin thickness on the heat transfer rate and pressure drop is negligible for two different geometrical models. Decreasing fin thickness affects Colburn factor positively. The effect of the fin thickness on the friction factor is negligible for two different geometries.

- The tube diameter has an important effect on heat transfer and pressure drop. From Figure 8.17 to 8.21 shows the tube diameter effect depending on the air inlet velocity. Figures 8.22 and 8.23 shows the temperature and pressure contours. Figure 8.24 shows the velocity vectors. The heat transfer rate and pressure drop increases as the tube diameter increases. For all tube diameters, the Colburn factor decreases as the air inlet velocity increases from 2 m/s to 4 m/s. As the tube diameter decreases, the friction factor drops more severely with increasing air inlet velocity.

- Tube arrangement is another important parameter on heat transfer and pressure drop. From Figure 8.25 to 8.29 shows the tube arrangement effect depending on air inlet velocity. Figures 8.30 and 8.31 shows the temperature and pressure contours. Figure 8.32 shows the velocity vectors. Staggered tube arrangement increases heat transfer and pressure drop. Colburn j-factor and friction factor is higher in staggered tube arrangement.

- Transverse tube pitch has an insignificant effect on heat transfer, but has an important effect on pressure drop. From Figure 8.33 to 8.37 shows the transverse tube pitch effect depending on air inlet velocity. Figures 8.38 and 8.39 shows the temperature and pressure contours. Figure 8.40 shows the velocity vectors. The transverse tube pitch effect on heat transfer rate is negligible. Pressure drop has a considerable increase when the transverse tube pitch decreases. Colburn j-factors are nearly the same for different transverse tube pitches. Friction factor increases when the transverse tube pitch decreases.

- Longitudinal tube pitch affects heat transfer and pressure drop. From Figure 8.41 to 8.45 shows the longitudinal tube pitch effect depending on air inlet velocity. Figures 8.46 and 8.47 shows the temperature and pressure contours. Figure 8.48 shows the velocity vectors. Greater heat transfer rates are obtained as the longitudinal tube pitch increases, due to the increased heat transfer area. The pressure drop increases with a reduction of longitudinal tube pitches. The longitudinal tube pitch has an important effect on Colburn factor. As the longitudinal tube pitch decreases, the Colburn factor decreases. Generally, the friction factor increases with a reduction of longitudinal tube pitches.

- Fin material affects the heat transfer too much. From Figure 8.49 to 8.53 shows the fin material effect depending on air inlet velocity. Figures 8.54 and 8.55 show the temperature and pressure drop contours. Figure 8.56 shows the velocity vectors. Greater heat transfer rates are obtained as the copper fins selected. The fin material has no change on pressure drop. Greater Colburn factors are obtained when the copper is selected as fin material whereas the friction factor has no change.

REFERENCES

Abu Madi, M., Johns, R.A., Heikal, M.R. (1998). Performance characteristics correlation for round tube and plate finned heat exchangers. *Int. J. Refrig. 21* (7) 507–517.

ASHRAE (2002) *Refrigeration Handbook.*

Elmahdy, A.H., & Biggs, R.C. (1979). Finned tube heat exchanger: Correlation of dry surface heat transfer data. *ASHRAE Transactions, Volume 85, Issue Pt 2,* 262 – 273.

Fluent, User Manuals & Tutorials

Friterm Brochures & Catalogues

Gambit, User Manuals & Tutorials

Graham, J. (2001). *Installing an Air Blast Freezer?* TORRY Research Station; TORRY Advisory Note No.35.

Gray, D.L., & Webb, R.L. (1986). Heat transfer and friction correlations for plate-finned tube heat exchangers having plain fins. *Heat Transfer, Proceedings of the International Heat Transfer Conference, Volume 6,* 2745 – 2750.

Horuz, I., Yamankaradeniz, R., Kurem, E., (1998). Experimental and theoretical performance analysis of air-cooled plate-finned-tube evaporators. *Int. Comm. Heat Mass Transfer, Vol.25,* No.6, pp. 787–798.

Incropera, F. (2002). *Fundamentals of Heat and Mass Transfer*. (5^{th} ed.), John Wiley & Sons, Inc.

Jang, J.Y., Wu, M.C., Chang, W.J. (1996). Numerical and experimental studies of three-dimensional plate-fin and tube heat exchanger. *Int. J. Heat Mass Transfer, 39,* 3057–3066.

Jang, J.Y., & Chen, L.K. (1997). Numerical analysis of heat transfer and fluid flow in a three-dimensional wavy-fin and tube heat exchanger. *Int. J. Heat Mass Transfer, Vol.40,* No.16, pp. 3981 – 3990.

Jang, J.Y., Lai, J.T., Liu, L.C. (1998). The thermal-hydraulic characteristics of staggered circular finned-tube heat exchangers under dry and dehumidifying conditions. *Int. J. Heat Mass Transfer, 41*, 3321 – 3337.

Kakaç, S. (1991). *Boilers, Evaporators, and Condensers*. CRC Press.

Kakaç, S. (1998). *Heat Exchangers: Selection, Rating, and Thermal Design*. CRC Press.

Kays, W.M., & London, A.L. (1984). *Compact Heat Exchangers*, (3rd ed.), Mc Graw Hill.

Kim Y., & Kim, Y. (2005). Heat transfer characteristics of flat plate finned-tube heat exchangers with large fin pitch. *International Journal of Refrigeration, 28,* 851–858.

Mendez, R.R., Sen, M., Yang, K.T., McClain, R. (2000). Effect of fin spacing on convection in a plate fin and tube heat exchanger. *Int. J. Heat Mass Transfer, 43,* 39–51.

Mon, M.S., & Gross, U. (2004). Numerical study of fin-spacing effects in annular-finned tube heat exchangers. *Int J Heat Mass Transfer, 47,* 1953–1964.

Rich D.G. (1973). The effect of fin spacing on the heat transfer and friction performance of multirow, smooth plate fin tube heat exchangers. *ASHRAE Transactions, 79*, 137–45.

Rich D.G. (1975). The effect number of tube rows on heat transfer performance of smooth-plate fin tube heat exchangers. *ASHRAE Transactions, 81,* 307–17.

Rocha, L.A.O., Saboya, F.E.M., Vargas, J.V.C. (1997). A comparative study of elliptical and circular sections in one and two row tubes and plate fin heat exchangers. *Int. J. Heat Fluid Flow, 18*, 247–252.

Rosman, E.C., Carajilescov P., Saboya, F.E.M. (1984). Performance of one and two-row tube and plate fin heat exchangers. *J. Heat Transfer, 106*, 627–632.

Saboya, F.E.M., & Sparrow, E.M. (1974). Local and average transfer coefficients for one-row plate fin and tube heat exchanger configurations. *J. Heat Transfer, 96*, 265–272.

Saboya, F.E.M., & Sparrow, E.M. (1976a). Transfer characteristics of two-row plate fin and tube heat exchanger configurations. *Int. J. Heat Mass Transfer,19,* 41–49.

Saboya, F.E.M., & Sparrow, E.M. (1976b). Experiments on a three-row fin and tube heat exchanger. *J. Heat Transfer, 98,* 520 – 522.

Shepherd, D.G. (1956). Performance of one-row tube coils with thin-plate fins, low velocity forced convection. *Heating, Piping Air Cond. 28*, 137–144.

Shih, Y. C. (2003). Numerical study of heat transfer performance on the air side of evaporator for a domestic refrigerator. *Numerical Heat Transfer, Part A, 44*, 851–870.

Şahin, N. (2005). Konvansiyonel Odalarda Havalı Şok Dondurma Uygulamaları, Friterm.

Trott, A.R., & Welch, T. (2000). *Refrigeration and Air-Conditioning*. (3rd ed.) Butterworth – Heinemann.

Turaga, M., Lin, S., Fazio, P.P. (1988). Performance of direct expansion plate finned tube coils for air cooling and humidification. *Int. Journal of Refrigeration, Volume 11, Issue 2,* 78 – 86.

VDI – Heat Atlas (1993)

Wang CC, Fu WL, Chang CT. (1997). Heat transfer and friction characteristics of typical wavy fin and tube heat exchangers. *Exp Thermal Fluid Sci, 14(2)*, 174–86.

Wang CC, Tsi YM, Lu DC. (1998). A comprehensive study of convex-louver and wavy fin and tube heat exchangers. *AIAA J Thermophys Heat Transfer, 12(3),* 423–30.

Wang CC, Lin YT, Lee CJ, Chang YJ. (1999). Investigation of wavy fin and tube heat exchangers: a contribution to databank. *Exper. Heat Transfer, 12*, 73–89.

Wang, C.C., Chi, K.Y. (2000). Heat transfer and friction characteristics of plain fin-and-tube heat exchangers, part I: new experimental data. *Int. J. Heat Mass Transfer 43*, 2681–2691.

Wang, C.C., Chi, K.Y., Chang, C.J. (2000). Heat transfer and friction characteristics of plain fin-and-tube heat exchangers, part II: Correlation. *Int. J. Heat Mass Transfer 43*, 2693–2700.

Wang, C.C., Lee, W.S., Sheu, W.J. (2001). A comparative study of compact enhanced fin-and-tube heat exchangers. *Int. J. Heat Mass Transfer, 44,* 3565 – 3573.

APPENDICES

A.1 Standard Designation of Refrigerants (ASHRAE, 2002)

Table 1 Standard Designation of Refrigerants (ASHRAE *Standard* 34)

Refrigerant Number	Chemical Name or Composition (% by mass)	Chemical Formula
Methane Series		
10	tetrachloromethane (carbon tetrachloride)	CCl_4
11	trichlorofluoromethane	CCl_3F
12	dichlorodifluoromethane	CCl_2F_2
12B1	bromochlorodifluoromethane	$CBrClF_2$
12B2	dibromodifluoromethane	CBr_2F_2
13	chlorotrifluoromethane	$CClF_3$
13B1	bromotrifluoromethane	$CBrF_3$
14	tetrafluoromethane (carbon tetrafluoride)	CF_4
20	trichloromethane (chloroform)	$CHCl_3$
21	dichlorofluoromethane	$CHCl_2F$
22	chlorodifluoromethane	$CHClF_2$
22B1	bromodifluoromethane	$CHBrF_2$
23	trifluoromethane	CHF_3
30	dichloromethane (methylene chloride)	CH_2Cl_2
31	chlorofluoromethane	CH_2ClF
32	difluoromethane (methylene fluoride)	CH_2F_2
40	chloromethane (methyl chloride)	CH_3Cl
41	fluoromethane (methyl fluoride)	CH_3F
50	methane	CH_4
Ethane Series		
110	hexachloroethane	CCl_3CCl_3
111	pentachlorofluoroethane	CCl_3CCl_2F
112	1,1,2,2-tetrachloro-1,2-difluoroethane	CCl_2FCCl_2F
112a	1,1,1,2-tetrachloro-2,2-difluoroethane	CCl_3CClF_2
113	1,1,2-trichloro-1,2,2-trifluoroethane	CCl_2FCClF_2
113a	1,1,1-trichloro-2,2,2-trifluoroethane	CCl_3CF_3
114	1,2-dichloro-1,1,2,2-tetrafluoroethane	$CClF_2CClF_2$
114a	1,1-dichloro-1,2,2,2-tetrafluoroethane	CCl_2FCF_3
114B2	1,2-dibromo-1,1,2,2-tetrafluoroethane	$CBrF_2CBrF_2$
115	chloropentafluoroethane	$CClF_2CF_3$
116	hexafluoroethane	CF_3CF_3
120	pentachloroethane	$CHCl_2CCl_3$
123	2,2-dichloro-1,1,1-trifluoroethane	$CHCl_2CF_3$
123a	1,2-dichloro-1,1,2-trifluoroethane	$CHClFCClF_2$
124	2-chloro-1,1,1,2-tetrafluoroethane	$CHClFCF_3$
124a	1-chloro-1,1,2,2-tetrafluoroethane	CHF_2CClF_2
125	pentafluoroethane	CHF_2CF_3
133a	2-chloro-1,1,1-trifluoroethane	CH_2ClCF_3
134a	1,1,1,2-tetrafluoroethane	CH_2FCF_3
140a	1,1,1-trichloroethane (methyl chloroform)	CH_3CCl_3
141b	1,1-dichloro-1-fluoroethane	CCl_2FCH_3
142b	1-chloro-1,1-difluoroethane	$CClF_2CH_3$
143a	1,1,1-trifluoroethane	CF_3CH_3
150a	1,1-dichloroethane	$CHCl_2CH_3$
152a	1,1-difluoroethane	CHF_2CH_3
160	chloroethane (ethyl chloride)	CH_3CH_2Cl
170	ethane	CH_3CH_3
Propane Series		
216ca	1,3-dichloro-1,1,2,2,3,3-hexafluoropropane	$CClF_2CF_2CClF_2$
218	octafluoropropane	$CF_3CF_2CF_3$
245cb	1,1,1,2,2-pentafluoropropane	$CF_3CF_2CH_3$
290	propane	$CH_3CH_2CH_3$
Cyclic Organic Compounds		
C316	1,2-dichloro-1,2,3,3,4,4-hexafluorocyclobutane	$C_4Cl_2F_6$
C317	chloroheptafluorocyclobutane	C_4ClF_7
C318	octafluorocyclobutane	C_4F_8
Zeotropic Blends (% by mass)		
400	R-12/114 (must be specified)	
401A	R-22/152a/124 (53/13/34)	
401B	R-22/152a/124 (61/11/28)	
401C	R-22/152a/124 (33/15/52)	
402A	R-125/290/22 (60/2/38)	
402B	R-125/290/22 (38/2/60)	
403A	R-290/22/218 (5/75/20)	
403B	R-290/22/218 (5/56/39)	
404A	R-125/143a/134a (44/52/4)	
405A	R-22/152a/142b/C318 (45/7/5.5/42.5)	
406A	R-22/600a/142b (55/4/41)	
407A	R-32/125/134a (20/40/40)	
407B	R-32/125/134a (10/70/20)	
407C	R-32/125/134a (23/25/52)	
407D	R-32/125/134a (15/15/70)	
408A	R-125/143a/22 (7/46/47)	
409A	R-22/124/142b (60/25/15)	
409B	R-22/124/142b (65/25/10)	
410A	R-32/125 (50/50)	
410B	R-32/125 (45/55)	
411A	R-1270/22/152a (1.5/87.5/11.0)	
411B	R-1270/22/152a (3/94/3)	
412A	R-22/218/142b (70/5/25)	
413A	R-218/134a/600a (9/88/3)	
Azeotropic Blends (% by mass)		
500	R-12/152a (73.8/26.2)	
501	R-22/12 (75.0/25.0)*	
502	R-22/115 (48.8/51.2)	
503	R-23/13 (40.1/59.9)	
504	R-32/115 (48.2/51.8)	
505	R-12/31 (78.0/22.0)*	
506	R-31/114 (55.1/44.9)	
507A	R-125/143a (50/50)	
508A	R-23/116 (39/61)	
508B	R-23/116 (46/54)	
509A	R-22/218 (44/56)	
Miscellaneous Organic Compounds		
Hydrocarbons		
600	butane	$CH_3CH_2CH_2CH_3$
600a	2-methyl propane (isobutane)	$CH(CH_3)_3$
Oxygen Compounds		
610	ethyl ether	$C_2H_5OC_2H_5$
611	methyl formate	$HCOOCH_3$
Sulfur Compounds		
620	(Reserved for future assignment)	
Nitrogen Compounds		
630	methyl amine	CH_3NH_2
631	ethyl amine	$C_2H_5NH_2$
Inorganic Compounds		
702	hydrogen	H_2
704	helium	He
717	ammonia	NH_3
718	water	H_2O
720	neon	Ne
728	nitrogen	N_2
732	oxygen	O_2
740	argon	Ar
744	carbon dioxide	CO_2
744A	nitrous oxide	N_2O
764	sulfur dioxide	SO_2
Unsaturated Organic Compounds		
1112a	1,1-dichloro-2,2-difluoroethene	$CCl_2=CF_2$
1113	1-chloro-1,2,2-trifluoroethene	$CClF=CF_2$
1114	tetrafluoroethene	$CF_2=CF_2$
1120	trichloroethene	$CHCl=CCl_2$
1130	1,2-dichloroethene (trans)	$CHCl=CHCl$
1132a	1,1 difluoroethene (vinylidene fluoride)	$CF_2=CH_2$
1140	1-chloroethene (vinyl chloride)	$CHCl=CH_2$
1141	1-fluoroethene (vinyl fluoride)	$CHF=CH_2$
1150	ethene (ethylene)	$CH_2=CH_2$
1270	propene (propylene)	$CH_3CH=CH_2$

*The exact composition of this azeotrope is in question.

A.2 Thermophysical Properties of R404A (ASHRAE, 2002)

Refrigerant 404A [R-125/143a/134a (44/52/4)] Properties of Liquid on the Bubble Line and Vapor on the Dew Line

Pressure, MPa	Temperature, °C		Density, kg/m³	Volume, m³/kg	Enthalpy, kJ/kg		Entropy, kJ/(kg·K)		Specific Heat c_p, kJ/(kg·K)		c_p/c_v	Velocity of Sound, m/s		Viscosity, μPa·s		Thermal Cond., mW/(m·K)		Surface Tension, mN/m	Pressure, MPa
	Bubble	Dew	Liquid	Vapor	Liquid	Vapor	Liquid	Vapor	Liquid	Vapor	Vapor	Liquid	Vapor	Liquid	Vapor	Liquid	Vapor		
0.00500	−94.18	−93.00	1444.4	3.05033	83.20	310.67	0.4810	1.7496	1.147	0.637	1.163	959.	132.8	760.4	7.20	123.6	6.00	17.77	0.00500
0.00600	−91.96	−90.80	1438.3	2.57089	85.75	311.99	0.4952	1.7415	1.149	0.643	1.162	947.	133.4	723.1	7.29	122.3	6.12	17.57	0.00600
0.00700	−90.03	−88.89	1432.9	2.22501	87.98	313.15	0.5074	1.7347	1.151	0.649	1.161	937.	134.0	693.2	7.37	121.2	6.23	17.39	0.00700
0.00800	−88.31	−87.19	1428.1	1.96336	89.95	314.17	0.5181	1.7290	1.153	0.653	1.161	928.	134.5	668.3	7.44	120.2	6.33	17.23	0.00800
0.00900	−86.77	−85.67	1423.8	1.75831	91.74	315.10	0.5277	1.7240	1.155	0.657	1.160	920.	134.9	647.2	7.50	119.3	6.42	17.08	0.00900
0.01000	−85.36	−84.27	1419.9	1.59315	93.36	315.94	0.5364	1.7196	1.157	0.661	1.160	913.	135.3	628.9	7.56	118.5	6.50	16.95	0.01000
0.02000	−75.43	−74.45	1392.0	0.83310	104.92	321.94	0.5963	1.6923	1.171	0.690	1.159	863.	137.8	520.6	7.97	113.1	7.10	15.99	0.02000
0.04000	−64.18	−63.29	1359.7	0.43580	118.21	328.80	0.6617	1.6680	1.191	0.725	1.159	807.	140.3	429.8	8.43	107.2	7.77	14.84	0.04000
0.06000	−56.87	−56.03	1338.3	0.29818	126.98	333.25	0.7028	1.6553	1.206	0.749	1.161	772.	141.7	383.1	8.73	103.5	8.25	14.07	0.06000
0.08000	−51.30	−50.50	1321.7	0.22768	133.73	336.63	0.7336	1.6470	1.218	0.769	1.164	745.	142.5	352.4	8.96	100.8	8.65	13.47	0.08000
0.10000	−46.75	−45.98	1308.0	0.18460	139.30	339.37	0.7584	1.6410	1.228	0.786	1.166	723.	143.1	329.8	9.14	98.6	8.97	12.97	0.10000
0.10132b	−46.48	−45.71	1307.2	0.18233	139.64	339.53	0.7599	1.6406	1.229	0.787	1.166	722.	143.2	328.5	9.15	98.4	8.99	12.94	0.10132
0.12000	−42.87	−42.12	1296.1	0.15547	144.09	341.70	0.7793	1.6364	1.238	0.801	1.169	705.	143.5	312.1	9.28	96.7	9.25	12.54	0.12000
0.14000	−39.47	−38.74	1285.5	0.13440	148.33	343.72	0.7975	1.6327	1.246	0.815	1.172	689.	143.8	297.6	9.42	95.1	9.51	12.16	0.14000
0.16000	−36.42	−35.72	1276.0	0.11844	152.14	345.52	0.8136	1.6296	1.254	0.828	1.175	674.	144.0	285.4	9.54	93.7	9.74	11.81	0.16000
0.18000	−33.66	−32.97	1267.2	0.10591	155.62	347.14	0.8282	1.6270	1.262	0.840	1.177	661.	144.2	274.9	9.65	92.4	9.95	11.50	0.18000
0.20000	−31.13	−30.45	1259.1	0.09580	158.83	348.61	0.8414	1.6248	1.269	0.851	1.180	649.	144.3	265.7	9.75	91.3	10.15	11.20	0.20000
0.22000	−28.79	−28.12	1251.5	0.08747	161.81	349.97	0.8536	1.6228	1.276	0.861	1.183	638.	144.3	257.5	9.84	90.2	10.33	10.93	0.22000
0.24000	−26.61	−25.95	1244.4	0.08049	164.61	351.22	0.8650	1.6211	1.282	0.871	1.186	628.	144.3	250.2	9.93	89.2	10.51	10.68	0.24000
0.26000	−24.56	−23.91	1237.6	0.07454	167.25	352.39	0.8756	1.6196	1.288	0.881	1.189	618.	144.3	243.5	10.02	88.3	10.66	10.44	0.26000
0.28000	−22.63	−21.99	1231.2	0.06941	169.75	353.48	0.8855	1.6182	1.294	0.891	1.192	609.	144.3	237.4	10.10	87.4	10.83	10.22	0.28000
0.30000	−20.80	−20.17	1225.1	0.06494	172.13	354.51	0.8949	1.6169	1.300	0.900	1.195	601.	144.2	231.8	10.13	86.6	11.11	10.00	0.30000
0.32000	−19.06	−18.44	1219.2	0.06101	174.40	355.48	0.9038	1.6158	1.306	0.908	1.198	593.	144.1	226.6	10.21	85.9	11.26	9.80	0.32000
0.34000	−17.40	−16.80	1213.5	0.05753	176.57	356.40	0.9123	1.6147	1.312	0.917	1.201	585.	144.0	221.8	10.29	85.1	11.40	9.60	0.34000
0.36000	−15.82	−15.22	1208.0	0.05442	178.65	357.27	0.9203	1.6138	1.317	0.925	1.204	577.	143.9	217.3	10.36	84.4	11.54	9.41	0.36000
0.38000	−14.30	−13.71	1202.8	0.05163	180.66	358.09	0.9280	1.6129	1.322	0.934	1.207	570.	143.8	213.1	10.43	83.8	11.67	9.23	0.38000
0.40000	−12.84	−12.26	1197.7	0.04910	182.60	358.88	0.9354	1.6120	1.328	0.942	1.210	563.	143.7	209.1	10.49	83.2	11.80	9.06	0.40000
0.42000	−11.44	−10.86	1192.7	0.04681	184.47	359.64	0.9425	1.6113	1.333	0.949	1.213	557.	143.5	205.4	10.56	82.5	11.93	8.89	0.42000
0.44000	−10.09	−9.51	1187.9	0.04472	186.28	360.36	0.9494	1.6105	1.338	0.957	1.216	550.	143.4	201.8	10.62	82.0	12.05	8.73	0.44000
0.46000	−8.78	−8.21	1183.2	0.04280	188.04	361.05	0.9560	1.6098	1.343	0.965	1.219	544.	143.2	198.5	10.68	81.4	12.18	8.57	0.46000
0.48000	−7.51	−6.95	1178.6	0.04104	189.75	361.71	0.9624	1.6092	1.348	0.972	1.222	538.	143.0	195.3	10.74	80.9	12.30	8.42	0.48000
0.50000	−6.28	−5.73	1174.1	0.03941	191.41	362.35	0.9685	1.6085	1.353	0.980	1.225	532.	142.9	192.2	10.79	80.3	12.41	8.28	0.50000
0.55000	−3.37	−2.83	1163.4	0.03584	195.37	363.84	0.9831	1.6071	1.365	0.998	1.234	518.	142.4	185.1	10.93	79.1	12.70	7.93	0.55000
0.60000	−0.65	−0.12	1153.1	0.03285	199.10	365.21	0.9968	1.6058	1.377	1.016	1.242	505.	141.9	178.8	11.06	77.9	12.97	7.60	0.60000
0.65000	1.90	2.42	1143.4	0.03030	202.64	366.46	1.0095	1.6046	1.389	1.033	1.250	493.	141.3	172.9	11.18	76.9	13.24	7.29	0.65000
0.70000	4.32	4.82	1134.0	0.02810	206.00	367.62	1.0215	1.6036	1.400	1.051	1.259	481.	140.8	167.6	11.30	75.8	13.50	7.00	0.70000
0.75000	6.60	7.10	1124.9	0.02619	209.21	368.69	1.0329	1.6025	1.412	1.068	1.268	470.	140.2	162.7	11.41	74.9	13.75	6.73	0.75000
0.80000	8.77	9.26	1116.1	0.02450	212.29	369.69	1.0437	1.6016	1.424	1.085	1.277	460.	139.6	158.1	11.52	74.0	14.01	6.47	0.80000
0.85000	10.85	11.33	1107.6	0.02301	215.26	370.62	1.0540	1.6007	1.435	1.102	1.287	450.	139.0	153.9	11.63	73.1	14.26	6.22	0.85000
0.90000	12.83	13.30	1099.3	0.02167	218.11	371.48	1.0639	1.5998	1.447	1.120	1.296	440.	138.4	149.9	11.74	72.3	14.51	5.98	0.90000
0.95000	14.74	15.20	1091.2	0.02047	220.87	372.29	1.0733	1.5989	1.459	1.137	1.306	431.	137.7	146.1	11.84	71.5	14.76	5.75	0.95000
1.00000	16.57	17.02	1083.3	0.01939	223.54	373.04	1.0824	1.5981	1.471	1.155	1.317	422.	137.1	142.6	11.94	70.7	15.00	5.53	1.00000
1.10000	20.03	20.47	1068.0	0.01750	228.65	374.41	1.0996	1.5965	1.495	1.190	1.339	404.	135.8	136.0	12.14	69.3	15.50	5.12	1.10000
1.20000	23.27	23.69	1053.1	0.01592	233.50	375.60	1.1158	1.5949	1.520	1.228	1.363	388.	134.4	130.0	12.34	67.9	16.00	4.74	1.20000
1.30000	26.31	26.72	1038.7	0.01457	238.12	376.65	1.1309	1.5933	1.547	1.266	1.388	373.	133.0	124.5	12.54	66.7	16.51	4.38	1.30000
1.40000	29.18	29.58	1024.5	0.01340	242.54	377.55	1.1453	1.5916	1.574	1.307	1.416	358.	131.6	119.5	12.74	65.5	17.04	4.05	1.40000
1.50000	31.90	32.29	1010.7	0.01238	246.80	378.34	1.1590	1.5900	1.603	1.350	1.446	344.	130.2	114.8	12.93	64.3	17.58	3.74	1.50000
1.60000	34.49	34.86	997.0	0.01148	250.91	379.00	1.1721	1.5882	1.634	1.397	1.480	330.	128.7	110.4	13.13	63.3	18.14	3.44	1.60000
1.70000	36.96	37.32	983.4	0.01068	254.89	379.55	1.1847	1.5864	1.667	1.447	1.516	317.	127.2	106.2	13.34	62.2	18.73	3.16	1.70000
1.80000	39.32	39.67	970.0	0.00996	258.76	380.00	1.1968	1.5846	1.703	1.501	1.556	305.	125.7	102.3	13.54	61.2	19.35	2.90	1.80000
1.90000	41.59	41.92	956.5	0.00932	262.53	380.35	1.2085	1.5826	1.741	1.560	1.601	292.	124.2	98.6	13.75	60.3	20.00	2.65	1.90000
2.00000	43.76	44.09	943.1	0.00873	266.22	380.59	1.2198	1.5805	1.784	1.625	1.651	280.	122.6	95.0	13.97	59.3	20.69	2.42	2.00000
2.10000	45.86	46.17	929.6	0.00819	269.83	380.74	1.2308	1.5783	1.830	1.697	1.708	268.	121.0	91.6	14.20	58.4	21.43	2.20	2.10000
2.20000	47.87	48.18	916.0	0.00770	273.38	380.79	1.2416	1.5760	1.882	1.778	1.772	257.	119.5	88.3	14.43	57.6	22.21	1.98	2.20000
2.30000	49.82	50.11	902.2	0.00724	276.87	380.73	1.2521	1.5735	1.940	1.869	1.845	246.	117.8	85.1	14.68	56.7	23.06	1.78	2.30000
2.40000	51.71	51.99	888.2	0.00682	280.32	380.57	1.2624	1.5709	2.006	1.974	1.929	235.	116.2	82.0	14.93	55.9	23.97	1.60	2.40000
2.50000	53.53	53.80	874.0	0.00643	283.74	380.31	1.2725	1.5680	2.081	2.095	2.027	224.	114.6	79.0	15.21	55.1	24.97	1.42	2.50000
2.60000	55.30	55.56	859.4	0.00606	287.14	379.92	1.2826	1.5649	2.169	2.238	2.143	213.	112.9	76.1	15.50	54.4	26.05	1.25	2.60000
2.70000	57.02	57.26	844.4	0.00571	290.53	379.42	1.2925	1.5616	2.272	2.407	2.282	202.	111.2	73.2	15.81	53.7	27.24	1.09	2.70000
2.80000	58.68	58.91	828.8	0.00538	293.92	378.77	1.3024	1.5580	2.397	2.613	2.451	191.	109.5	70.3	16.15	53.0	28.56	0.94	2.80000
2.90000	60.30	60.52	812.5	0.00507	297.32	377.97	1.3122	1.5540	2.552	2.868	2.662	180.	107.8	67.5	16.52	52.3	30.05	0.79	2.90000
3.00000	61.87	62.08	795.4	0.00476	300.76	376.99	1.3222	1.5496	2.748	3.195	2.931	170.	106.0	64.6	16.93	51.8	31.74	0.66	3.00000
3.20000	64.88	65.07	757.6	0.00419	307.87	374.35	1.3425	1.5391	3.366	4.224	3.781	148.	102.3	58.7	17.92	50.9	36.05	0.42	3.20000
3.40000	67.74	67.89	711.4	0.00362	315.62	370.30	1.3645	1.5249	4.792	6.551	5.695	126.	98.4	52.4	19.31	51.0	42.77	0.22	3.40000
3.775c	72.5	72.5	574.	0.00174	334.8	334.8	1.419	1.419	—	—	—	—	—	—	—	—	—	0.00	3.775

*Temperatures are on the ITS-90 scale b = bubble and dew points at one standard atmosphere c = critical point

A.3 Pressure - Enthalpy Diagram of R404A (ASHRAE, 2002)